Nodule inception NIN plays a dual role in the establishment of root nodule symbiosis in *Lotus japonicus*

vorgelegt von

Jayne Carol Lambert

München, Oktober 2016

Dissertation zur Erlangung des Doktorgrades

der Naturwissenschaften an der Fakultät für Biologie

der Ludwig-Maximilians-Universität München

"It always seems impossible until it's done."

Nelson Mandela

Dissertation eingereicht am 27. Oktober 2016

Tag der mündlichen Prüfung: 19. Januar 2017

Erstgutachter: Prof. Dr. Martin Parniske

Zweitgutachterin: PD Dr. Cordelia Bolle

For
my family

Table of contents

1 List of Publications

Binder, A., **Lambert, J.**, Morbitzer, R., Popp, C., Ott, T., Lahaye, T., and Parniske, M. (2014). A modular plasmid assembly kit for multigene expression, gene silencing and silencing rescue in plants. PLoS ONE 9, e88218.

Singh S, Katzer K, **Lambert J**, Cerri M, Parniske M. CYCLOPS, a DNA-binding transcriptional activator, orchestrates symbiotic root nodule development, Cell Host Microbe. 2014 Feb 12;15(2):139-52.

Manuscript:

Lambert J, Rosa Andrade, Katzer K and Parniske M. NIN plays a dual role in the establishment of the root nodule symbiosis in *Lotus japonicus*, in preparation

2 List of presentations at scientific conferences

Poster presentation at the ENFC 2014 in Teneriffe, "*Lotus japonicus* NIN plays a dual role in the establishment of the root nodule symbiosis", awarded with **1st Posterprize**

Poster presentation at the ENFC 2012 in Munich

Poster presentation at the Botaniker-Tagung 2011 in Berlin

Poster presentation at the Plant Calcium Signaling Meeting 2010 in Münster

3 Abstract

The symbiosis between legume plants and nitrogen-fixing rhizobia leads to the formation of a novel organ, the root nodule. Bacterial secreted lipo-chitooligosaccharides, so-called nodulation factors (NF) are recognized at the surface of plant root hairs, leading to the initiation of calcium spiking in the nucleus. These calcium oscillations are decoded by a complex comprising CCaMK, a calcium and calmodulin dependent kinase, and the transcription factor CYCLOPS, a nuclear-coiled-coil protein. CCaMK phosphorylates CYCLOPS at two serines (S50 and S154) essential for symbiosis. Activated CYCLOPS (CYCLOPS-DD) binds to the *NIN* promoter in a sequence specific manner and in turn drives its expression. *NIN* encodes a transcription factor with a highly conserved RWP-RK DNA-binding domain. Homologous NIN-like proteins control nitrate signalling in presumably all land plants. Since its discovery, NIN has been considered a positive regulator in nodulation based on its rapid upregulation after NF perception and its requirement for root hair infection and the initiation of cortical cell division. Nevertheless, a negative role of NIN in the process of infection thread formation was recently described, raising the question how NIN can play a bifunctional role in infection and nodule organogenesis. In this study, we demonstrated that NIN and CYCLOPS interact in yeast and in the nucleus *in planta*. Furthermore, the co-expression of NIN, CYCLOPS and CCaMK was investigated and the results suggest the formation of a trimeric complex. Moreover, a negative regulatory role of NIN on the CYCLOPS-DD mediated activation was observed in transactivation assays using the *NIN* promoter. In addition, NIN can efficiently bind to a *cis*-element of the *NIN* promoter in close vicinity of the CYCLOPS binding site in electrophoretic mobility shift assays (EMSA). Strikingly, both proteins can bind simultaneously to the *NIN* promoter, resulting in a supershift in EMSA. Lastly, overexpression of *NIN* in *L. japonicus* Gifu wild-type plants and different nodulation mutants led to an inhibition of nodulation independent of the autoregulation of nodulation process. In our model NIN regulates its own expression via a negative feedback loop by binding to the *NIN* promoter and through protein-protein interaction between NIN and CYCLOPS thus preventing further activation of the CYCLOPS-mediated signalling pathway and restricting further infection by rhizobia.

4 Zusammenfassung

Die Symbiose zwischen Leguminosen und Stickstoff-fixierenden Rhizobien führt zur Bildung eines neuen Organs, dem Wurzelknöllchen. Bakterielle sekretierte Lipo-chitooligosaccharide, sogenannte Nodulationsfaktoren (NF), werden an der Oberfläche von Pflanzenwurzelhärchen erkannt und führen zu symbiotischem „Calcium spiking" im Kern. Diese Kalziumoszillationen werden durch einen Komplex dekodiert, der aus CCaMK, einer Calcium- und Calmodulin- abhängigen Kinase und dem Transkriptionsfaktor CYCLOPS, einem Zellkern-lokalisierten coiled-coil Protein besteht. CCaMK phosphoryliert CYCLOPS an zwei Serinen (S50 und S154), die von wesentlicher Bedeutung für die Symbiose sind. Aktiviertes CYCLOPS (CYCLOPS-DD) bindet sequenzspezifisch an den *NIN* Promotor und induziert anschließend die *NIN* Expression. *NIN* kodiert für einen Transkriptionsfaktor mit einer hochkonservierten „RWP-RK" DNA-Bindungsdomäne. Homologe NIN-ähnliche Proteine steuern die Signalweiterleitung in der Nitratassimilation in vermutlich allen Landpflanzen. Seit seiner Entdeckung galt NIN als ein positiver Regulator in der Knöllchensymbiose, basierend auf der schnellen Hochregulierung der *NIN* Genexpression nach NF Wahrnehmung und der Notwendigkeit von NIN für die Wurzelhaar-Infektion und für die Einleitung der kortikalen Zellteilung. Für NIN wurde jedoch kürzlich auch eine negative regulatorische Funktion beim Prozess der Infektionsschlauchbildung demonstriert, was die Frage aufwirft, wie NIN eine bi-funktionelle Rolle bei Infektion und Knöllchenbildung spielen kann.

In dieser Studie haben wir gezeigt, dass NIN und CYCLOPS im Zellkern von Pflanzen und in Hefe miteinander interagieren können. Darüber hinaus wurde die Co-Expression von NIN, CYCLOPS und CCaMK untersucht und die Ergebnisse zeigen, dass diese Proteine einen trimeren Komplex bilden. Zudem wurde eine negative regulatorische Rolle von NIN auf die von CYCLOPS-DD vermittelte Aktivierung in Transaktivierungsassays unter Verwendung des *NIN* Promotors beobachtet. Außerdem konnte in Electrophoretic Mobility Shift Assays (EMSAs) gezeigt werden, dass NIN effizient an ein *cis*-Element des eigenen Promotors binden kann, welches sich in unmittelbarer Nähe der CYCLOPS-Bindungsstelle befindet.

Beide Proteine können gleichzeitig nebeneinander an den *NIN* Promotor binden, was zu einem Supershift im EMSA führte. Schließlich kommt es durch die Überexpression von *NIN* zu einer Hemmung der Knöllchenbildung in Gifu Wildtyp Pflanzen und verschiedenen nodulierenden Mutanten, die unabhängig vom Prozess der Autoregulation der Nodulation reguliert ist. In unserem Modell reguliert NIN seine eigene Expression durch eine negative Feedback-Schleife, indem es an den *NIN* Promotor bindet und durch Protein-Protein Interaktion von NIN und CYCLOPS eine weitere Aktivierung des durch CYCLOPS vermittelten Signalwegs verhindert und dadurch für eine Einschränkung weiterer Infektionen durch Rhizobien sorgt.

5 Introduction

5.1 The Root Nodule Symbiosis and Arbuscular Mycchorizha Symbiosis

The symbiosis between legume plants and nitrogen-fixing soil bacteria (rhizobia) is a beneficial interaction for both partners (Den Herder and Parniske, 2009). Rhizobia live in a newly formed plant organ, named nodule (Brewin et al., 1999; Oldroyd and Downie, 2008; Oldroyd et al., 2011). In this environment, rhizobia fix atmospheric nitrogen under oxygen-restricted conditions and provide the plant with ammonium, leading to an improved survival of the plant in nitrogen-poor soil (Gage, 2004). In exchange the microsymbiont receives carbon sources (including dicarboxylates and amino acids) deriving from photosynthesis and mineral nutrients (iron, molybdenum, sulphur and others) from the plant.

Microbial partners efficiently engage in root nodule symbiosis (RNS) with various flowering plant species, which belong to the Eurosid I clade, specifically those from the four orders of Fagales, Fabales, Cucubitales and Rosales, also referred to as nodulating clade (Kistner and Parniske, 2002; Cermak et al., 2011). RNS with rhizobia is restricted to legumes (Fabaceae), with one exception for the non-legume Parasponia (Op den Camp et al., 2012; Remigi et al., 2016). There is, however, another RNS between filamentous actinomycetes of the genus *Frankia* (Actinobacteria) and so-called "actinorhizal" plants (e.g. Datisca and Casuarina) (Li et al., 2015; Pawlowski and Sprent, 2008).

In all RNSes, several symbiotic genes were co-opted from the signalling pathway of the more ancient association between plants and arbuscular mycorrhizal fungi (Delaux et al., 2013; Delaux et al., 2015). About 80% of all land plants are able to establish the arbuscular mycorrhizal symbiosis (AMS) with fungi from the phylum Glomeromycota (Schüβler et al., 2001; Parniske, 2008). The plant receives phosphorus and other inorganic nutrients from the fungus in exchange for carbon sources (Harrison, 1999; Parniske, 2008). In this association the fungus is able to colonize the plant by invasion of the root and forms highly branched structures in the cortex, named arbuscules (Gutjahr and Parniske, 2013).

Both symbioses share a common set of genes (common symbiosis genes), which are required for the initiation of the signalling cascade within the plant (Kistner and Parniske, 2002).

5.2 Signal perception and symbiotic calcium signalling

Under nitrogen limiting conditions, leguminous plants secret flavonoids that attract compatible symbiosis partners (Peters et al., 1986). In turn, bacteria respond with the activation of *nod* genes, leading to the production and secretion of nodulation factors (NF) into the soil (Fisher and Long, 1992). Variations of NFs exist among different rhizobial species, which ensures the perfect match of interaction partners between host plant and microsymbiont (Roche et al., 1991; Denarie et al., 1996). The chemical compositions of NFs is a chitooligosaccharide backbone with four to five N-actetylglucosamine residues with β-1,4 linkeages decorated with further species-specific groups such as methyl, acetyl or sulphate groups (Denarie et al., 1996).

This first signal exchange initiates a complex signalling cascade to activate the common signalling pathway leading to gene activation (Figure 1). In the past 30 years several genes required for the two major subsequent events, bacterial infection and nodule formation, have been identified and characterised (Oldroyd, 2013).

Firstly, NFs are recognised by the two Lysin Motif (LysM)–type receptors Nod Factor Receptor 1 (NFR1) and NFR5, on the root hair plasma membrane (Madsen et al., 2003; Radutoiu et al., 2003). NFR1 shows a typical domain structure of a receptor kinase, which is an active intracellular kinase domain that is capable of auto-phosphorylation and trans-phosphorylation of other proteins, including NFR5 (Radutoiu et al., 2003; Madsen et al., 2011). In contrast to NFR1, NFR5 has a pseudokinase that lacks important motifes of a functional kinase and is not able to phosphorylate other proteins (Madsen et al., 2003; Madsen et al., 2011). Interestingly, the receptors feature an additional LysM domain in the extra-cytoplasmic domain exclusively in plants, which has been shown to be crucial for NF binding (Bateman and Bycroft, 2000; Zhang et al., 2007; Broghammer et al., 2012). Both receptors localise to the plasma membrane and form a heterodimeric complex (Madsen et al., 2011; Lefebvre et al., 2012; Pietraszewska-Bogiel et al., 2013).

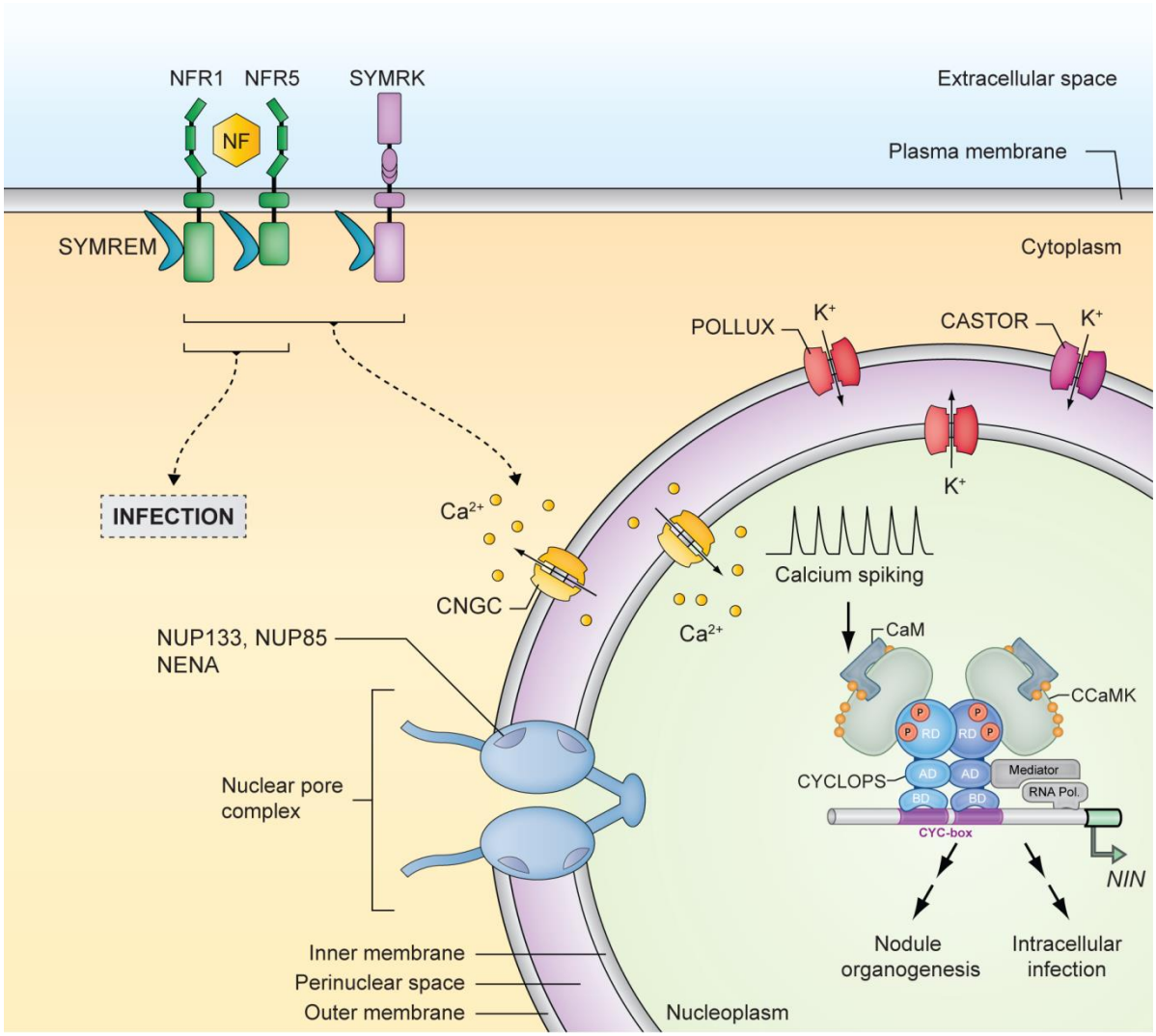

Figure 1: symbiotic signal transduction in root nodule symbiosis

Nod factor (NF) is recognised and bound by the NF receptors NFR1 and NFR5 at the plasma membrane. SYMRK, a plasma membrane bound receptor-like kinase and SYMREM1, a remorin upregulated during symbiosis, are interacting with both NFRs. Calcium channels (CNGCs) are responsible for calcium release from the nuclear envelop. Three components of the nuclear pore complex NUP133, NUP85 and NENA as well as two ion-channels CASTOR and POLLUX are required for the generation of calcium spiking. The nuclear calcium and calmodulin-dependent kinase CCaMK is the decoder of these calcium oscillations. CCaMK and CYCLOPS form a complex and activate *NIN* expression. Figure modified from (Singh and Parniske, 2012)

SYMRK is a receptor-like kinase (RLK) that is indispensable for both RNS and AMS (Endre et al., 2002; Stracke et al., 2002; Yoshida and Parniske, 2005; Markmann et al., 2008; Kosuta et al., 2011; Antolin-Llovera et al., 2014; Ried et al., 2014). SYMRK consists of an extra-cytoplasmic region including Leucin-rich repeats (LRRs), a malectin-like domain and a functional intracellular protein kinase domain (Stracke et al., 2002; Yoshida and Parniske, 2005; Kosuta et al., 2011; Antolin-Llovera et al., 2014).

An active role for SYMRK in the signalling pathway of root nodule symbiosis was demonstrated with the overexpression in hairy root experiments, which lead to the formation of spontaneous nodules in the absence of rhizobia (Ried et al., 2014). The interaction of SYMRK and NFR5 places them at an early recognition point for RNS and suggests a role of SYMRK as a co-receptor (Antolin-Llovera et al., 2014; Ried et al., 2014).

Furthermore, the interaction between these receptors and a plasma membrane associated remorin, SYMREM1, was demonstrated. Remorins function as scaffold proteins and are assumed to be involved in the organization of microdomains and thus may facilitate bacterial entry (Lefebvre et al., 2010; Jarsch and Ott, 2011; Toth et al., 2012). The interplay of these receptors is the earliest recognition step between the symbiotic partners to verify the specificity of the host and allow for colonisation.

Two of the earliest readouts in the plant after contact with bacteria are calcium influx at the root-hair tip and nuclear calcium spiking (Kosuta et al., 2008; Chabaud et al., 2011; Sieberer et al., 2012). The same response is triggered with purified NF extracted from rhizobia (Kosuta et al., 2008; Chabaud et al., 2011; Sieberer et al., 2012). Recently, three calcium channels have been identified, which encode cyclic nucleotide-gated channels (CNGCs) and probably account for calcium release from the nuclear envelope (Charpentier et al., 2016). In the nuclear envelope CASTOR and POLLUX, two cation channels with a preference for K^+ ions, are both required for the establishment of the symbiosis in *Lotus japonicus* (Ané et al., 2004; Imaizumi-Anraku et al., 2005; Charpentier et al., 2008). Moreover, proteins of the nuclear pore complex, NUP85, NUP133 and NENA, are required for calcium spiking within the plant (Bonfante et al., 2000; Kistner et al., 2005; Kanamori et al., 2006; Saito et al., 2007; Groth et al., 2010).

Binding of NFs to the receptors leads to a rapid response within the plant, including calcium spiking, rearrangement of the cytoskeleton and the curling of responsive root hairs in a typical "shepherd's crook" structure (Jones et al., 2007; Broghammer et al., 2012). The first event is an influx of calcium within one minute, actin rearrangement happens within three to five minutes of NF perception (Weerasinghe et al., 2005), followed by calcium spiking in the nucleus within 15 minutes and root hair deformation within one to three hours (Ehrhardt et al., 1996; Miwa et al., 2006; Oldroyd, 2013).

Infection is initiated by the attachment of rhizobia to the growing root tip. Then, the plant cell wall is modified to facilitate rhizobial uptake. The entrapped rhizobium divides and multiplies to a microcolony in the "shepherd's crock" curl structure, within an infection pocket. Within 10 to 20 hours the full process of infection thread formation is initiated (Fournier et al., 2015). Then, rhizobia enter the plant through a tube like structure (infection thread) bound by the plant membrane and cell wall, which guides them to the root cortex (Esseling et al., 2003; Geurts et al., 2005; Fournier et al., 2008; Murray, 2011). Cortical cell division in close proximity to the infection thread leads to the formation of a nodule primordium, where the bacteria are released into the cytoplasm of nodule cells and then differentiate into nitrogen-fixing bacteroids (Timmers et al., 1999; Bolanos et al., 2004). Genes required for cell-cycle activation and for hormone biosynthesis are induced during the process of infection thread formation (Yang et al., 1994; Breakspear et al., 2014).

5.3 Decoding of the calcium signal

In the nucleus there are several proteins that are responsible for inducing gene expression downstream of calcium spiking. A calcium and calmodulin dependent serine/threonine kinase (CCaMK) is considered to be the central player in the signalling transduction pathway and the decoder of calcium spiking (Levy et al., 2004; Mitra et al., 2004; Tirichine et al., 2006; Hayashi et al., 2010; Singh and Parniske, 2012).

CCaMK harbours a calmodulin binding domain (CaMBD), an active kinase domain and a C-terminal visinin-like domain (VLD) with three calcium binding EF hands (Gleason et al., 2006; Tirichine et al., 2006). Interestingly, CCaMK only exists in symbiotic plants (Hrabak et al., 2003) and it becomes active after calcium binding to the EF hand, leading to auto-phosphorylation of the kinase (Tirichine et al., 2006; Shimoda et al., 2012; Swainsbury et al., 2012). Then, binding of CaM to the CaMBD results in a release of auto-inhibition of the kinase, inducing a conformational change in the protein structure and activating the kinase for transphosphorylation (Gleason et al., 2006; Shimoda et al., 2012; Singh and Parniske, 2012).

The central role of CCaMK in symbiotic sinalling was demonstrated by the study of an autoactive version of CCaMK that carries a replacement of threonine at position 265 by aspartic acid or isoleucine (T265D or I). Plants that express this autoactive CCaMK form spontaneous nodules in the absence of bacteria (Tirichine et al., 2006; Hayashi et al., 2010; Madsen et al., 2010). Expression of the kinase alone also leads to spontaneous nodule formation in *ccamk* plant mutants; however, infection is not restored (Gleason et al., 2006; Shimoda et al., 2012; Takeda et al., 2012). Moreover, spontaneous nodulation can also be triggered by expression of a gain-of-function version of CCaMK in a *cyclops* mutant background, with CYCLOPS being a phosphorylation target of CCaMK (Yano et al., 2008). The fact that an autoactive version of CCaMK is able to induce downstream signalling, suggestes that the primary purpose for all upstream symbiotic genes is to activate CCaMK (Gleason et al., 2006; Tirichine et al., 2006; Hayashi et al., 2010; Madsen et al., 2010).

CCaMK forms a complex with CYCLOPS in the nucleus (Yano et al., 2008; Singh et al., 2014). CYCLOPS is both required for RNS and AMS (Messinese et al., 2007; Yano et al., 2008; Horvath et al., 2011; Ovchinnikova et al., 2011). Furthermore, the phosphorylation of CYCLOPS via CCaMK leads to the activation of downstream transcription factors (Singh et al., 2014). Two phosphorylation sites of the CYCLOPS protein are essential for symbiosis, as replacements of S50D and S154D (CYCLOPS-DD) lead to an autoactive version of CYCLOPS that is able to trigger the nodulation process without the symbiont partner (Singh et al., 2014). In combination, CYCLOPS-WT and gain-of-function CCaMKT265D are able to transactivate the *NODULE INCEPTION (NIN)* promoter in *Nicotiana benthamiana* leaves and *L. japonicus* hairy roots, a gene required for bacterial entry and nodule formation (Schauser et al., 1999; Singh et al., 2014). Moreover, the same effect was achieved by only expressing CYCLOPS-DD, suggesting that the two phosphorylation residues are required for *NIN* activation (Singh et al., 2014).

Furthermore, the CYCLOPS binding site was pinpointed to a *cis*-responsive element *"CYC"* (*CYC-RE*) within the *NIN* promoter (Singh et al., 2014), demonstrating that CYCLOPS confers both DNA-binding and transactivation abilities. Both functional domains of CYCLOPS were further analysed, with the activation domain (AD) mapped to a central part of the protein (aa 267 to 380), while the DNA binding domain (BD) was

delimited to the C-terminal region (aa 364 to 518), harbouring a coiled-coil domain (Singh et al., 2014). A minimal version of CYCLOPS, consisting of only the AD and BD part of the protein (CYC-min, aa 255 to 518), was demonstrated to be sufficient for mimicking CYCLOPS-DD behaviour (Singh et al., 2014). The function of CYCLOPS as a transcriptional activator is dependent on its phosphorylation by CCaMK at the phosphorylation sites S50 and S154, which induces a structural change, releasing CYCLOPS from auto-inhibition of the activation domain and promoting its potential for DNA binding capability (Singh et al., 2014).

5.4 The symbiotic transcriptional network

Furthermore, several nuclear-associated transcriptional regulators, including NODULATION SIGNALLING PATHWAY 1 and 2 (NSP1 and NSP2) are required for the expression of downstream genes and initation of nodule development (Kaló et al., 2005; Smit et al., 2005; Heckmann et al., 2006; Hirsch and Oldroyd, 2009). Both proteins belong to the family of GRAS transcription factors that are conserved throughout the plant kingdom and have diverse roles in plant development (Bolle, 2004). A function during mycorrhorzial colonisation was only demonstrated for NSP2 (Liu et al., 2011).

Moreover, three Ethylene response factors (ERF) required for nodulation (ERN1, ERN2 and ERN3) have been shown to associate with the *ENOD11* promoter, an early nodulin gene encoding a repetitive proline-rich protein (Journet et al., 2001; Charron et al., 2004; Andriankaja et al., 2007; Fournier et al., 2015).

Interestingly, ERN1 and ERN2 function as transcriptional activators, while ERN3 acts as a repressor on the identified *cis* binding element (NF box) on the *ENOD11* promoter (Andriankaja et al., 2007). Expression profiles and cross-complementation studies suggested a functional reduncancy (Cerri et al., 2012). This was recently corroborated by *ern2* single and *ern1ern2* double mutant phenotypic characterisation. ERN1 and ERN2 are acting together to regulate epidermal infection, but ERN1 seems to be the major factor orchestrating infection in the cortex (Cerri et al., 2016).

NSP1 and NSP2 form a complex, which upregulates symbiosis-related marker-genes such as *ENOD11* or *NIN*. Only NSP1 demonstrated DNA-binding properties to the target promoters (Murakami et al., 2006; Hirsch et al., 2009). NSP1 binds to *NIN* (-893 to -13 bp) on a *cis* regulatory element containing an AATTT motif (Hirsch et al., 2009). The heterodimeric complex of NSP1 and NSP2 induces the expression of *NIN* and *ERN1* (Marsh et al., 2007; Middleton et al., 2007; Cerri et al., 2012).

5.5 NIN - a transcription factor

In 1999, the first gene involved in RNS was identified, a putative transcription factor named NODULE INCEPTION (NIN) (Schauser et al., 1999). A transposon-inactivated *nin* was shown to be responsible for a defect in nodulation, while "revertants", which had lost the transposon, nodulated normally (Schauser et al., 1999).

NIN is involved in bacterial entry, cortical cell division and nodule formation (Schauser et al., 1999; Borisov et al., 2003; Schauser et al., 2005). *nin* mutants show excessive root hair curling in response to NF treatment, indicating that the NF signal is recognized, but further signal trandcution is arrested (Schauser et al., 1999; Borisov et al., 2003; Marsh et al., 2007). Recently, a role of *NIN* in remodelling the infection pocket was demonstrated (Fournier et al., 2015).

The *NIN* cDNA sequence consists of 2,634 bp with a 3' untranslated region of 140 bp, coding for a protein of 878 aa (Schauser et al., 1999). The nucleotide identity is around 60% between *Lotus japonicus* and *Pisum sativum NIN* (*LjNIN* and *PsNIN*, respectively) and the intron/exon structure is conserved (Borisov et al., 2003).

The open reading frame of *PsNIN* encodes a protein with 922 aa in comparison to 878 aa in *LjNIN* (Borisov et al., 2003). The transcription of *NIN* was upregulated upon rhizobia treatment after one day (8 fold) and at 10 days (Marsh et al., 2007; Yano et al., 2008), suggesting a two-phase *NIN* response. The expression of *PsNIN* was localized in the meristematic cells (zone I) and infection cells (zone II), whereas in the fixation zone (zone III) no expression was detected (Borisov et al., 2003). In Lotus *NIN* expression was shown to be dependent on *NFR1*, *NFR5* and *SYMRK* (Radutoiu et al., 2003), furthermore calcium spiking is normal in *nin* mutant (Miwa et al., 2006). Overexpression

of *SYMRK*, *NFR1*, *NFR5* and gain-of-function versions of *CCaMK* or *CYCLOPS* triggered spontaneous *NIN* expression in the plant (Ried et al., 2014; Singh et al., 2014).

5.6 Transcriptional targets of NIN

Several genes have been identified in the past years, which are dependent on *NIN* expression and respond in a positive or negative regulatory way. 19 putative target genes of NIN were identified in the transcriptome database and 9 candidates were verified by real time (RT)-PCR (Soyano et al., 2013).

One transcriptional target is pectate lyase (NPL), a gene involved in infection thread formation. For the formation of infection treads, cell walls are degraded by a pectate lyase activity to break down polygalacturonic acid and pectin (methyl esterified PGA) via a beta-elimination reaction (Xie et al., 2012). Direct regulation of NPL was demonstrated, as NIN´s DNA binding domain was able to bind to the *NPL* promoter (Xie et al., 2012).

Other downstream regulation genes are *NF-YA* and *NF-YB*, which belong to a hetero-trimeric complex with NF-YC (Soyano et al., 2013). NIN directly bound to the promoters of *NF-YA1* and *NF-YB1* and upregulated their transcription (Soyano et al., 2013). The heterodimeric NF-Y complex has been described to trigger the entry into the cell cycle division (Laloum et al., 2013; Laloum et al., 2014).

Soyano and collegues could show that overexpression of *NIN* induces *NF-YA* and *NF-YB* expression and in turn induces initiation of lateral root organs resembling nodule-like structures (Soyano et al., 2013).

Although the nitrogen fixing bacteria inside a nodule are beneficial for the plant, a negative feedback loop exists that prevents hypernodulation, as the bacteria require large amounts of photosynthate (Reid et al., 2011). The autoregulation of nodulation AON is dependent on two signals being exchanged, one coming from the root and the other from the shoot of the plant (Mortier et al., 2012). Furthermore, CLAVATA3/ENDOSPERM SURROUNDING REGION (CLE)-related peptides, CLE ROOT SIGNAL (CLE-RS1) and CLE-RS2, are transcriptional targets of NIN (Soyano et al., 2014).

These factors are assumed to function as root-derived signals that are perceived by the shoot acting AON receptor, the HYPERNODULATION ABERRANT ROOT FORMATION (HAR1) (Wopereis et al., 2000; Okamoto et al., 2009; Soyano et al., 2014; Kucukoglu and Nilsson, 2015; Nishida et al., 2016). The number of nodules per plant is strictly regulated via an AON pathway (Magori and Kawaguchi, 2009).

A negative regulatory role of NIN was demonstrated in the *daphne* mutant, which harbours a chromosomal translocation 7 kb upstream of *NIN*s transcriptional start site (Yoro et al., 2014). *daphne* shows an increased level of infection thread formation, while nodule formation is inhibited (Yoro et al., 2014). Interestingly, hyperinfection was suppressed by the overexpression of *NIN* (Yoro et al., 2014). Downstream of CCaMK, the autoactivation of Lotus Histidine Kinase (LHK1), encoding a cytokine receptor protein, also triggers spontaneous nodule formation (*snf2*) (Murray et al., 2007; Tirichine et al., 2007). Here, a single nucleotide exchange, leading to the replacemnet of leucine 266 to phenylalanine (L266F) in the receptor, was sufficient to continuously trigger cytokinin signalling to induce nodule formation. Strikingly, the mutation in LHK1 leads to a local activation of cell division rather than prolific cell division along the entire root (Murray et al., 2007). As the *daphne snf2* double mutant formed no nodules, the phenotype of *daphne* is likely caused downstream of the cytokinin signalling (Yoro et al., 2014).

5.7 NIN domain structure

Six conserved modular domains were identified by alignment of the NIN protein of legumes and NIN-like proteins from different land plants (Figure 2) (Schauser et al., 2005). Domains I to III are NIN family specific domains with unknown function. A transmembrane domain is predicted for domain IV, which is inconsistent with its localisation in the nucleus *in planta* (Yokota et al., 2010; Soyano et al., 2013). Domains V and VI are the RWP-RK, involved in DNA binding and the PB1 domain, which functions in protein heterodimerization, respectively (Schauser et al., 2005). The secondary structure predicted for the RWP-RK domain is a helix-turn-helix and a helical leucine zipper (Schauser et al., 2005).

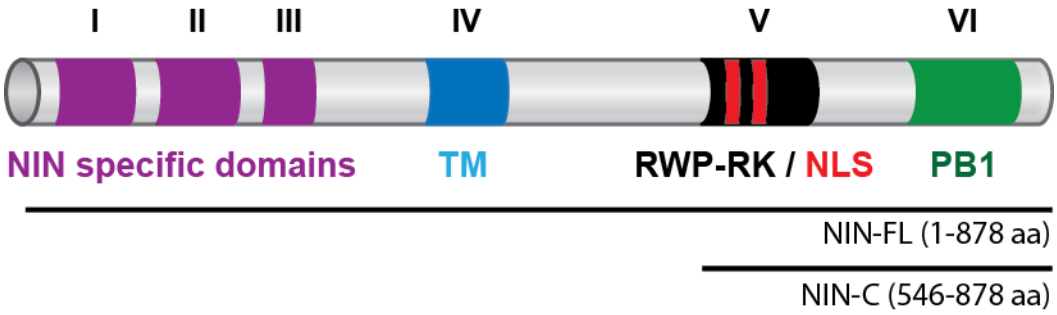

Figure 2: Domain structure of NIN.

Domains I to III are NIN family specific domains with unknown function. A transmembrane region is predicted for domain IV. NIN harbours two NLS within its conserved RWP-RK domain (V), which confers DNA binding capability. A protein-protein interaction domain is proposed for domain VI due to its homology to a PB1 domain. The full-length NIN protein consists of 878 aa and has a molecular weight of 97 kDa. NIN-C (546-878 aa) is a truncated version of NIN only harbouring both the RWP-RK domain (571-621 aa) and PB1 domain (780-863 aa).

5.8 NIN like proteins (NLPs)

Due to the conserved DNA binding domain (RWP-RK), NIN belongs to the protein family of NIN-like proteins (NLPs), which are required in nitrate signalling (Schauser et al., 2005; Castaings et al., 2009; Suzuki et al., 2013). Strikingly, NLPs feature an additional functional domain, the GAF domain, which was lost in an ancestor NLP turning into the symbiotic *NIN* gene (Schauser et al., 2005).

This 210 bp deletion in the N-terminal part of the gene probably preceded the recruitment of NIN for its special function in RNS (Schauser et al., 2005). *NIN* lost its responsiveness towards nitrate, which is crucial for its role in nodule development, as nodules are only formed under N-deficient conditions (Streeter and Wong, 1988; Schauser et al., 2005).

Blast searches of a *L. japonicus* genomic database identified 4 NLPs, with NLP1 being the closest homolog to NIN (Suzuki et al., 2013). A 43 bp sequence of a nitrate responsive *cis*-element (NRE), which is conserved in nitrate inducible genes, was bound by the RWP-RK domain of NLPs and NIN (Konishi and Yanagisawa, 2013). In particular the activity of NLP6 was examined, where the N-terminal part of NLP6 is post-translationally actived by nitrate signals and in turn can interact with the NRE (Konishi and Yanagisawa, 2013).

Another well characterized NLP is NLP7 from *Arabidopsis*, which is regulated by nitrate via a nuclear retention mechanism (Marchive et al., 2013). NLP7 is transported actively from the nucleus to the cytoplasm via exportin, which is consistent with the presence of a predicted leucine-rich nuclear export signal (Marchive et al., 2013). A ChIP-chip approach identified 851 targets of NLP7, which were mainly involved in N-metabolism and related metabolic pathways, including hormone signalling (Marchive et al., 2013). Interestingly, NLP7 was found to be both an activator and a repressor (Marchive et al., 2013). Nitrate plays an active role in converting NLPs from an inactive to an active form.

Despite the high homology between NIN and NLPs, in a cross-species transformation the *pNIN-OsNLP1* could not rescue the infection phenotype of the *nin-1* mutant (Yokota et al., 2010). In contrast, expression of the rice homologs of NSP1 and NSP2 could fully complement the Lotus mutant phenotypes, restoring infection and nodule organogenesis (Yokota et al., 2010).

6 Aim of the thesis

Understanding the molecular crosstalk and the interplay between the symbiotic players might allow us to transfer this symbiosis to non-legumes with the goal of reducing fertilizer use in agriculture.

NIN is a nuclear-localised transcription factor that plays an essential role in the root nodule signalling pathway and is required for both infection and organogenesis (Schauser et al., 1999). Despite beeing the first symbiosis transcription factor identified in 1999, the mechanistic action of the NIN protein remains poorly understood.

In the past, *NIN* was primarily used as a genetic marker to study nodulation during symbiotic signalling, as it is rapidly induced after inoculation with rhizobia. However, the function of the NIN protein during nodulation at the molecular level was not well understood.

My project aimed to characterise NIN at the molecular level and to test whether NIN is part of the CCaMK/CYCLOPS complex. To do so, I made use of not only the full-length protein, but also a truncated version referred to hereafter as "NIN-C" comprising two conserved C-terminal domains, namely RWP-RK and PB1. Both were previously described as DNA-binding and protein-protein interacting domains respectively (Schauser et al., 2005). I analysed them in order to better understand how NIN functions as a transcription factor.

The main goals of the thesis were to I) confirm the protein-protein interaction between NIN and the CCaMK/CYCLOPS complex, II) understand the molecular mechanism of this interaction and III) to elucidate the role of NIN in nodulation.

7 Results

7.1 NIN accumulates in the nucleus

NIN harbours a predicted transmembrane domain and two nuclear localisation signals (NLS) (Figure 2), indicating that it could localise to a membrane or be targeted to the nucleus. Due to the predicted domains, a model was proposed were NIN is located at either the plasma or the nuclear membrane and then undergoes a cleavage process in which the NIN-C part is released and moves to the nucleus (Schauser et al., 1999; Borisov et al., 2003).

In order to characterise the subcellular localisation of NIN, I generated YFP-tagged NIN translational fusions (C-terminal fusion tags) and transiently expressed them under the control of the constitutive cauliflower mosaic virus 35S promoter in *N. benthamiana* leaves. Free YFP was observed in both the cytosol and the nucleus (Figure 3A), in line with the absence of a NLS. A YFP signal for both the full-length NIN and NIN-C was detected in the nucleus (Figure 3B and C), indicating that the NLS is functional. However, the predicted transmembrane domain did not localise NIN to either the plasma or nuclear membrane.

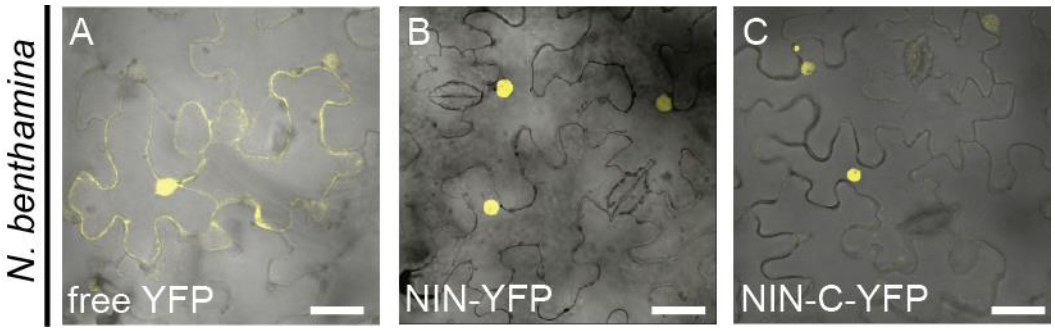

Figure 3: Localisation of NIN protein *in planta.*

(A) Free YFP is expressed in the cytosol and the nucleus. NIN-YFP (B) and NIN-C-YFP (C) localised to the nucleus in *N. bentamiana* leaf cells. The YFP signal is shown in yellow in an overlay image of the bright field with the micrograph using an YFP filter. *N. benthamiana* leaf epidermis cells were transformed by *Agrobacterium*-mediated transformation and all proteins were transiently expressed under the *35S* promoter. Protein expression was examined 3 days post infiltration. Bar: 50 μm.

7.2 NIN interacts with CYCLOPS in the nucleus

CYCLOPS and CCaMK form a tight complex in the nucleus that activates the transcription of *NIN* upon perception of calcium signals. As NIN also localized within the nuclear compartment, we asked whether NIN could be part of this complex. To test this hypothesis, three different protein-protein interaction techniques were performed.

7.2.1 Yeast two-hybrid analysis

An deletion series of the CYCLOPS protein was available (Yano et al., 2008) and was used in yeast two-hybrid (Y2H) assays to further investigate the interaction between CYCLOPS and NIN. This technique is based on the reconstitution of the split transcription factor Gal4, which is then able to activate a downstream reporter gene, by binding to the upstream activated sequence (UAS). Thus, the DNA binding domain (BD) of GAL4 is fused to one protein (bait) while the activation domain (AD) is fused to the other protein (prey), in order to test for protein-protein interaction. In this study the yeast strain AH109 was used, which contains the reporter gene *HIS3*, required for the biosynthesis of histidine. Yeast is able to grow on minimal agar plates lacking the amino acid if the two proteins tested interact. In addition two markers, LEU2 and TRP, are present on the plasmids for selecting positive transformants.

Using NIN as bait and CYCLOPS as prey, we observed growth on selection media, indicating an interaction (Figure 4). The co-expression of N-terminal CYCLOPS (1-159 aa) fused to BD and NIN fused to the GAL4 activation domain did not show any yeast growth on selection media, indicating that the N-terminal part of CYCLOPS is not sufficient for the interaction with NIN in yeast (Figure 4). For the positive control, the combination of CYCLOPS-AD and CCaMK-BD demonstrated yeast growth on minimal agar in all dilutions (Figure 4). The yeast two-hybrid analysis indicates an interaction between NIN and CYCLOPS.

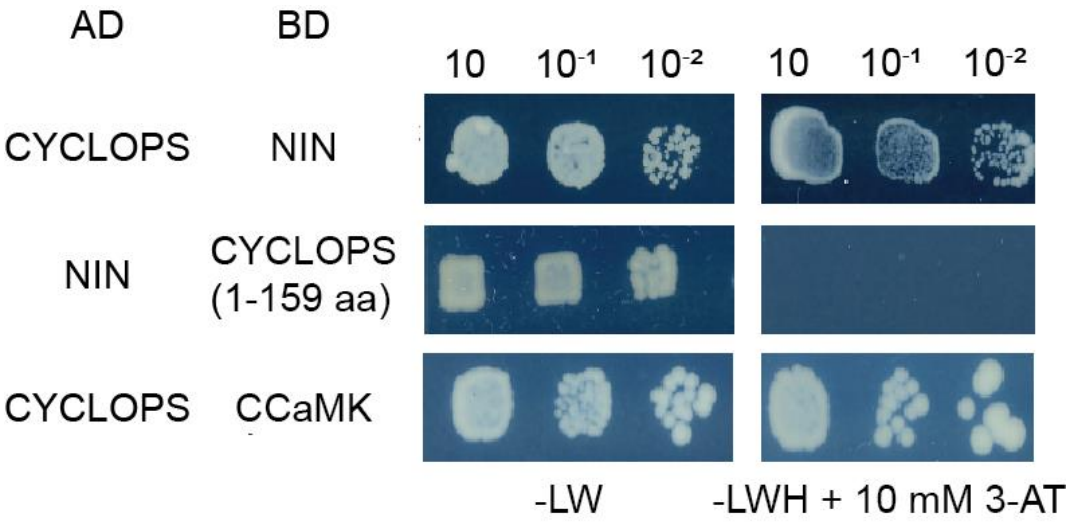

Figure 4: Interaction of NIN and CYCLOPS in yeast

Yeast two-hybrid GAL4 based assay was performed for the identification of interaction domains for NIN and CYCLOPS. Positive interaction was detected between NIN and CYCLOPS, while CYCLOPS (aa 1-159) did not interact with NIN. CYCLOPS and CCAMK were used as positive control. Interaction assays were performed in the yeast strain AH109 cotransformed with prey (AD) and bait (BD) vectors containing NIN, CYCLOPS variants and CCaMK. The cotransformants and interacting partners were analysed on synthetic dropout nutrient medium lacking leucine and tryptophan (-LW) and lacking leucine, tryptophan and histidine (-LWH) plus 10 mM 3-AT respectively. The assay was performed with undiluted, 10^{-1} and 10^{-2} diluted suspension of co-transformation with 10 µl spotted on the plate.

7.2.2 Bimolecular fluorescence complementation (BIFC)

Second, a targeted split-YFP experimental approach was performed to test the interaction of NIN with the CCaMK/CYCLOPS complex. This technique enables *in vivo* visualization of protein-protein interaction. Each potential interactor is fused to one half of the YFP protein, which by itself is non-fluorescent. If our candidates are in close proximity, an active YFP is reconstituted and a fluorescent signal should be visible upon excitation. Candidate proteins were either fused to the N-terminal half or C-terminal half of YFP and were transiently expressed in *N. benthamiana* leaves using *A. tumefaciens* transformation.

When NIN-YFP_N was co-expressed with YFP_C-CYCLOPS-WT, a nuclear YFP signal was observed (Figure 5A), suggesting protein-protein interaction. As CCaMK interacts with different phosphosite variants of CYCLOPS (Singh et al., 2014), we wanted to test if this is also the case for NIN.

Hence, NIN-YFP_N was co-expressed with two CYCLOPS phosphosite variants, YFP_C-CYCLOPS-AA and YFP_C-CYCLOPS-DD. Both CYCLOPS variants, when co-expressed with NIN, led to a fluorescent signal in the nucleus, demonstrating that they both interact with NIN *in planta* (Figure 5B and C). The interaction between CCaMK-YFP_N and YFP_C-CYCLOPS was included as positive control in this assay (Figure 5D). Interestingly, no fluorescence was observed when NIN-YFP_N and CCaMK-YFP_C where co-expressed (Figure 5E), indicating no direct interaction with CCaMK within this approach. However, in the presence of CYCLOPS-DD, a positive YFP signal for NIN-YFP_N and CCaMK-YFP_C was detected in the nucleus, strongly suggesting the formation of a trimeric complex (Figure 5F).

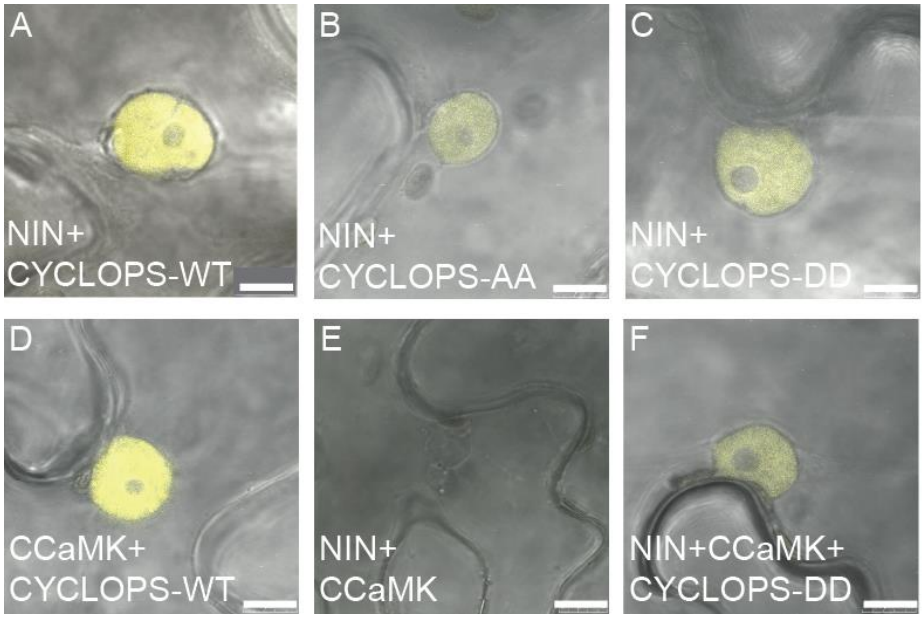

Figure 5: NIN interacts with different variants of CYCLOPS in *N. benthamiana* leaf cells.

Analysis of the interaction between NIN and the CCaMK/CYCLOPS complex by bimolecular fluorescence complementation in *N. benthamiana* leaf cells. Positive interaction was visualised in the nucleus between NIN and CYCLOPS-WT (A) as well as with CYCLOPS-AA (B) and with CYCLOPS-DD (C). As positive control, the interaction between CCaMK and CYCLOPS showed an YFP signal in the nucleus (D). No YFP fluorescence was detected for the combination of NIN and CCaMK (E), however, in the presence of CYCLOPS-DD, an interaction between NIN and CCaMK was detected in the nucleus (F). Candidate proteins were fused to the N- or C-terminal part of YFP (YFPn attached to a c-Myc tag or YFPc attached to a HA tag) and driven by the cauliflower mosaic virus *35S* promoter. Interaction is indicated by a yellow YFP signal and was visualized 60 hpi. Pictures show an overlay of bright field with micrographs recorded with an YFP filter. Bars: 10 μm

The BiFC technique is often subject to creating false positives, inducing a random association of the two separated fluorophore halves (Kerppola, 2008). Therefore, it is necessary to include suitable controls such as non-interacting proteins. In the performed experiments no interaction was observed between NIN and CCaMK. Still, the lack of interaction could be due to various reasons. To ensure that this result is not a false negative, western blot analyses were performed to verify that all proteins are correctly expressed, at comparable level. The expression level of all proteins was detected with an immunoblot analysis to verify that the lack of fluorescence was not due to altered expression of the proteins (data not shown).

7.2.3 FLIM–FRET approach

To validate the previous results and to further quantify the observed interaction between NIN and CYCLOPS variants, Fluorescence-Lifetime-Imaging-Microscopy (FLIM) was performed in *N. benthamiana* epidermal leaf cells.

As this technique was new in the lab, I first established FLIM as a reliable technique for protein-protein interaction studies using a Leica SP5 confocal microscope and applicable software from Becker and Hickl.

FLIM is based on the lifetime change of a fluorescent protein due to Förster Resonance Energy Transfer (FRET). After excitation by laser light and transition into the first excited state every fluorescent protein has a molecule specific fluorecence lifetime before it sends out a fluorescent photon and transitions back to the ground state. If two molecules called donor and acceptor are in close proximity (below 10 nm) the energy of the first excited state can be transferred from the donor to the acceptor. This energy transfer results in a decreased lifetime of the donor. By analysing either the lifetime change or the decrease of the donor fluorescence and increase of the acceptor fluorescence an energy transfer rate can be calculated.

In this work TSapphire (TS) was used as the donor and mOrange (mO) as the acceptor molecule. This FLIM-FRET pair was described to be efficient and functional in plant cells (Bayle et al., 2008) and it allows to directly visualise the proximity of both molecules.

In this FLIM-FRET set-up the fluorescence lifetime of the donor was used as probe. A repetitive pulsing 80 mHz Multi-Photon (MP) laser was tuned to 800 nm and used to excite the donor fluorophore TSapphire. The excited state of the donor fluorophore was analysed by a time correlated single photon counting FLIM measurement for a number of 20 scanning cycles (5 sec/cycle), to acquire a suitable photon count rate in our set-up.

First, the functional set-up and the resulted measurements of this technique had to be verified. So, the lifetime of free TSapphire co-expressed with free mOrange was measured to estimate the lifetime for non-interacting protein partners. For mimicking the possible interaction of two proteins we made use of a chimeric construct that separates TSapphire and mOrange by a 16 aa linker (Bayle et al., 2008). To analyse the fluorescent lifetime changes of the donor TSapphire in the presence of the acceptor mOrange, *N. benthamia* leaves were infiltrated with equimolar amounts of p35S::TSapphire-nos and p35S::mOrange-nos or with p35S::TSapphire-mOrange-nos, and all proteins were transiently expressed in the plant. The TSapphire fluorophore lifetime is coded in pseudo colours ranging from blue (2.6 nanoseconds) to red (1.5 nanoseconds), as depicted in the representative lifetime images of each measured combination (Figure 6).

A lifetime was successfully and consistently detected with 2.49±0.09 ns (Figure 6) for TSapphire when co-expressed with free mOrange, showing that the FLIM measurements were adequate and within the expected lifetime range. As also expected, the lifetime measured for the TSapphire and mOrange fusion construct resulted in a significant shift to 2.17±0.11 ns, amounting for an energy transfer of 13% (Figure 6;

Table **1**).

To confirm that intermolecular interactions are appropriately detected with our FLIM-FRET set-up, the donor and acceptor were fused to the known interaction pair CCaMK and CYCLOPS (Yano et al., 2008; Singh et al., 2014). The coexpression of CCaMK and CYCLOPS resulted in a lifetime shift of the donor from 2.35±0.09 ns for TS-CYCLOPS in combination with free mOrange to 2.06±0.10 ns for TS-CYCLOPS in the presence of CCaMK-mOrange (Figure 6). This amounted for a FLIM-FRET efficiency of around 12% (

Table 1).

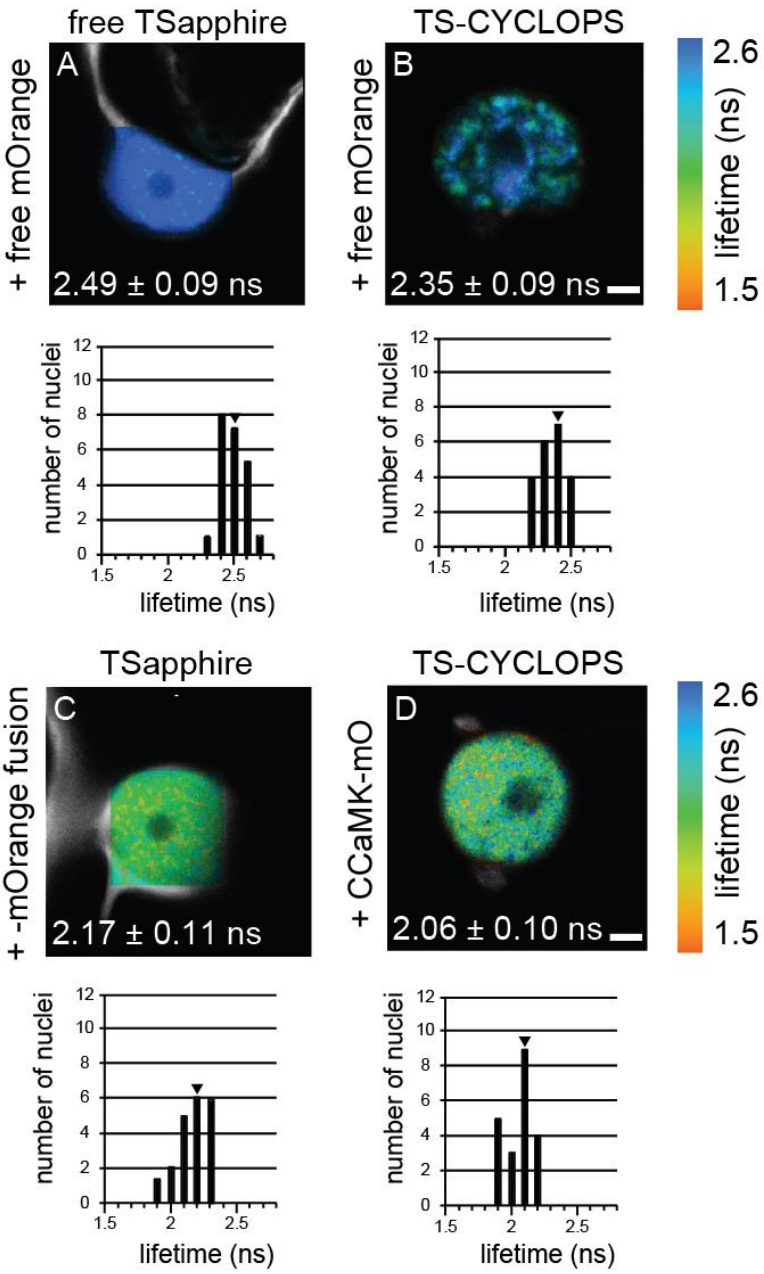

Figure 6: FRET FLIM analysis of control combinations in *N.benthamiana* cells.

Lifetime images of TSapphire in a cell co-expressing either free TSapphire and free mOrange (A) or TSapphire-mOrange fusion (C). Fluorescent lifetimes were significantly reduced for the chimeric contruct, mimicking interaction (t-test: $p=3.76^{-12}$). Lifetime images of TSapphire in a cell co-expressing either TS-CYCLOPS and free mOrange (B) or TS-CYCLOPS and CCaMK-mO (D). Fluorescent lifetimes were significantly reduced in the presence of CCaMK-mOrange, indicating interaction (t-test: $p=5.63^{-12}$). In a colour code ranging from blue (2.6 ns) to red (1.5 ns) representative lifetime images show the analysed fluorescent lifetime for one nucleus per combination. Below the image, histograms illustrate the distribution of all measured lifetimes of TSapphire in the nucleus in context of the combination. Arrowheads point to the lifetime of the depicted nuclei. Insets show mean value and standard deviation. Measurements were performed in *N.benthamiana* leaf cells 60 hours post infiltration. TS: TSapphire; mO: mOrange; Bars: 2 µm

For the paper Singh et al., I performed FLIM-FRET analysis for further characterisation of the CCaMK/CYCLOPS complex. Then, I could show that the complex formation takes place independent of the phosphorylation status of CYCLOPS, as all analysed CYCLOPS variants (CYCLOPS-WT, CYCLOPS-AA and CYCLOPS-DD) showed interaction with CCaMK in FLIM-FRET experiments. Furthermore, the dimerization properties of CYCLOPS variants were tested, with all combinations resulting in interactions, and interestingly with CYCLOPS-DD showing a stronger association compared to CYCLOPS-AA and CYCLOPS-WT. These results were published in Figure1 (Singh et al., 2014).

To quantify the interaction of CYCLOPS and NIN, they were fused to either TSapphire at the N-terminus or to mOrange at the C-terminus of the proteins. Expression of all proteins was driven by the *35S* promoter. The averaged mean lifetime was measured for TS-CYCLOPS-WT/AA/DD in the presence of free mOrange and was found to be 2.33 ± 0.08 ns, 2.32 ± 0.08 ns and 2.32 ± 0.05 ns, respectively, in four independent experiments (Figure 7). These measurements were taken as the control, and used as reference values for non-interacting proteins. To examine the changes in lifetime in the presence of a potential interactor, TS-CYCLOPS-WT/AA/DD and NIN-mOrange (NIN-mO) were co-expressed in *N. bethamiana* leaf cells. In comparison the average mean lifetime for TS-CYCLOPS-WT/AA/DD in the presence of NIN-mO resulted in a significant shift in the lifetime profile of the donor, in detail to 2.08 ns ± 0.09 ns, 2.12 ± 0.07 ns and 2.06 ns ± 0.09 ns, respectively (Figure 7). The overall FRET-FLIM efficiency for the energy transfer was 11%, 9% and 11 % respectively (**Table 1**).

In conclusion, FLIM-FRET analysis confirmed the interaction between NIN and CYCLOPS variants.

Taken together, the results of the BiFC, FRET-FLIM and Yeast-two hybrid experiments strongly corroborate that NIN interacts with CYCLOPS.

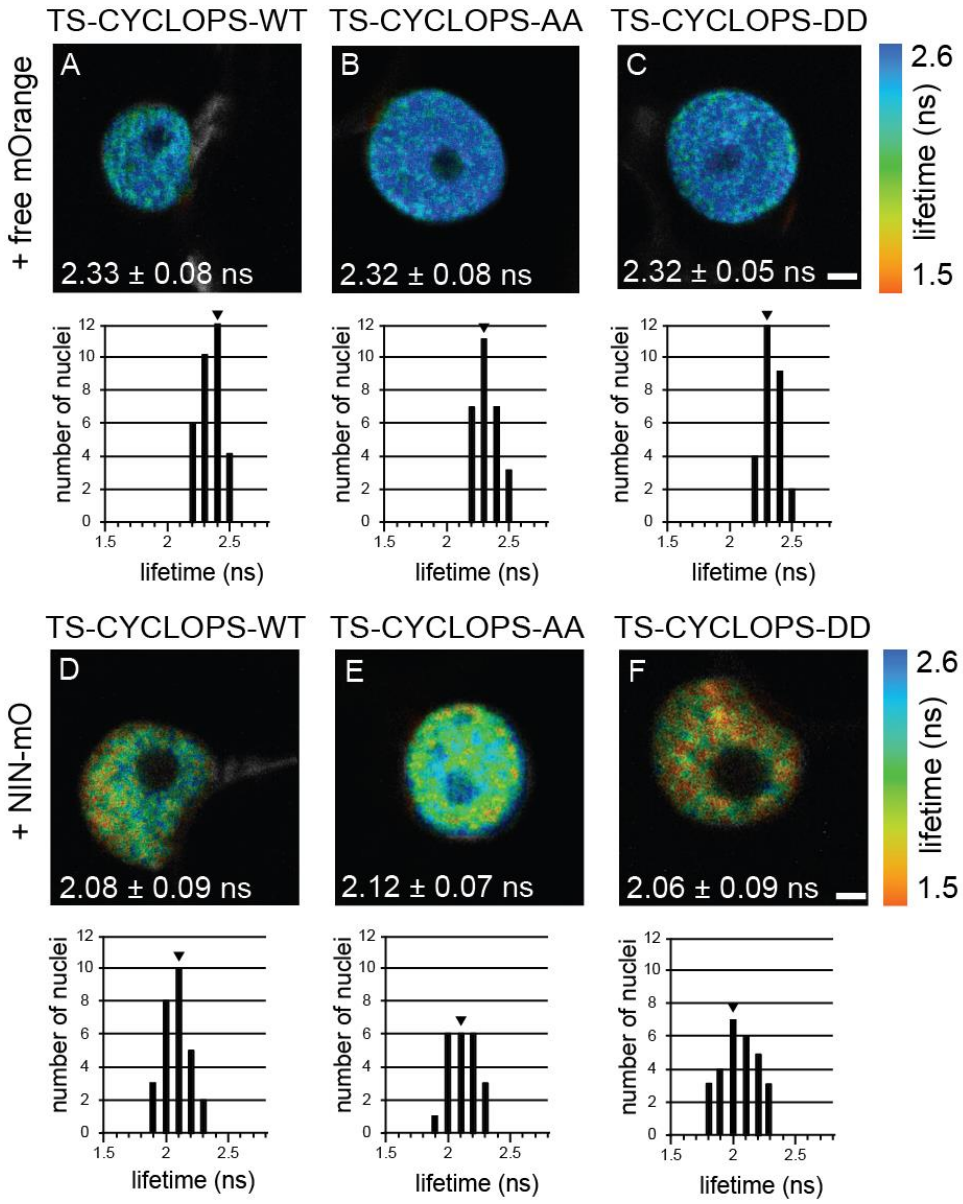

Figure 7: FLIM-FRET analysis confirms the interaction between NIN and CYCLOPS variants

(A-C) For control measurements, TSapphire-CYCLOPS and phospho-site mutants were co-expressed with free mOrange, and the fluorescent lifetime of TSapphire-CYCLOPS variants was measured as reference for non interacting proteins with no lifetime difference (ANOVA: $F_{2,85}$=0.195; p=0.823). (D-E) A significant reduction in lifetime of TS-CYCLOPS-WT/-AA/-DD was detected when co-expressed with NIN-mO, suggesting an interaction of CYCLOPS phosphorilation-site mutants and NIN in the nucleus (t-test: $p=1.894^{-13}$; $p= 7.457^{-9}$, $p=2.626^{-10}$) without any difference in lifetime for the variants (ANOVA: $F_{2,74}$=0.76; p=0.471). FLIM-FRET measurements were performed in *N. benthamina* 60 hours post transformation. In a colour code ranging from blue (2.6 ns) to red (1.5 ns) representative lifetime images show the analysed fluorescent lifetime for one nucleus per combination. The histogram depicts all measurements obtained for individual nuclei; the arrowhead shows the lifetime of the nucleus in the image. For each combination the mean value and standard deviation is indicated below the representative nucleus. TS: TSapphire; mO: mOrange; Bar: 2 µm

expressed proteins	average lifetimes (ns)	n	FRET efficiency (%)
free TSapphire + free mOrange	2.49 ± 0.09	22	
TSapphire-mOrange fusion	2.17 ± 0.11	20	13
TSapphire-CYCLOPS-WT+ free mOrange	2.33 ± 0.08	32	
TSapphire CYCLOPS-WT + CCaMK-mOrange	2.06 ± 0.10	21	12
TSapphire-CYCLOPS-WT+ NIN-mOrange	2.08 ± 0.09	28	11
TSapphire-CYCLOPS-AA+ free mOrange	2.32 ± 0.08	28	
TSapphire-CYCLOPS-AA+ NIN-mOrange	2.12 ± 0.07	22	9
TSapphire-CYCLOPS-DD+ free mOrange	2.32 ± 0.05	27	
TSapphire-CYCLOPS-DD+ NIN-mOrange	2.06 ± 0.09	28	11

Table 1: Average mean lifetimes and calculated FRET-FLIM efficiencies for protein-protein interaction

Fluorescent lifetimes of the donor TSapphire in the presence of the acceptor mOrange fused to either a protein or the free mOrange alone was measured in plants to determine protein-protein interaction between CCaMK, CYCLOPS variants and NIN. For control measurements, CYCLOPS and free mOrange or free fluorophores were used. In addition, corresponding FRET efficiencies were calculated.

7.3 NIN inhibits CYCLOPS-DD mediated *pNIN* activation in N.benthamiana leaf cells

It was previously shown that the expression of CYCLOPS-DD is sufficient to transactivate the *NIN* promoter *in planta* (Singh et al., 2014). Based on the interaction data of NIN with CYCLOPS-WT and with two CYCLOPS phosphorylation-site variants in the nucleus, we asked if this interaction could have an impact on the previously published CYCLOPS-DD transcriptional properties (Singh et al., 2014).

Therefore, we examined if the interaction of NIN and CYCLOPS can modulate the transactivation properties of CYCLOPS-DD for the *NIN* mediated activation in a transient expression assay in *N. benthamiana*. Leaves were co-infiltrated with a reporter construct comprising the *NIN* promoter (-870 bp) fused to the *uidA* gene (*pNIN:GUS*) and the coding squences of the effector proteins NIN-FL and CYCLOPS-DD (Figure 8). All combinations were analysed by both fluorimetric and histochemical GUS assays.

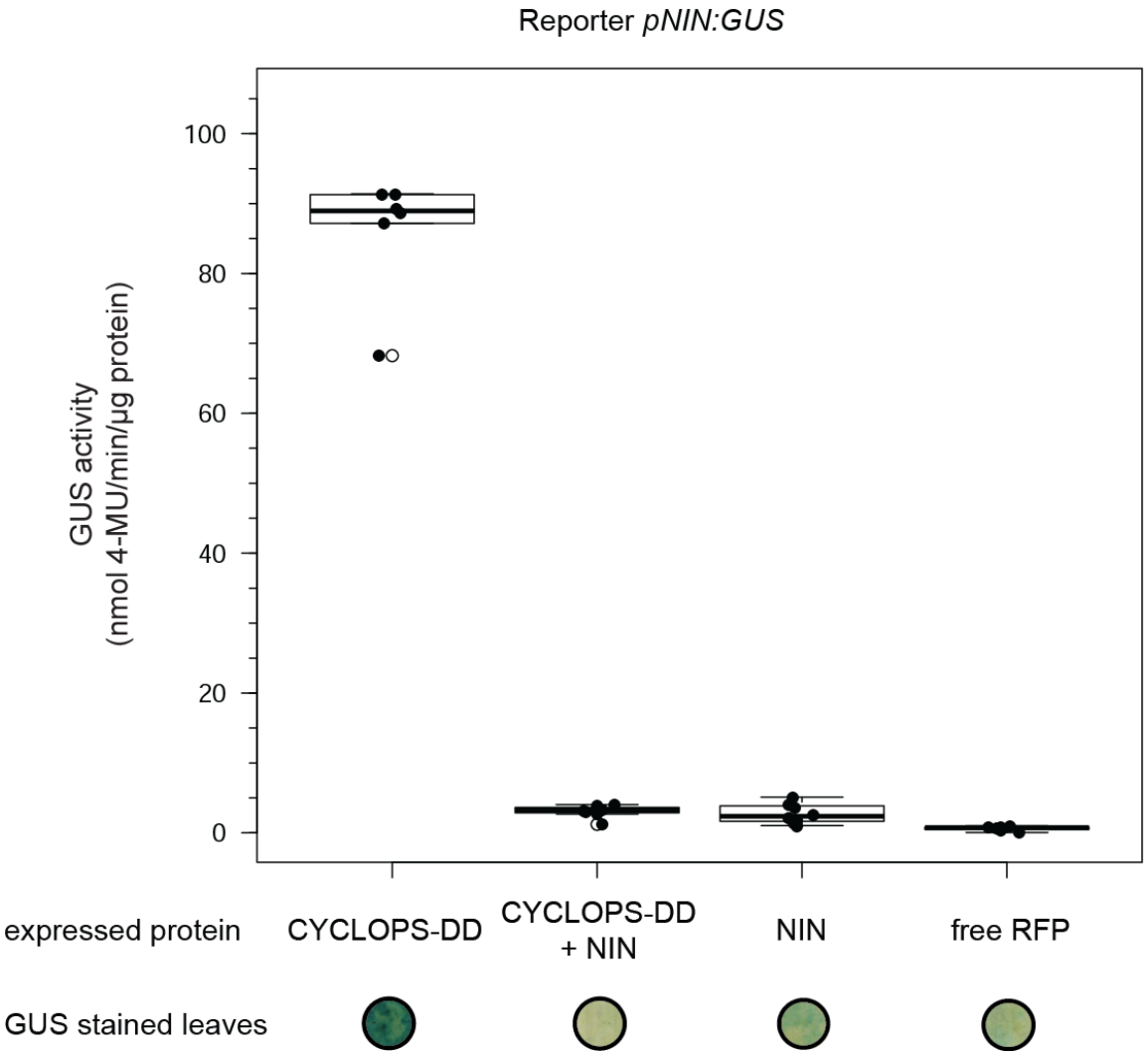

Figure 8: NIN inhibits CYCLOPS-DD mediated activation of the *NIN* promoter in *N. benthamiana*.

The expression of CYCLOPS-DD alone led to a strong transactivation of the *NIN* promoter, while NIN alone showed no transactivation activity of its own transcription. CYCLOPS-DD in combination with NIN showed a reduction in transcriptional activity compared to the CYCLOPS-DD alone. The expression of free RFP functioned as an internal control for a possible autoactivation of the reporter construct. Respective T-DNAs of 35S:*NIN-myc* and/or *35S:HA-CYCLOPS-DD* were co-expressed with a *pNIN:GUS* (-870 bp) reporter. GUS activity was quantified with a histochemical and fluorimetric assay from infiltrated tobacco leave cells 60 hours after infiltration. Mean value and standard deviation were determined from seven biological replicates. The image of one leaf-disc is representative for each combination.

CYCLOPS-DD strongly induced *pNIN:GUS* reporter expression, as already shown previously (Singh et al., 2014). When expressed alone, NIN only induced a faint *GUS* expression, indicating that NIN is not able to transactivate its own promoter (Figure 8). Strikingly, the co-expression of NIN and CYCLOPS-DD resulted in a significant reduction of the *GUS* reporter activity, indicating that CYCLOPS-DD, in presence of NIN is no longer able to transactivate the reporter expression (Figure 8). To confirm that all proteins were correctly expressed, Western blot analysis were performed with respective antibodies (data not shown).

7.4 Development of a Golden Gate cloning system to facilitate co-expression of different genes in *Lotus japonicus*

In order to confirm our results from the *N. benthamiana* leaf assays in *Lotus* roots, it was necessary to co-express the different proteins in a hairy root system. To facilitate the assembly of suitable co-expression constructs we developed a Golden Gate based cloning toolbox, which was successfully published (Binder et al., 2014).

The golden gate system offers the possibility to assemble multiple DNA fragements in a certain order in a single cut-ligation reaction with high efficiency (Engler et al., 2008; Engler et al., 2009; Engler and Marillonnet, 2011). For the assembly of a certain construct, one combines promotors, genes, protein tags, terminators and fluorophore markers. The correct assembly order of different elements is guaranteed through the use of predefinded overhangs that link all elements in a certain order. Furthermore, golden gate cloning exclusively uses type IIS restriction enzymes in the cutting reaction to create sticky overhangs. In our case, we used BsaI, BpiI and Esp3I, which generate a 4 base-pairs overhang upon cleavage. This powerful tool has been used already for other applications, such as the cloning of designer transcription-activator-like effectors (TALEs) (Cermak et al., 2011; Morbitzer et al., 2011; Weber et al., 2011; Sakuma et al., 2013).

Our toolbox of Level I (LI) vectors consisted of a collection of promoters, N-terminal tags, Gene of interest (GOI), C-terminal tags, terminators and a miscellenous module, which are all equipted with BsaI restriction sites at both ends. For the successful assembly of a Level II construct (synthetic gene), you combine six LI vectors and a Level II (LII) backbone. For co-expression of more than one gene you use a Level III (LIII) backbone for the assembly of different LII constructs.

I generated serveral contructs for our toolbox, including a promoter, various fluorescent protein tags for N and C terminal fusion, dummies as placeholders, LI backbones, LII and LIII backbones.

For reliable co-expression of both *NIN* and *CYCLOPS-DD* with equal gene dosage within one root system, both genes were cloned into the same golden gate LIII backbone. To enable efficient assembly in a single cut-ligation reaction, the recognition sites of the Type IIS restriction enzymes BsaI, BpiI and Esp3 were removed from both genes by introduction of silent point mutations. For the LII construct the genomic sequence of NIN was recombined with the *L. japonicus* polyubiquitin promoter (*pUb*) and with the sequence of c-myc (coding for a C-terminal tag).

7.5 NIN inhibits CYCLOPS-DD mediated *pNIN* activation in roots of *L. japonicus*

To verify the results of the transactivation assays from *N. benthamiana* in *L. japonicus,* hairy root transformation was performed in a wild-type line harbouring a stable integrated 2 kb *pNIN:GUS* transcriptional fusion (Radutoiu et al., 2003).

As expected, CYCLOPS-DD induced a strong and specific GUS activity in 90 % of the analysed root systems (Figure 9B;

Table 2). In line with the results obtained in *N. benthamiana* leaf cells previously, no GUS staining was visible in roots transformed with the empty vector control or expressing *pUb:NIN*, demonstrating that NIN, at least when overexpressed, is also not able to activate its own transcription in *Lotus* roots (Figure 9C).

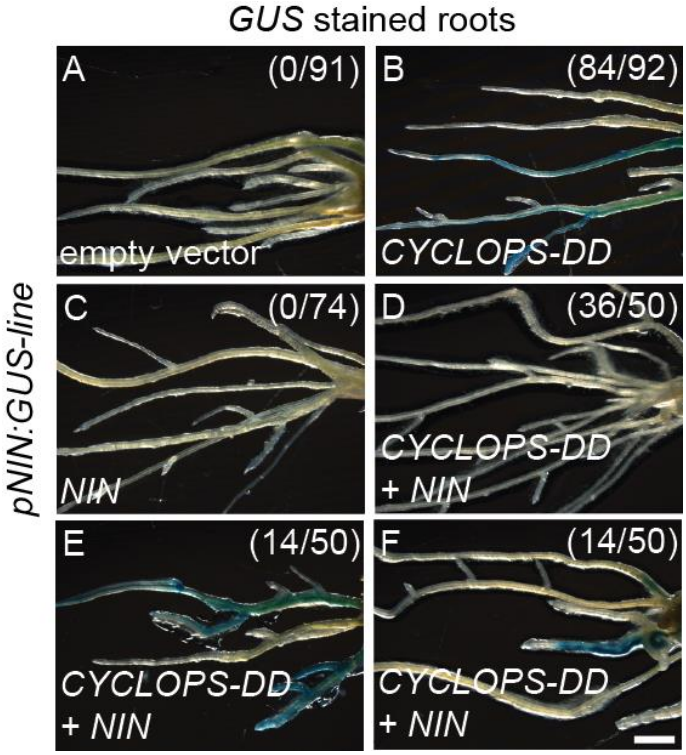

Figure 9: NIN inhibits CYCLOPS-DD mediated activation of the *NIN* promoter in *Lotus* roots.

No GUS activity was observed in transformed roots of the empty vector control (A) and overexpressing *NIN* alone (B). Strong GUS activity was detected in roots expressing *CYCLOPS-DD* alone (C). The co-expression of *CYCLOPS-DD* with *NIN* led to a reduction of GUS staining in approximately 2/3 of the analysed root systems (D). Some blue-stained patterns were observed with the co-expression of *CYCLOPS-DD* and *NIN* in 1/3 of the analysed root systems (E and F). Analysis of GUS induction in a *pNIN:GUS* reporter *Lotus* line, transformed with constructs expressing *pUb:CYCLOPS-DD*, *pUb:NIN* or co-expressing *pUb:NIN* and *pUb:CYCLOPS-DD* (golden gate construct) was performed 4 weeks post transformation. Reporter activity was determined by GUS staining of transformed plants carrying the inserted T-DNA. Transformed plants were identified by expression of GFP. Bar: 2 mm

Interestingly, the co-expression of *CYCLOPS-DD* and *NIN* led to a reduced induction of *pNIN:GUS*. In 72% of the observed transformed root systems, no GUS activity was detected (referred to as GUS-, Figure 9D;

Table 2), while 28 % of the plants showed some GUS staining in different areas along the root (referred to as GUS+; Figure 9E and F;

Table 2). In 28% of transformed plants co-expressing *NIN* and *CYCLOPS-DD* together with the *pNIN:GUS* reporter resulted in a blue stained pattern shown in Figure 9 (E and F). The positive GUS pattern in the co-expression roots resembles the pattern observed

in the *CYCLOPS-DD* activated GUS in roots, indicating that overexpression of *NIN* was not always able to reduce CYCLOPS-DD mediated *pNIN* activation.

contructs	total plants	GUS-	GUS+
empty vector	91	91	0
CYCLOPS-DD	92	8	84
NIN	74	74	0
CYCLOPS-DD+NIN	50	36	14

Table 2: Quantification of GUS expression in roots of *pNIN:GUS* line

The total number of hairy roots are listed with respective number of roots presenting GUS activity (GUS +) or no GUS (GUS-) activity. The data were generated from 5 independent experiments.

Nevertheless, these results are in agreement with the data from *N. benthamiana*. Again, the co-expression led to a reduction of GUS staining compared to the CYCLOPS-DD transactivating activity on the *NIN* promoter. The pictures illustrate the results of the histochemical GUS activity that are representative for each construct (Figure 9), which is consistent with the observations in *N. benthamiana* (Figure 8). In conclusion, the co-expression experiments performed in leaf cells and in roots demonstrate that the transactivation activity of CYCLOPS-DD on the *NIN* promoter is strongly reduced in the presence of NIN.

7.6 NIN inhibits CYCLOPS-DD mediated *pNIN* activation at the previously identified CYCLOPS-responsive element

We showed that NIN and CYCLOPS interact *in planta* and that the presence of NIN reduces the transactivation of the *NIN* promoter by CYCLOPS-DD. *CYC-RE* was demonstrated to be the binding site for CYCLOPS-DD on the *NIN* promoter and sufficient to mimic *NIN* transactivation by CYCLOPS-DD (Singh et al., 2014).

We hypothesized that this could be potentially achieved via the the following mechanisms:

1) As CYCLOPS-DD was demonstrated to interact with the previously identified CYCLOPS-responsive element (*CYC-RE*, 30 bp), it is possible that NIN equally binds to *CYC-RE* in close proximity to the *CYC-box* and in turn blocks CYCLOPS-DD from transactivating the *NIN* promoter.

CYC-RE: CGATTGCCATGTGGCACGCAGAGAGGAGCC with CYC-box in red

2) Alternativly, since co-expression of NIN and CYCLOPS reduced *GUS* activity by inhibiting *pNIN* activation in *Nicotiana* and in *Lotus*, the protein-protein interaction of NIN and CYCLOPS could prevent the binding of CYCLOPS-DD to DNA and thereby inhibit CYCLOPS-DD mediated *pNIN* transactivation.

In order to test if NIN can also reduce CYCLOPS-DD mediated *pNIN* activation at *CYC-RE*, the same set of combinations was performed in transactivation assays as previously described (Figure 8), but using this time *2xCYC-RE:GUS* as a reporter (Figure 10).

The 2x*CYC-RE:GUS* reporter was transactivated when co-infiltrated with CYCLOPS-DD, whereas no *GUS* activity was detected in the presence of NIN alone, as expected (Figure 10). The co-expression of CYCLOPS-DD and NIN led to a reduction in *GUS* activity compared to the CYCLOPS-DD activated *2xCYC-RE* (Figure 10), suggesting that the transactivation activity of *CYC-RE* can be reduced with NIN co-expression by either competitive binding of CYCLOPS-DD and NIN or by no binding of either transcription factor due to their protein-protein interaction capability.

In general the overall GUS activity readout of the *2xCYC-RE:GUS* reporter was weaker for all tested combinations in comparison to the *pNIN:GUS* promoter in previous experiments. Still, the same tendency of reporter expression and repression effect was triggered as with the *pNIN:GUS* reporter (Figure 8). In conclusion, NIN seems to function as a transcriptional repressor of the CYCLOPS-DD activated *NIN* expression *in planta*

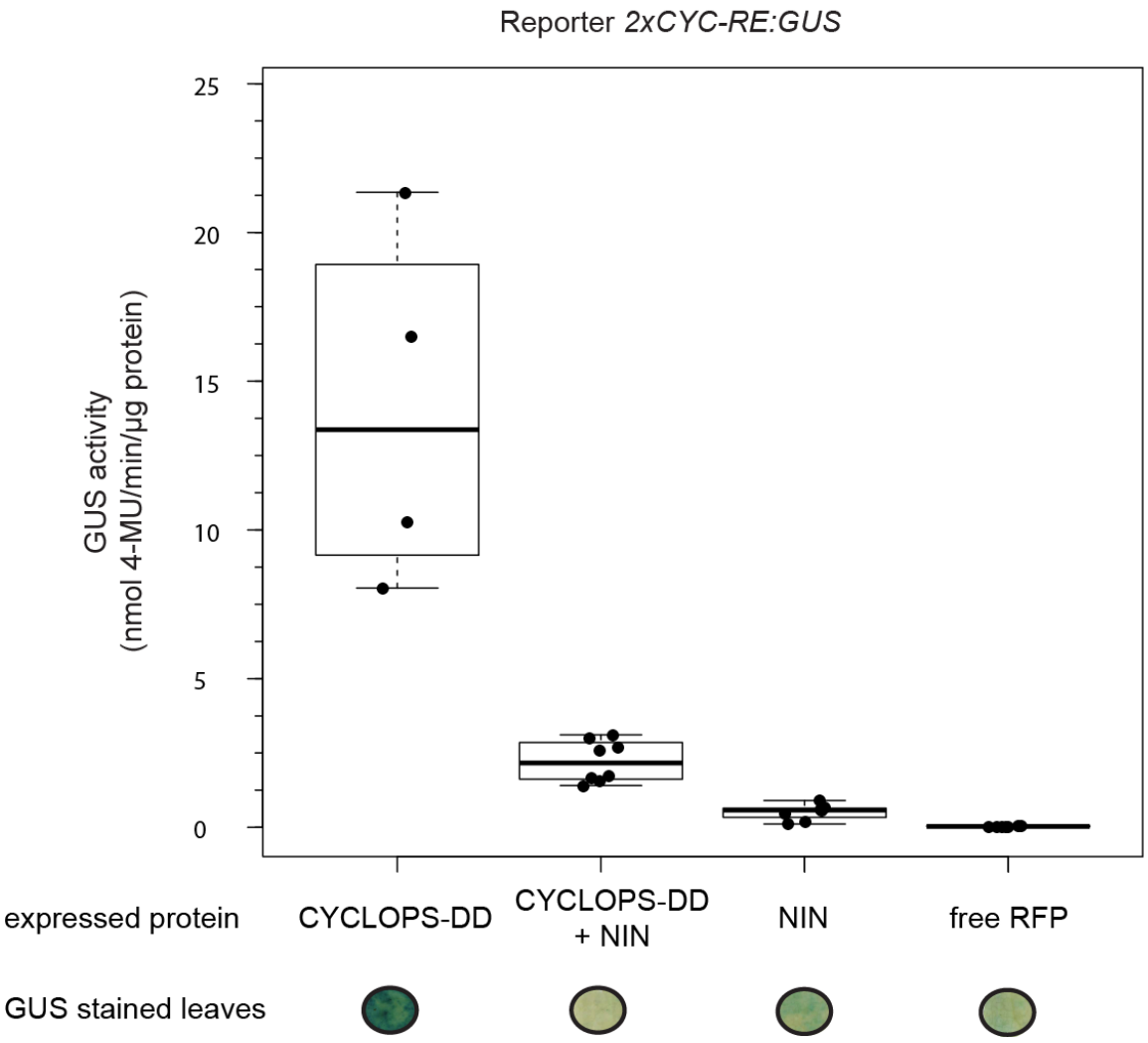

Figure 10: NIN inhibits CYCLOPS-DD transactivation of *2xCYC-RE:GUS* in *N. benthamiana*

Pinpointing the inhibitory site of NIN interfering with the CYCLOPS-DD mediated transactivation to the cis responsive element *CYC-RE*. The expression of *CYCLOPS-DD* alone led to a strong activation of the *2xCYC-RE:GUS*, while NIN alone showed no transactivation activity of *GUS*. Co-expression of both CYCLOPS-DD and NIN led to a reduction in transactivation of GUS expression. Respective T-DNAs of *35S:NIN-myc* and *35S:HA-CYCLOPS-DD* were co-expressed with a *2xCYC-RE:GUS* (-717 to -683 bp) reporter. Free RFP was used as control and showed no transactivation activity of *2xCYC-RE:GUS*.

.

7.7 NIN binds to its own promoter, located in close vicinity to the CYC-box, in a sequence-specific manner

As NIN can reduce the activation of *2xCYC-RE:GUS* expression mediated by CYCLOPS-DD *in planta*, we then tested whether NIN could directly bind to DNA on the *CYC-box* element or in the vicinity of that element. In turn, NIN binding could prevent CYCLOPS-DD from binding to the *CYC-box* or both proteins might simultaneously bind next to each other on the *CYC-RE*.

Electrophoretic mobility shift assays (EMSA) provide a powerful tool to study DNA-protein interactions (Fried, 1989). This method relies on the principle that a DNA-protein complex (bound probe) will have different mobility during electrophoresis than non-bound linear DNA (free probe) (Ryder et al., 2008). These shifts can be visualized by a native acrylamide gel using labeled DNA to form the DNA-protein binding complex (Ryder et al., 2008). Near infrared (IR) fluorescence EMSA offer a safe and sensitive alternative to radioactive EMSA techniques. Short linear DNA fragments that contain consensus binding sequences are used as probe and are 5' end-labeled with IR dye for the binding assay.

NIN binding site (NBS) motifs have already been identified (Soyano et al., 2013; Soyano et al., 2014), so we searched for similar bipartite consensus NBS *in silico* in order to find putative binding sites for NIN on the *NIN* promoter, in particular in the region surrounding the *CYC-RE*. One sequence was found in close proximity upstream of the *CYC-RE* element, which contains both bipartite consensus elements, a T-rich region and an AGG separated by 7 bp (named hereafter *NIN-RE*, Figure 11). Strikingly, another AGG sequence was found within the *CYC-RE* with 7 bp downstream of *CYC-box* element.

To test direct binding of NIN to the identified cis elements, EMSAs were performed using different IR-labeled DNA probes (*NIN-RE, CYC-RE* and *PAL*) (Figure 11). The *PAL* probe was included to distinguish between binding to the palindromic *CYC-box* sequence (highlighted in red) and the present AGG sequence (highlighted in green) within the *CYC-RE* (Figure 11).

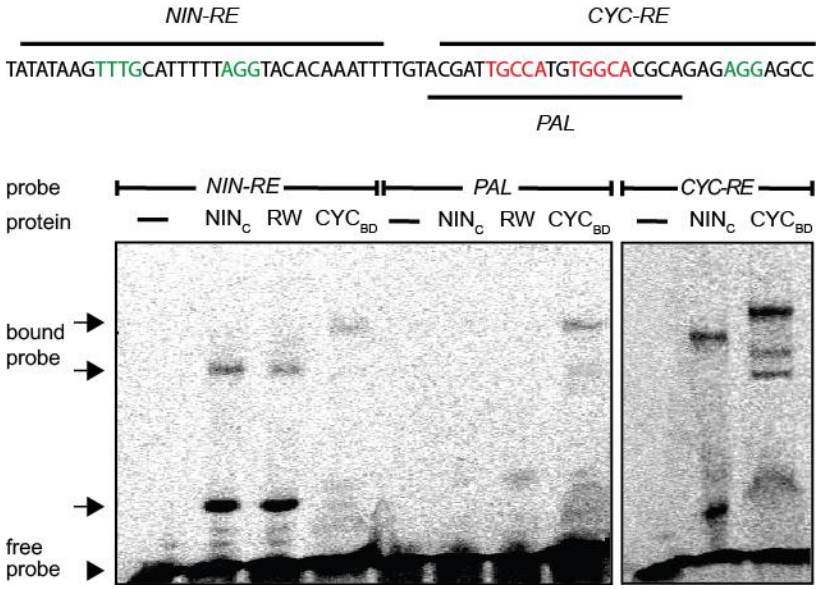

Figure 11: NIN can bind to different probes in close proximity and on the *CYC-RE*.

Different nucleotide binding sites (NBS) within the *NIN* promoter were used as probes in EMSAs. Sequences containing the consensus NBS of NIN are highlighted in green, the palindromic region of the *CYC-box* is indicated in red. The C-terminal part of NIN (NIN_C, aa 546-878), the DNA-binding domain of NIN (RW, aa 546-643) and CYCLOPS (CYC_{BD}, aa 364-518) were tested for ability to bind to different NBS within the *NIN* promoter (*NIN-RE, CYC-RE* and *PAL*) in EMSAs. CYC_{BD} was able to interact with all tested elements. NIN_C did bind to *NIN-RE* and *CYC-RE*, but did not interact with *PAL*. Arrow point towards the detected shifted bands, while arrow head marks the free probe in the gel. Data and this figure were generated by Katja Katzer.

We tested these probes with the C-terminal part of NIN (NIN_C, aa 546-878), which was already shown to successfully bind to the promoter of *LjNF-YA-1* and *LjNF-YB-1* (Soyano et al., 2013). This NIN fragment contains the RWP-RK domain and the PB1 domain, which are predicted to function in DNA binding and in protein-protein interaction, respectively (Schauser et al., 1999; Schauser et al., 2005). This protein was further reduced to contain only the DNA binding domain (RW, aa 546-643). Two shifted bands (two bound probes) of the *NIN-RE* probe were detected upon incubation with NIN_C (Figure 11), indicating protein-DNA binding. Interestingly, IR-labeled *CYC-RE* was also shifted by NIN_C, whereas the probe containing the palindromic *CYC-box* (Rodríguez-Llorente et al.) alone did not show a mobility shift (Figure 11), sugessting that the AGG region within the *CYC-RE* is responsible for NIN-DNA binding. RW also resulted in a mobility shift with *NIN-RE* and again with no binding affinity to *PAL*, confirming that NIN interacts with DNA in a sequence specific manner via its predicted DNA binding domain.

In conclusion, NIN can interact with DNA on *NIN-RE* and *CYC-RE*, but not *PAL*, confirming the hypothesis that NIN can bind to DNA on the *CYC-RE* and on another site in close vicinity likely via its RWP-RK domain.

It was demonstrated that the binding domain of CYCLOPS (aa 364 – 518, CYC_{BD}) can bind in a sequence specific manner to a palindromic element named *CYC-box* (highlighted in red in Figure 11) (Singh et al., 2014). Hence, we also tested if CYC_{BD} can bind to the *NIN-RE in vitro*, although there is no sequence similar to the *CYC-box* on this element. Interestingly, CYC_{BD} caused a mobility shift with *NIN-RE* as with *CYC-RE* and *PAL* in EMSA (Figure 11), suggesting that CYC_{BD} can bind to other elements on DNA other than the previously identified *CYC-box* (Singh et al., 2014).

Striking is the observation that NIN binds the probed DNA with two shifted bands while CYC_{BD} only binds DNA with one specific mobility shift band, suggesting that NIN binds in different complexes or to additional motifs.

To verify that NIN_C binds to *NIN-RE* in a sequence specific manner, different competition analyses were performed. A NIN binding sequence has already been described, which is conserved in two parts within the identified consensus sequence, namely on the left with a richness in T and on the right with the sequence AGG (Soyano et al., 2013). Consequently, *NIN-RE* was mutated in the conserved regions of the element (highlighted in red, Figure 12). Sequence specificity of *NIN-RE* was demostrated as the binding can be out-competed by addition of unlabeled *NIN-RE* DNA in a large molecular excess (40x and 200x), but not with mutated competitor *NIN-RE* DNA (*mNIN-RE*) with 4 bps substituted on the bipartite NBS or *PAL* DNA (Figure 12).

Moreover, we confirmed that a higher NIN_C protein concentration results in a thicker shifted band detected in EMSAs, refecting the higher amount of bound probe (Figure 12). NIN binds with two mobility shifted bands on *NIN-RE*; however, we observed that the lower mobility shift interacts less specifically than the upper one with *NIN-RE*. One explanation might be that different stoichiometric complexes of NIN_C or unspecific DNA-protein complexes are represented. As expected, unlabeled *Pal* DNA comprising the *CYC-box* did not compete for the binding of NIN_C to labeled *NIN-RE* probe (Figure 12), as it was previously shown to not interact with this element (Figure 11).

These results demonstrate that NIN has sequence-specific DNA-binding properties and can directly bind to a NBS in close vicinity to the *CYC-box in vitro*.

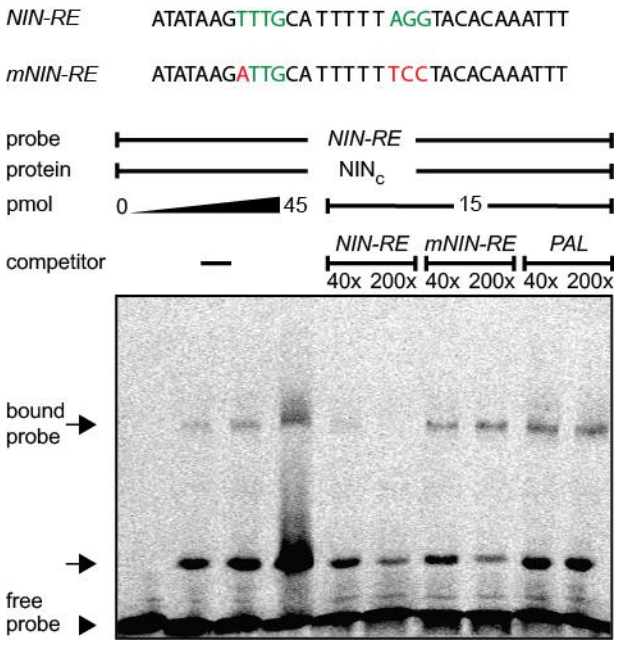

Figure 12: NIN$_C$ specifically binds to *NIN-RE in vitro*.

Sequences of *NIN-RE* and *mNIN-RE* are shown above the gel. Regions related to the consensus NBS of NIN and mutated base pairs are highlighted in green and red, respectively. Mobility shifted bands of NIN$_C$ bound to *NIN-RE* are enhanced with increasing concentration of NIN$_C$ (0-45 pmol). Unlabeled wild-type or mutated versions of *NIN-RE* (*mNIN-RE*) or wild-type *PAL* were used as competitor DNA in 40- and 200-fold excess. Arrows point towards the detected shifted bands, while the arrow head marks the free probe in the gel. Data and this figure were generated by Katja Katzer.

7.7.1 Competition of NIN and CYCLOPS for *NIN* promoter regulatory elements

As CYCLOPS and NIN can both bind to the same *NIN-RE* DNA element within the *NIN* promoter (Figure 11), we asked about the binding affinity both NIN and CYCLOPS would have in the same binding reaction with *NIN-RE*. To test which transcription factor has a higher affinity for *NIN-RE*, competition experiments between NIN$_C$ and CYC$_{BD}$ were performed (Figure 13).

We observed that equal molar amounts of NIN_C and CYC_{BD} incubated with *NIN-RE* as probe caused a shift, which was shifted to an intermediate position, between the mobility shift of individually bound NIN_C or CYC_{BD}. Excess of CYC_{BD} over NIN_C was able to out-compete the upper specific mobility shift of NIN_C, whereas the unspecific lower shift remained bound to *NIN-RE*. On the other hand, NIN_C was less effective to prevent CYC_{BD} from binding to *NIN-RE* (Figure 13).

While a 5-fold excess of CYC_{BD} over NIN_C strongly shifted the complex stoichiometry towards *NIN-RE*+CYC_{BD}, the same molar excess of NIN_C over CYC_{BD} only insufficiently competed for the DNA element. Instead the lower unspecific shift of NIN_C bound to *NIN-RE* increased.

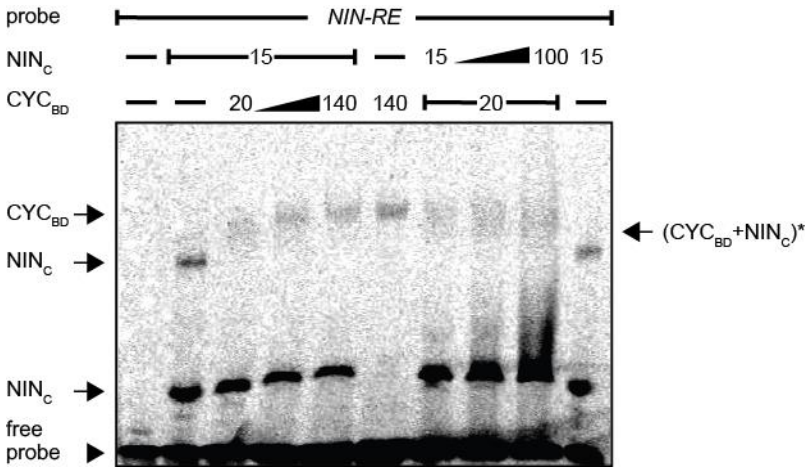

Figure 13: Competition experiments between NIN_C and CYC_{BD} for *NIN-RE*.

CYC_{BD} shows a higher affinity for *NIN-RE* and can out-compete NIN_C for binding. Equal quantities of NIN_C and CYC_{BD} caused a shift of intermediate mobility (CYC_{BD}, NIN_C)* which is moving towards the band height of *NIN-RE*+CYC_{BD} complex with increasing concentration of CYC_{BD}. Molar amounts of proteins used for each binding reaction are indicated above the gel. Data and this figure were generated by Katja Katzer.

These results indicate that CYC_{BD} has a higher affinity for *NIN-RE* and can outcompete NIN_C for binding *in vitro*; and also that once *NIN-RE* is saturated with CYC_{BD}, high quantities of NIN_C are required to replace CYC_{BD} and shift the equilibrium towards *NIN-RE*+NIN_C complex.

7.7.2 Co-binding of NIN and CYCLOPS to the *NIN* promoter regulatory element

It was demonstrated that NIN binds specifically to *NIN-RE*, which is in close proximity to *CYC-box*, the binding site of CYCLOPS. Next, we asked whether NIN and CYCLOPS would both interact simultaneously with DNA or would compete for binding to the tested element, which combines both identified responsive sequences *NIN-RE* and *CYC-RE* (named *NC-RE*).

The activity of CYCLOPS to mediate DNA binding and transcriptional activation was previously verified for a minimal CYCLOPS version. So, to better distinguish this band from the mobility shifts of the individual proteins, the minimal CYCLOPS (CYC_{Min}, aa 255-518) was used, which has a higher molecular weight than CYC_{BD}.

When *NC-RE* was used as probe, both proteins could individually interact with the element (Figure 14B). Strikingly, when both proteins were simultaneously present in one binding reaction, an additional super shift of potentially trimeric *NC-RE*+CYC_{Min}+NIN_C complex was observed (Figure 14).

In accordance, since both NIN_C and CYC_{Min} bind to different NBS on the *CYC-RE*, CYLOPS to the *CYC-box* and NIN to the 3' region of the *CYC-RE*, both proteins can concurrently bind the probe in EMSA and create an additional super shift, as observed for *NC-RE* (Figure 14B). This result can only be explained by simultaneous binding of CYC_{Min} and NIN_C.

Interestingly, the auto-active, full-length CYCLOPS (CYC_{DD}) (Singh et al., 2014) did not cause an additional super shift of *CYC-RE* in the presence of NIN_C (Figure 14), which might be caused by sterical hindrance between the two proteins.

Finally, the results from the competition EMSAs are in agreement with the idea that NIN inhibits CYCLOPS-DD mediated NIN activation through its co-binding to DNA.

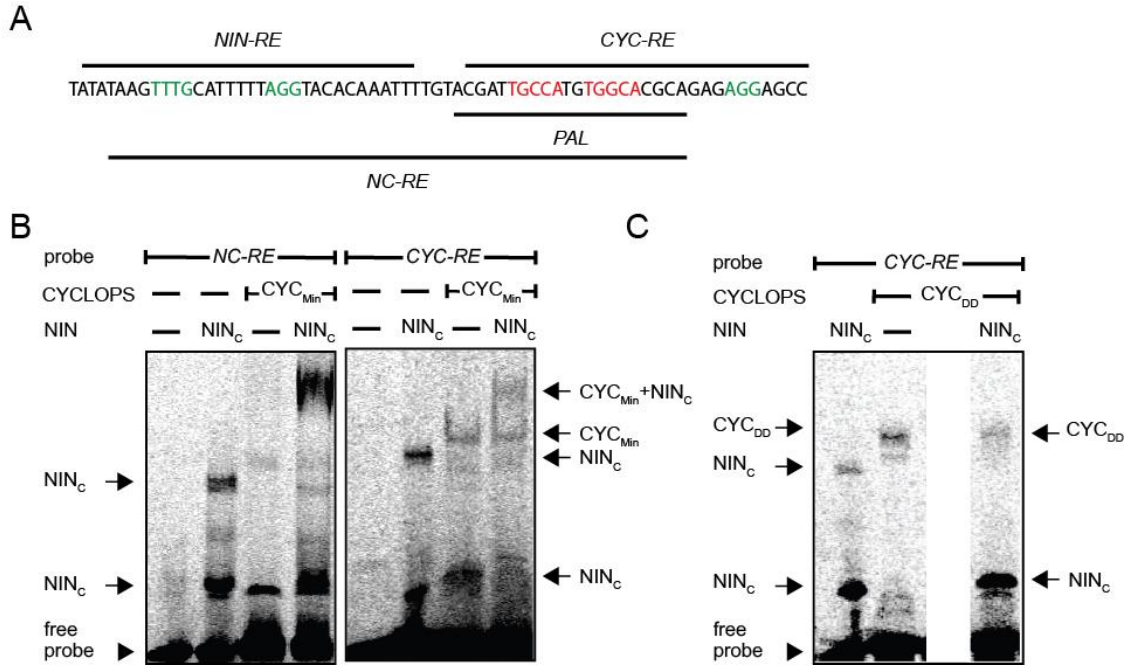

Figure 14: Competition analyses using *NC-RE* and *CYC-RE* together with CYCLOPS and NIN_C

(A) Different nucleotide binding sites (NBS) within the *NIN* promoter were used as probes in EMSAs. Sequences containing the consensus NBS of NIN are highlighted in green, the palindromic region of the *CYC-box* is indicated in red. (B) The minimal CYCLOPS (CYC_{Min}, aa 255-518) and NIN_C can individually and simultaneously bind to *NC-RE* and *CYC-RE* in EMSA. Super shifted band of trimeric DNA+CYC_{Min}+NIN_C complex is indicated. (C) When CYC_{DD} and NIN_C are incubated together with CYC-RE only CYC_{DD} can bind and not NIN_C. NIN_C does not interfere with binding of CYC_{DD} to *CYC-RE* in EMSA.The arrows and the arrowheads show positions of specifically bound and free probe, respectively. Data and figure were generated by Katja Katzer.

7.8 Overexpression of *NIN* leads to local inhibition of nodulation and infection

Due to the observed negative regulatory effect of the NIN protein on its own transcription in the CYCLOPS-DD mediated activation pathway shown in transactivation assays in *N. benthamiana* and *L. japonicus* roots (Figure 8 and Figure 9), we tested if overexpression of *NIN* would cause an effect on the nodulation efficiency in *L. japonicus*. Therefore, hairy root experiments were performed, where *NIN* was expressed under the strong and constitutive *poly-ubiquitin* promoter in Gifu wild-type roots. The transformed plants were inoculated with *Mesorhizobium loti* symbiont and nodulation was examined 4 weeks post infection (wpi).

As depicted in the pictures of representative samples for a successful hairy root transformation, the root systems often consisted of a mix of transformed (visualized in green, expressing the GFP transformation marker) and untransformed roots (no green colour, not expressing the GFP transformation marker)(Figure 15).

Strikingly, nodulation was blocked in GFP positive transformed roots overexpressing *NIN* (Figure 15D-F), indicating an inhibitory effect on nodulation. Nevertheless, the overall root system exhibited normal root architecture (Figure 15D-F).

To validate that this negative effect on nodulation is caused specifically by NIN, the overexpression of another transcription factor, CYCLOPS, which is relevant for symbiosis, was tested in Gifu hairy root systems. The overexpression of CYCLOPS in Gifu wild-type plants led to a normal nodulation efficiency (Figure 15G-I) that was comparable to the control plants transformed with an empty vector (Figure 15A-C).

Hence, no inhibition of nodulation was observed in this experiment, demonstrating that overexpression of *CYCLOPS* has no repressive effect on nodulation and that the inhibition of nodulation is specific to the overexpression of *NIN*.

Next, we tested if the inhibitory effect was restricted to nodule organogenesis or if it also had an impact on the infection process. As observed, infection was also blocked at the very early microcolony stage, restricted to the GFP positive roots overexpressing *NIN* and where nodule organogenesis was not concomitantly triggered (Figure 16B).

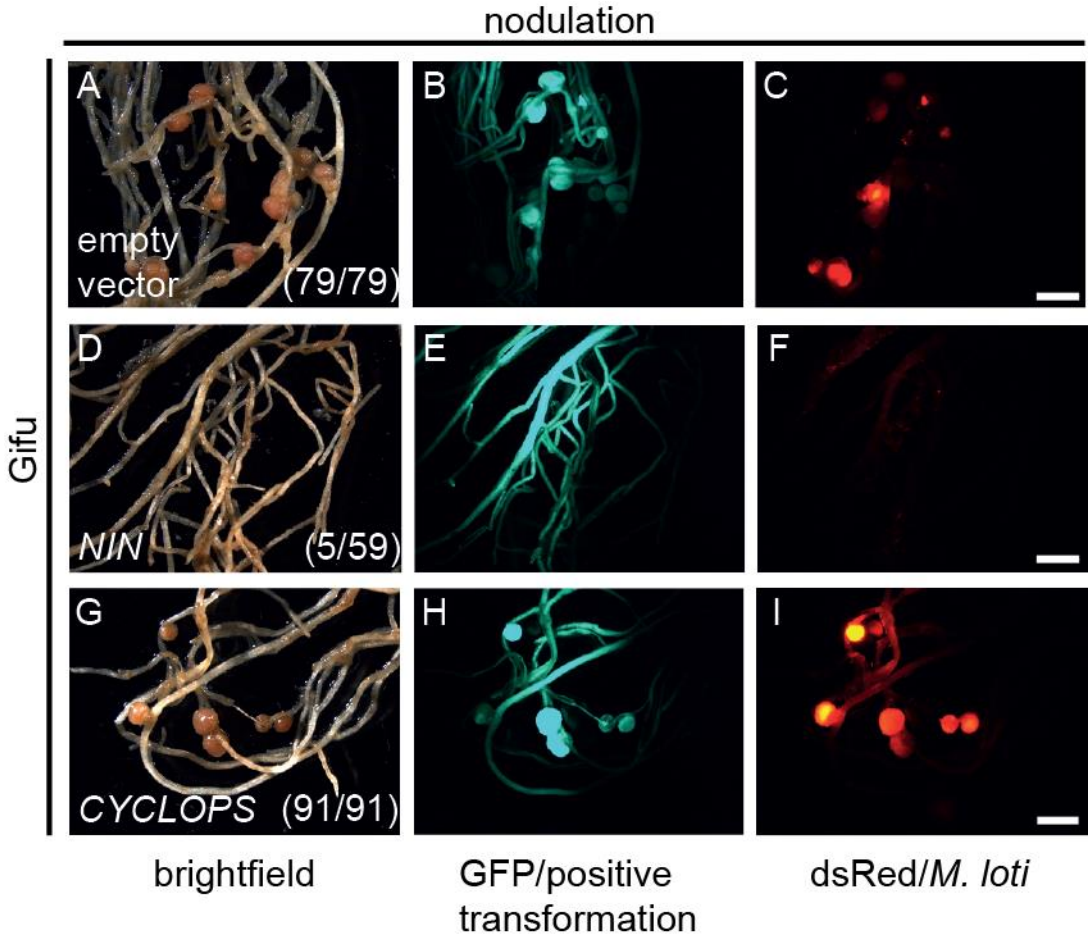

Figure 15: Nodulation is inhibited by overexpression of *NIN* in Gifu hairy roots.

(A-C) There were no effects on nodulation along the whole root system in roots transformed with the empty vector control. (D-F) Nodulation was suppressed in the transformed roots overexpressing *NIN*, but nodules were formed on non-transformed roots of the same root system. (G-I) Overexpression of *CYCLOPS* did not inhibit nodulation in Gifu hairy roots. Representative brightfield images with corresponding GFP fluorescent images as a transformation marker and DsRed expressing *M.loti* were taken 4 weeks past infection. Bar: 2 mm; Numbers in parentheses show: first number represents the amount of plants showing a normal wild-type phenotype, the second number represents the number of total plants tested in 4 independent hairy root experiments.

However, infection threads were normally formed on non-transformed roots of the same root system overexpressing *NIN* (Figure 16C). In comparison, the empty vector control showed normal nodulation and infection, in both GFP negative and GFP positive roots, on 100% of the observed root systems (Figure 15A-C and Figure 16A).

To further quantify the observed difference on nodulation in GFP positive and negative roots caused by the overexpression of *NIN*, the nodule numbers for GFP positive and GFP negative roots were counted separately for each root system in two *Lotus* wild-type ecotypes Gifu and MG-20 (Figure 17).

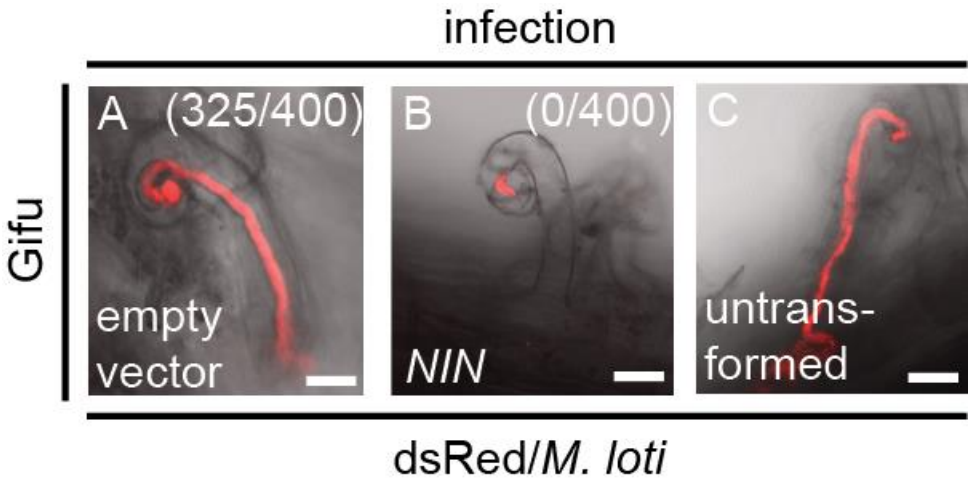

Figure 16: Infection is locally inhibited by overexpression of *NIN* in Gifu hairy roots.

A typical shepherd's crook curl is formed by a responsive root hair and an infection thread is formed in empty vector transformed plants (A). Infection is stopped at the entrapped microcolony stage with overexpression of *NIN* (B), however, infection threads are formed in non-transformed roots of the same root system (C). Representative infection events 14 dai on Gifu hairy roots are depicted. *M. loti* expressing dsRED are visualized in red. Bar: 100 µm; Numbers in parentheses represent individual infection events counted in 4 independent root systems in comparison to the average number of fully developed infection threads (average from 100 infection events per root system). Infection events were counted 14 dpi with *M.loti*.

The mean number of nodules formed on GFP positive roots overexpressing *NIN* was significantly lower in comparison to the GFP positive roots expressing the empty vector control, in both Gifu and MG-20.

In fact, nodule formation was completely inhibited in 80% of the plants overexpressing *NIN*, while the nodule number in roots transformed with the empty vector control showed a median of 13 nodules in Gifu and 8 nodules in MG-20. Consistently, the same effect on nodulation was observed in both ecotypes. The obtained results are summarized in Figure 17.

Interestingly the mean nodule number was around 16 in Gifu and 8 in MG-20 in the untransformed (GFP negative) roots overexpressing *NIN* in the same roots system, confirming the local effect of inhibition of nodulation caused via overexpression of *NIN* (Figure 17).

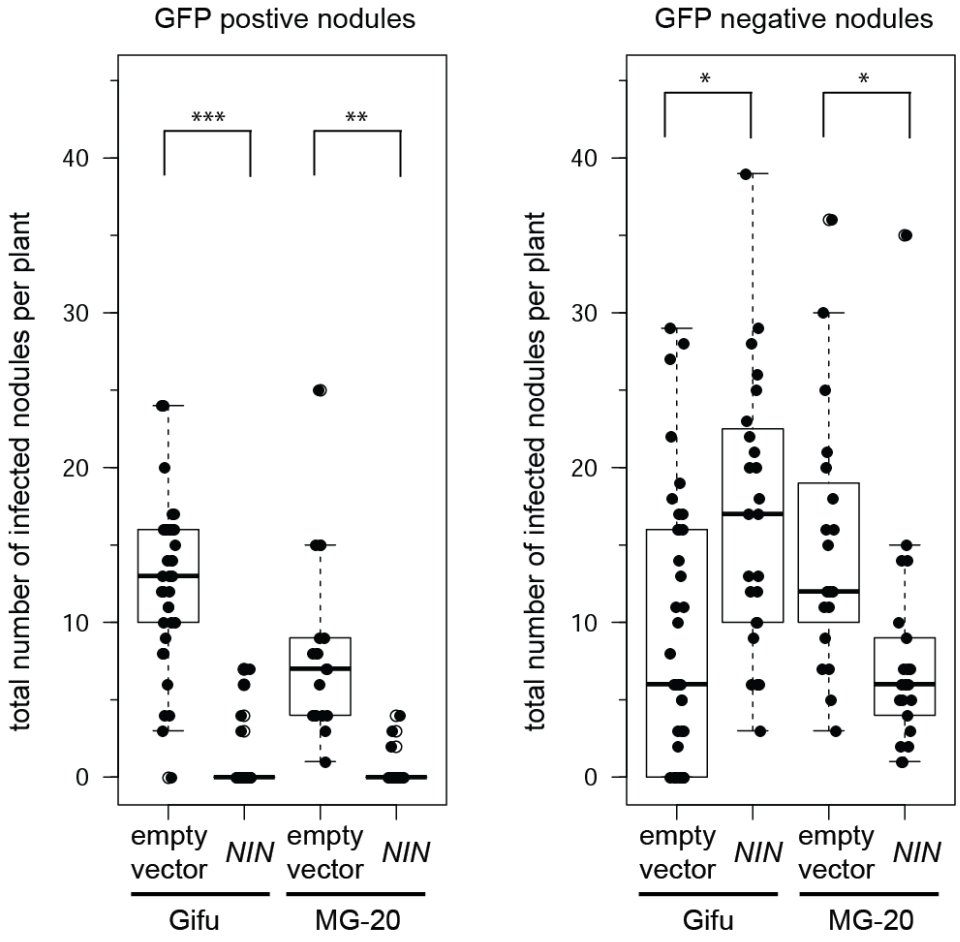

Figure 17: Local inhibition of nodulation is caused by overexpression of *NIN* in Gifu and MG-20 hairy roots

An inhibition of nodulation was observed in GFP positive roots transformed with *pUb:NIN* in Gifu and MG-20 plants (t-test: Gifu $p=7.08^{-11}$; ; MG-20 $p=1.33^{-5}$). In GFP negative roots overexpressing *NIN* more nodules are formed compared to roots transformed with the empty vector control in Gifu plants (t-test: Gifu p=0.001517). In contrast to GFP negative roots overexpressing *NIN* less nodules are formed compared to roots transformed with the empty vector control in MG-20 plants (t-test: MG-20 p=0.007161). Gifu and MG-20 were inoculated with the symbiont *M.loti* and nodule number was scored 4 wpi. Around 30 plants were analysed in each experiment.

As expected, the number of infected nodules along the root was independent of a transformation event in plants transformed with the empty vector, with nodules formed in non-transformed roots comparable to GFP positive roots. Looking only at the GFP negative roots in Gifu, the mean nodule number was higher in *NIN* overexpressing roots compared to the empty vector control.

The opposite was observed in MG-20, with more nodules in the empty vector control compared to the ones overexpressing *NIN* (Figure 17), indicating that there is a difference in the regulation of nodule inhibition in the different ecotype backgrounds.

These findings indicate that *NIN* overexpression locally inhibits nodulation in Gifu wild-type roots, as the number of nodules is solely reduced in GFP positive roots overexpressing *NIN*. It can be speculated that expression of *NIN* is reduced via *NIN* overexpression leading to a local inhibition of nodulation and infection. However, the observation in MG-20 suggests a systemic inhibition of nodulation caused by *NIN* overexpression.

7.9 *nin*-2 and -8 mutants cannot be complemented by overexpression of *NIN*

To test the hypothesis that *NIN* overexpression complements the *nin* mutant phenotype, hairy root experiments were performed in *nin-2* and *nin-8* (Schauser et al., 1999; Perry et al., 2009). The *nin-2* mutant has a transposon insertion that causes a frame shift at C_{145}. The *nin-8* mutant harbours a mutation at C_{1785} to T that leads to a stop codon and in addition contains a *har-1* mutation.

Both *nin* mutant alleles cause the same phenotype of non-nodulating and no infection thread formation and no nodulation after inoculation with the symbiont. Overexpression of *NIN* previously causing the repression effect on nodulation and infection in Gifu, was tested by *A. rhizogenes* mediated hairy root transformation in both *nin* mutants.

Representative pictures of the phenotype observed in the *nin-8* mutant are depicted in Figure 18. All plants transformed with the empty vector control showed the typical non-nodulating phenotype und infection blocked at the microcolony stage (Figure 18A-C). Nodulation and the infection process was not rescued with overexpression of *NIN* in *nin* hairy roots (Figure 18D-F). Consequently, it was not possible to complement the mutant phenotype with overexpression of *NIN*.

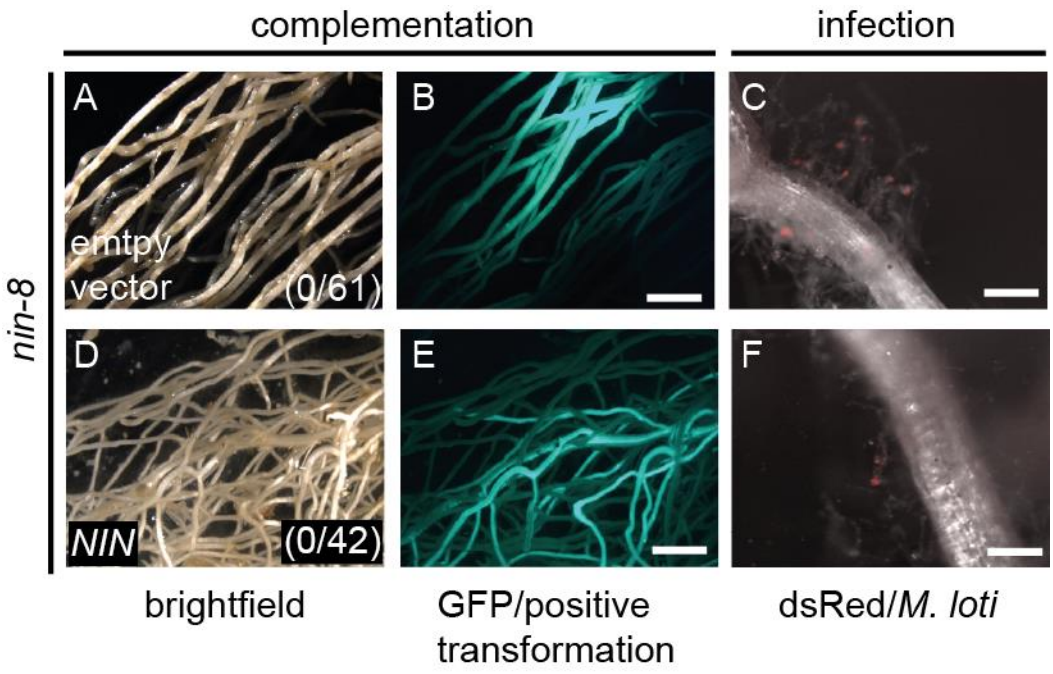

Figure 18: Overexpression of NIN did not rescue nodulation or infection in *nin* mutants

(A-C) Hairy roots of *nin-8* mutants were transformed with the empty vector control showed the mutant phenotype without any nodule formation or infection thread formation. (D-F) No complementation of nodulation and infection growth was observed with overexpression of *NIN* in hairy roots. The left panels (A,D) show bright field images, images in the middle panels (B,E) highlight only the transformed roots expressing free GFP as transformation marker, and the right panels (C,F) show *M. loti* expressing dsRed marker in red colour. Roots were analysed under the epifluorescence microscopy 4 weeks after inoculation with *M. loti*. Bar: 2 mm in B and E, 500 μm in C and F.

The results from the complementation experiments are in line with the idea of NIN acting as a repressor and strengthen the hypothesis of a tight regulation of the *NIN* gene. As both tested mutants are no genetic null mutants, it would be interesting if complementation of a null *nin* mutant might be possible. In *nin-2* and *nin-8* the N' terminal part of *NIN* is still expressed, which could also trigger the inhibitory effect on infection and nodulation.

7.10 The negative regulatory effect on nodulation caused by overexpression of *NIN* is independent of autoregulation of nodulation

Next, we wanted to determine at which point within the symbiosis signalling pathway the inhibition of nodulation is caused by overexpression of *NIN*. To pinpoint the negative mechanistic action caused by overexpression of *NIN*, several nodulation mutants were analysed for the effect on nodulation efficiency.

The nodule number is regulated by a key process named autoregulation of nodulation, preventing the production of an excessive number of nodules along the root (Wopereis et al., 2000; Magori and Kawaguchi, 2009). This mechanism is based on long-distance cell-to-cell communication between root and shoot. In *Lotus japonicus*, one shoot-acting receptor-like kinase HYPERNODULATION ABERRANT ROOT FORMATION 1 (HAR1) has been identified to be involved in this process (Krusell et al., 2002; Nishimura et al., 2002; Buzas and Gresshoff, 2007).

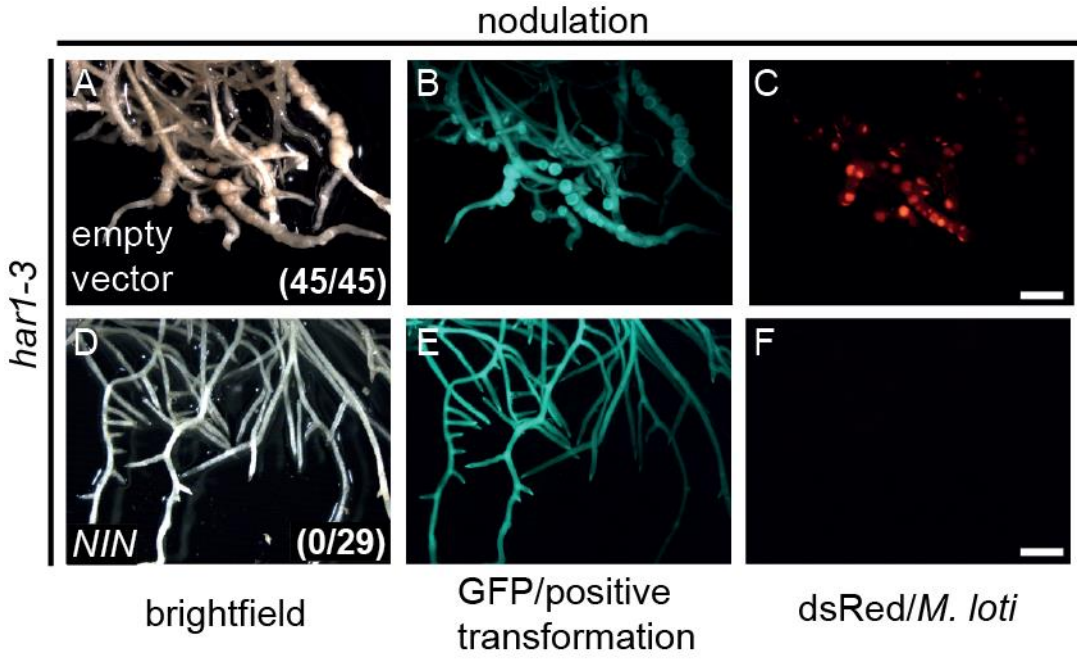

Figure 19: Overexpression of *NIN* inhibited nodulation in *har1-3* hairy roots

(A-C) In *har1-3* hairy roots transformed with the empty vector, hypernodulation was normal, which is in agreement with the respective mutant phenotype. (D-F) Nodulation is inhibited in transformed roots overexpressing *NIN* (GFP positive) in the *har1-3* mutant, but not in non-transformed roots (no GFP expression) of the same root system. Nodulation was examined after 4 weeks of inoculation with rhizobia. Bar: 2 mm

As HAR1 is required for AON to inhibit nodulation, the mutant phenotype is hyper-nodulating and thus forms an enormous amount of nodules (Wopereis et al., 2000). To investigate if the inhibitory effect on nodulation via *NIN* overexpression is dependent on HAR1 regulation and thus connected to AON, hairy root experiments were performed in the *har1-3* mutant background. While *har1-3* hairy roots transformed with the empty vector control showed a typical excessive nodulation phenotype (Figure 19A-C), the overexpression of *NIN* resulted in the inhibition of nodulation in GFP positive roots (Figure 19D-E), confirming a local inhibition of nodulation independent of AON.

Strikingly, the root length of transformed roots overexpressing *NIN* were longer (3.6 ± 0.8 cm) compared to the empty vector control (1.8 ± 0.4 cm) in the absence of rhizobia, indicating that the cell division process was still active (Figure 20).

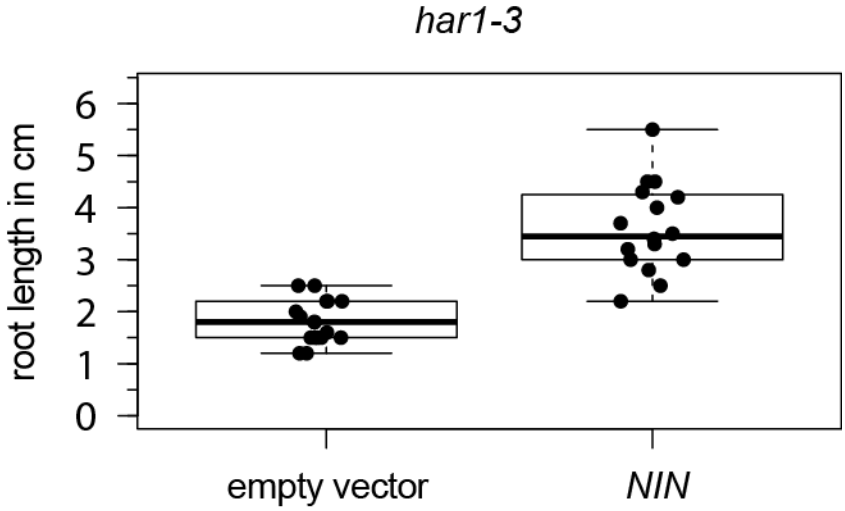

Figure 20: *har1-3* hairy roots overexpressing *NIN* were longer in root length

The analysis of *har1-3* hairy roots overexpressing *NIN* showed a longer root length, compared to the roots transformed with the empty vector control. Root length was measured 4 wpi with *M.loti*.

Taken together, these data demonstrate that overexpression of *NIN* is sufficient to block the process of infection and nodulation within the nodulation signalling pathway in a *har-1* independent manner.

7.11 Inhibition of nodulation caused by *NIN* overexpression is downstream of the common symbiosis pathway

Based on the previous result that NIN is part of the CCaMK/CYCLOPS complex (Figure 5), we asked ourselves whether the interference of NIN within the signalling pathway would be active either upstream or downstream of the common symbiosis pathway.

Interestingly, the complex nodule organogenesis program can be activated by the deregulation of CCaMK, which triggers spontaneous nodulation in the absence of rhizobia (Tirichine et al., 2006). Tirichine reported a spontaneous nodule formation (*snf1-1*) mutant, which harbours two mutations causing the induction of nodulation, one is a C to T transition leading to the replacement of threonine 265 by Isoleucine, and the second is a mutation in intron 1 (Tirichine et al., 2006).

To investigate if the inhibition of nodulation triggered by overexpression of *NIN* acts upstream or downstream of CCaMK, *snf1-1* was subjected to the overexpression of *NIN* in hairy root experiments and was further cultivated in the absence of rhizobia in order to test for spontaneous nodulation.

Interestingly, rhizobia-free spontaneous nodules were not formed on hairy roots overexpressing *NIN* (GFP positive), while the wild-type roots from the same root system showed normal nodulation (Figure 21C-F; Figure 22). This is in line with the observation using Lotus wild-type plants and *har1-3* plants, indicating a mechanism independent from rhizobial infection.

To verfy that overexpression of *NIN* is causing the inhibition of spontaneous nodule formation, NSP2, another transcription factor relevant for symbiosis, was equally tested in this experiment. Overexpression of *NSP2* slightly reduced spontaneous nodulation in *snf1-1* (Figure 21G and H; Figure 22), however, still showed nodulation on GFP positive roots as control plants transformed with the empty vector control (Figure 21; Figure 22).

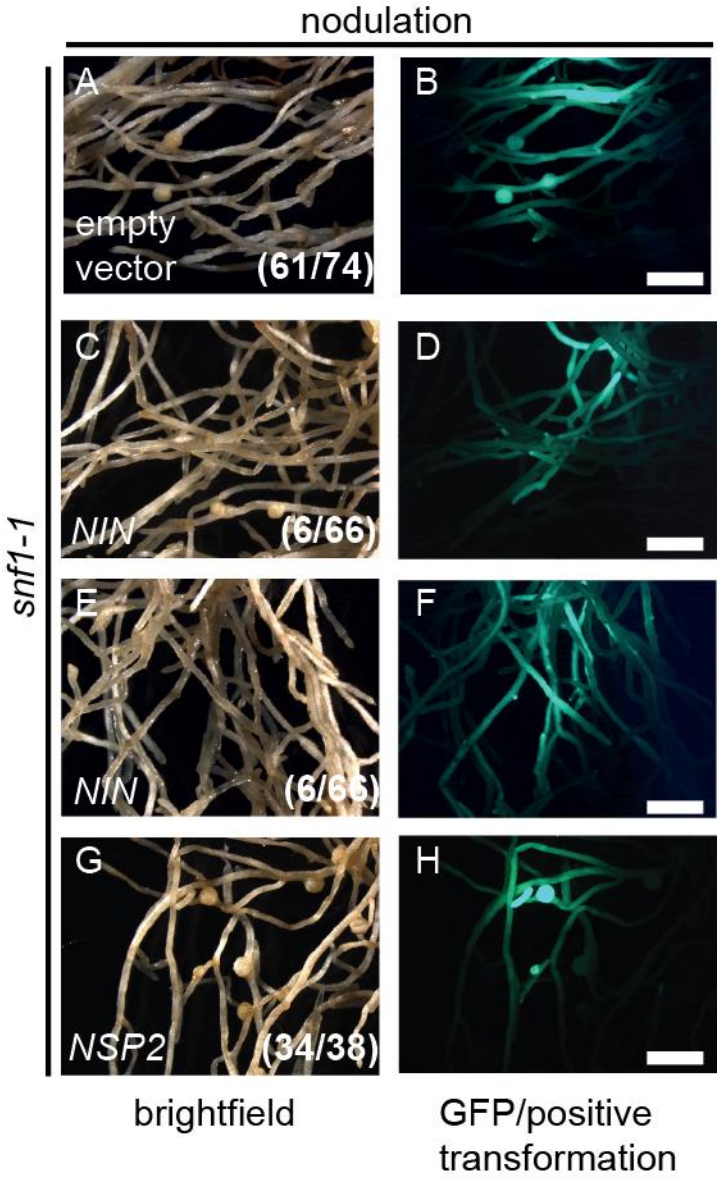

Figure 21: Inhibition of spontaneous nodulation in *snf1-1* is caused by overexpression of *NIN*.

(A and B) In *snf1-1* plants transformed with the empty vector control spontaneous nodules developed as expected for the *snf1-1* phenotype. (D-F) Spontaneous nodulation is inhibited in hairy roots overexpressing *NIN* in the *snf1-1* mutant, but is not blocked in GFP negative roots (non-transformed roots). (G and H) Overexpression of *NSP2* did not inhibit spontaneous nodule formation in snf1-1 hairy roots. Representative bright field images (on the left panels) with corresponding GFP fluorescent images highlighting GFP as transformation marker (right panels). The first number in parenthesis depicts the amount of nodulated plants, the second number represents the total number of plants tested in 4 independent hairy root experiments. Nodulation was assayed 5 weeks post transplantation in pots kept under sterile conditions. Bar: 2mm

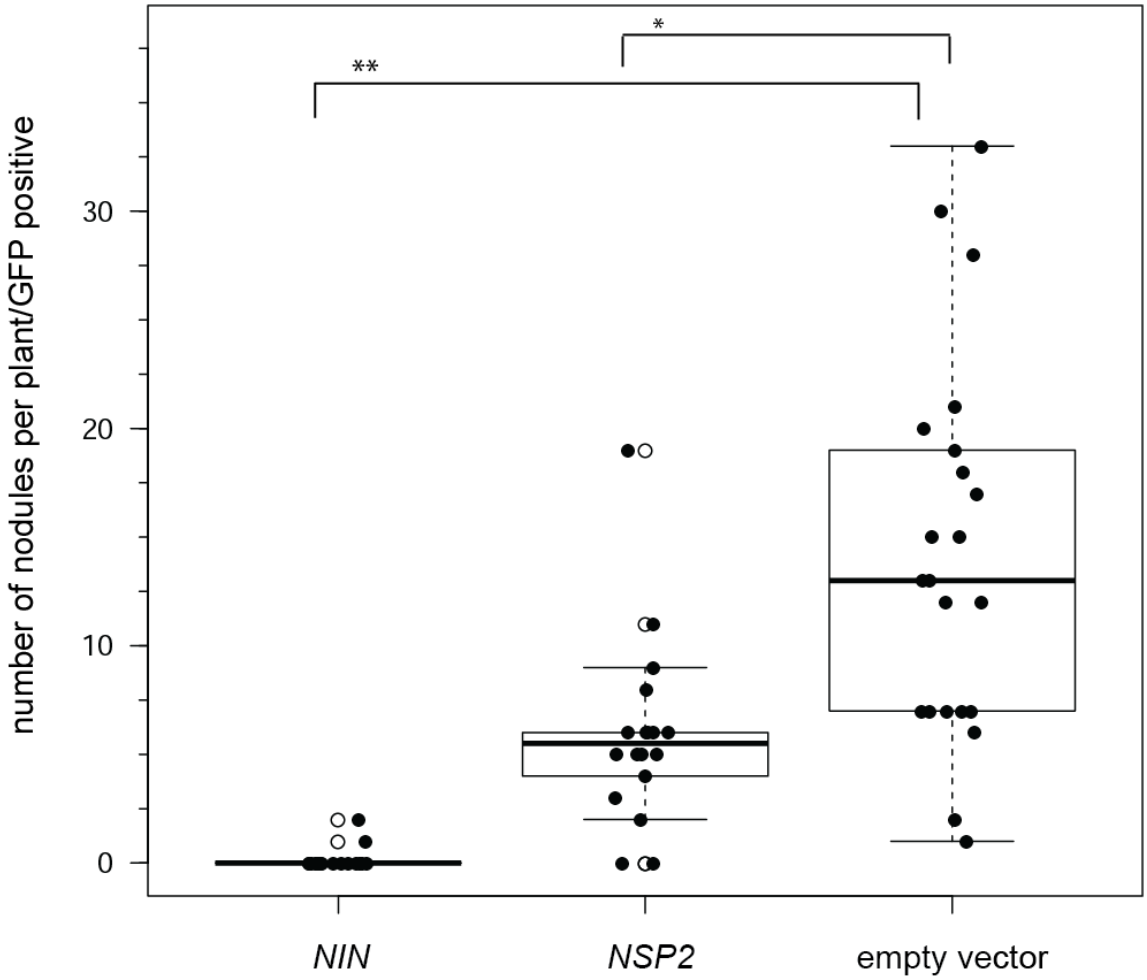

Figure 22: Quantification of spontaneous nodules formed in *snf1-1* hairy roots overexpressing *NIN* or *NSP2*

The number of spontaneous nodules was scored in *snf1-1* hairy roots overexpressing either *NIN* or *NSP2* and roots transformed with the empty vector control 5 weeks after transplantation to pots without infection of rhizobia. Statistical analysis showed a significant difference in nodule numbers with overexpression of *NIN* or *NSP2* compared to the empty vector control (ANOVA: $F_{2,54}=27.21$; $p=6.71^{-9}$; Tukey HSD: NIN:p=0.0; NSP2:p=0.0001), with less spontaneous nodules formed on hairy roots overexpressing *NIN* compared to the nodule number counted on hairy roots overexpressing *NSP2*.

Another spontaneous nodulation formation (*snf2-2*) mutant had been identified that harbours a gain-of-function mutation in a cytokinin receptor (Lotus Histidine Kinase: LHK1), caused by a single nucleotide transition C to T, replacing leucine 266 by phenylalanine (L266F) (Tirichine et al., 2007). Exogenous application of cytokinin to the plant is solo sufficient to induce non-infected nodule-like structures in a *NIN* expression dependent manner (Heckmann et al., 2011).

Due to a strong dependence of LHK1 on *NIN*, we were investigating if *NIN* overexpression would influence the efficiency of spontaneous nodule formation thus linking the previously observed negative feedback loop to the action of cytokinin regulation.

To test if cytokinin plays a role in the suppression of nodulation observed by overexpression of *NIN*, hairy root experiments were performed in *snf2-2* and the frequency of spontaneous nodulation was analysed.

Again, *NIN* overexpression restricted nodulation only in the GFP positive roots, while nodule formation was normal in the non-transformed roots of the same root system in *snf2-2* mutant (Figure 23C-F; Figure 24). *snf2-2* plants transformed with the empty vector control (Figure 23A and B; Figure 24) or overexpressing *NSP2* (Figure 23G and H; Figure 24) exhibited a homogenous distribution of spontaneous nodules on GFP positive and GFP negative roots of the same root system. These results suggest that the inhibition of nodulation caused by *NIN* overexpression is independent of the *LHK1* regulation and cytokinin perception.

These findings support the idea of a local inhibitory effect on nodulation induced by overexpression of *NIN*, which acts downstream of *CCaMK* and *LHK1* in the root nodule symbiosis signalling pathway.

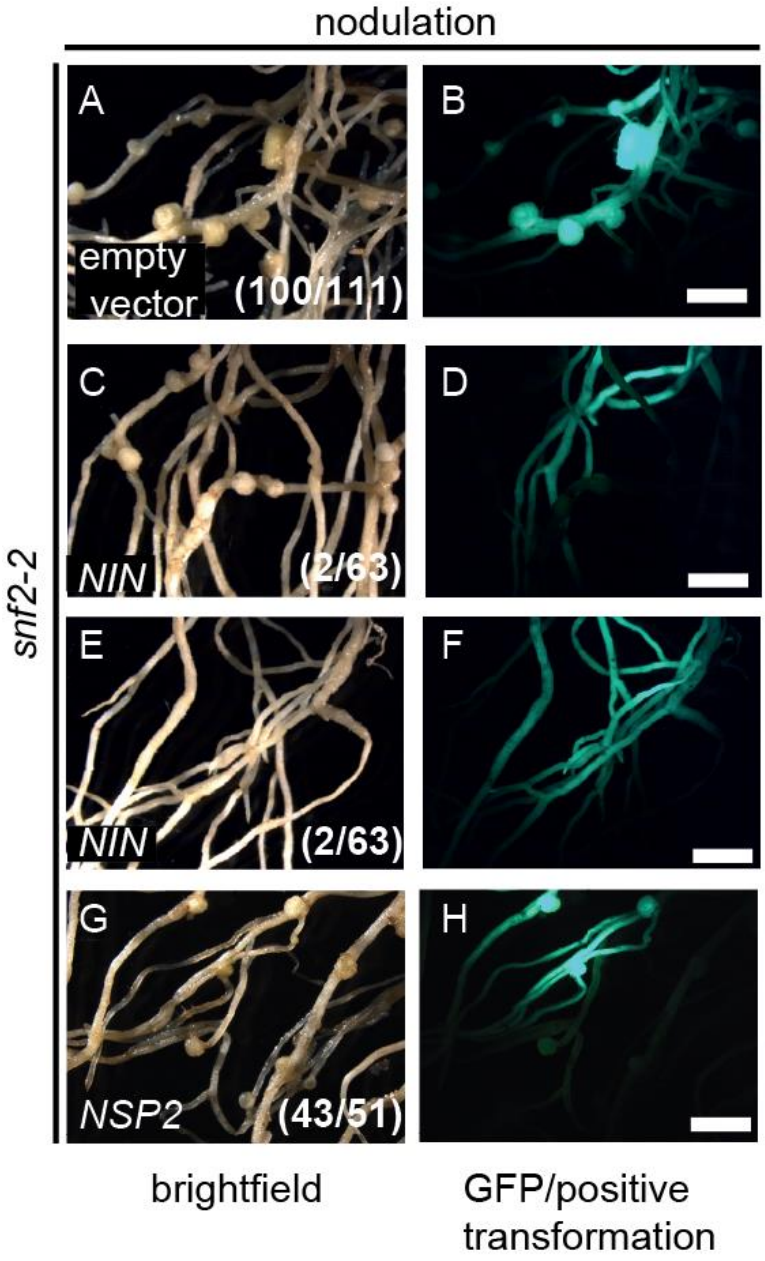

Figure 23: Spontaneous nodule formation is inhibited by *NIN* overexpression in *snf2-2.*

(A and B) In hairy roots transformed with the empty vector control, spontaneous nodules were formed in line with the *snf2-2* mutant phenotype, regardless of whether the roots were GFP positive or negative. (C-F) Overexpression of *NIN* inhibited spontaneous nodulation only in the positive transformed roots of *snf2-2* mutants, and not in the GFP negative roots (non-transformed roots). (G and H) In hairy roots overexpressing *NSP2* spontaneous nodulale were developed like in the empty vector control. Representative bright field images (left panels) are shown with corresponding GFP fluorescent images highlighting GFP as transformation marker (right panels). Numbers in parentheses indicate the amount of plants showing the nodulation phenotype compared with the total number of plants tested in 4 independent hairy root experiments. Bar: 2 mm

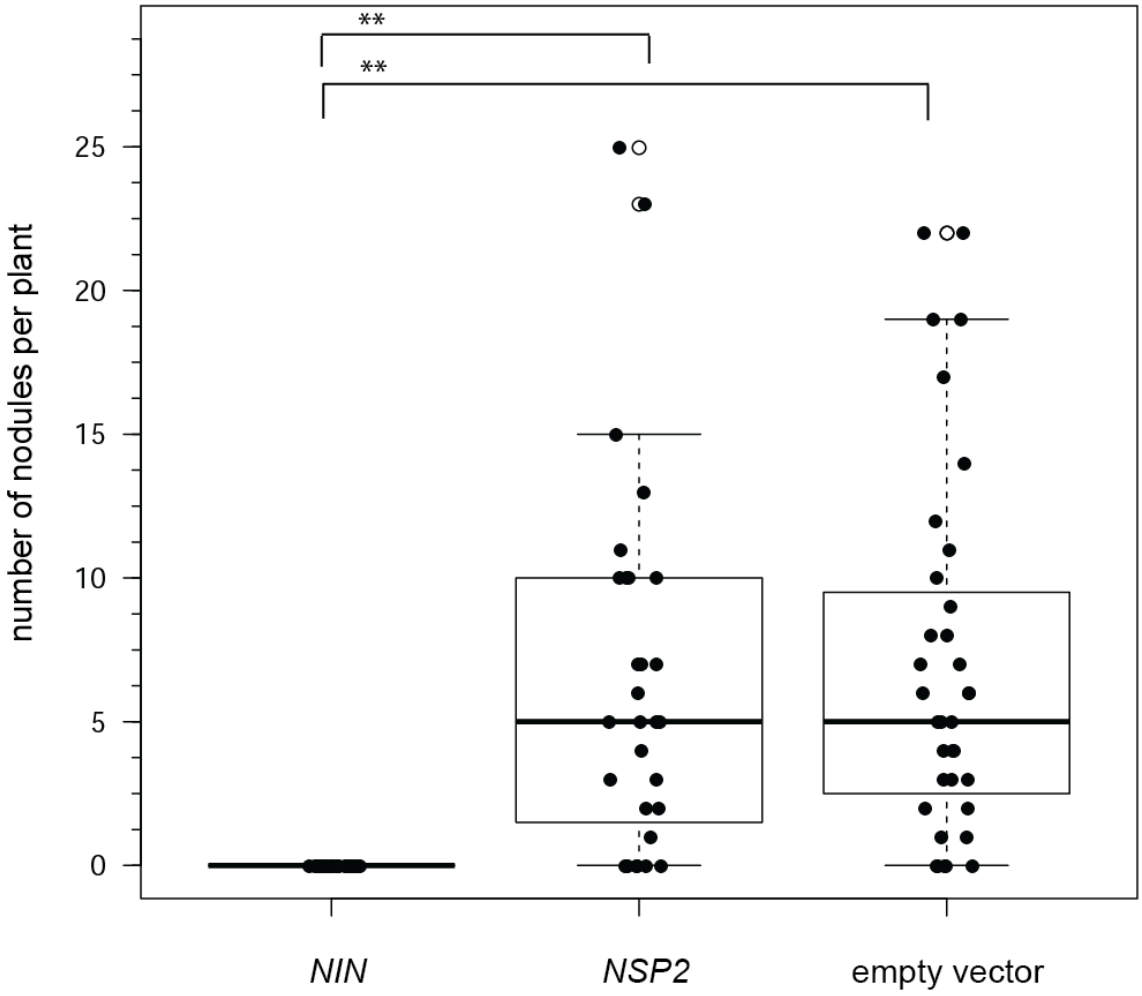

Figure 24: Quantification of spontaneous nodule development in *snf2-2* hairy roots overexpressing *NIN* or *NSP2*

Number of spontaneous nodules was scored in hairy roots overexpressing either *NIN* or *NSP2* and in addition transformed roots with the empty vector control in *snf2-2* after 5 weeks of transplantation to pots without infection of rhizobia. Statistical analysis showed a significant reduction in nodule numbers only with overexpression of *NIN*, but not with *NSP2* compared to the empty vector control **(**ANOVA: $F_{2,88}$=13.7; p=6.62^{-6}; Tukey`s HSD: NIN: p=0.0000122; NSP2: p=0.84;) Furthermore a significant reduction of spontaneous nodule number was detected for the overexpression of *NIN* in comparison to overexpression of *NSP2* in *snf2-2* hairy roots (Tukey`s HSD: *NSP2* and *NIN*: p=0.0001403)

7.12 *NIN* overexpression has no effect on the infection with the arbuscular mycorrhiza fungus *Rhizophagus irregularis*

NIN is dispensable for the more wide spread AMS among plants (Schauser et al., 1999; Marsh et al., 2007). Importantly, there is emerging evidence that *NIN* was specially recruited for RNS due to its loss in nitrate sensitivity (Suzuki et al., 2013).

Therefore, we expected that the overexpression of *NIN* would not influence the symbiosis between AM fungi and *L. japonicus*. In addition, it was reported that infection by *Rhizophagus irregularis* was fully functional in *nin* mutants (Schauser et al., 1999), suggesting no function of *NIN* in AM symbiosis.

Here, we tested our hypothesis by performing hairy root experiments overexpressing *NIN* in Gifu wild-type plants and infecting the transformed plants with AM fungi. Hairy roots transformed with the empty vector control or overexpressing *NIN* were identified with the GFP transformation marker. Later, only transformed roots were selected and stained with ink to highlight structures formed by the fungi within the root.

Both, hairy roots transformed with the empty vector control or roots overexpressing *NIN* showed successful AM colonisation in Gifu (Figure 25).

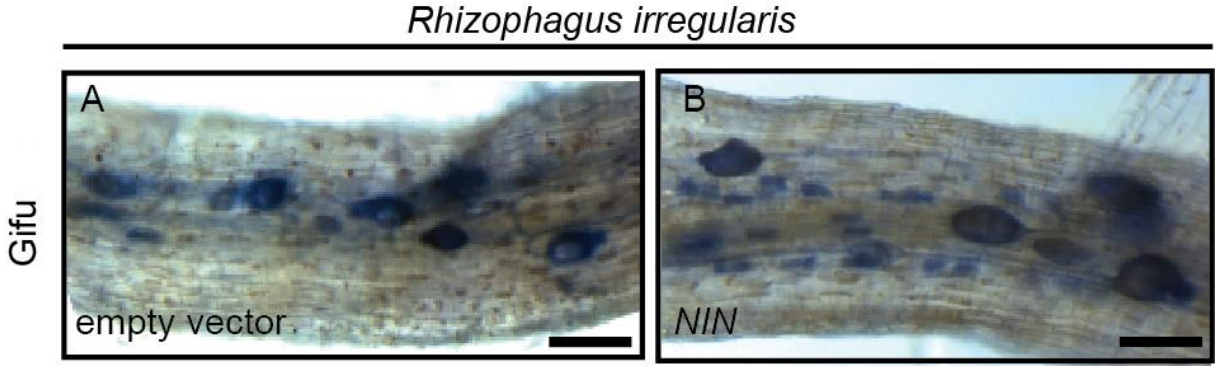

Figure 25: Overexpression of *NIN* did not inhibit AM colonization in Gifu hairy roots

(A) In Gifu hairy roots transformed with the empty vector control a fully colonized root by the fungus was also observed. (B) The whole root system overexpressing *NIN* was colonized by AM in Gifu hairy roots, showing different AM structures containing fully developed arbuscules and vesicles. Root samples of *Lotus japonicus* Gifu wild-type were harvested 4 wpi with *R. irregularis*, cultivated in chive pots with BEG195 in controlled climate chambers. AM fungal structures were stained with acid ink and analysed using a stereomicroscope. Bar: 100 µm

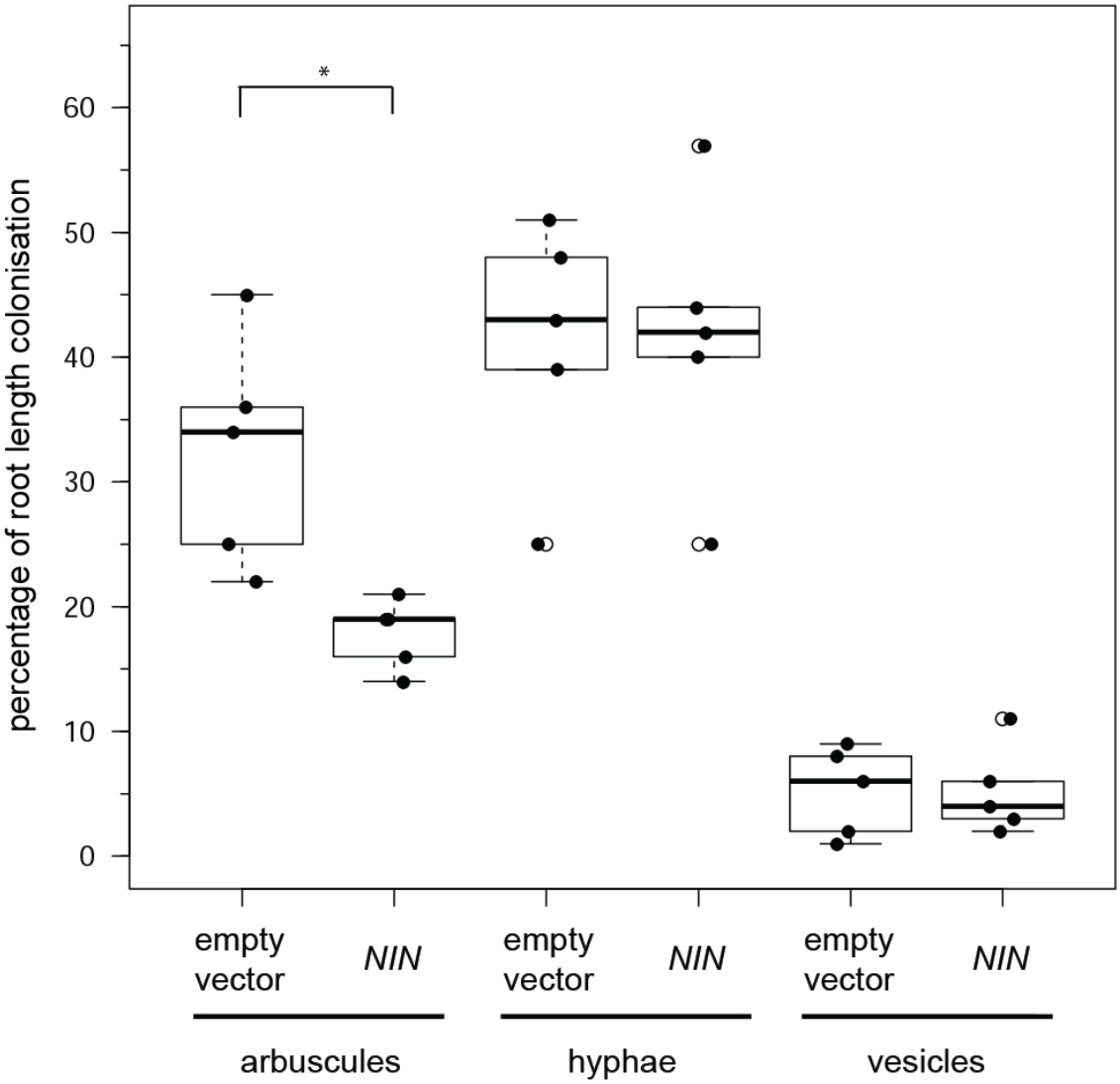

Figure 26: Quantification of percentage of root length colonized by AM in Gifu hairy roots overexpressing *NIN*.

No significant difference of colonised root length was observed for vesciles or hyphae (Vesicles: p=1;; hyphae: p=0.9548) between hairyroots transformed with the empty vector control or hairy roots overexpressing *NIN*. A higher percentage of arbuscular colonisation was observed in hairy roots overexpressing *NIN* (Arbuscules: p=0.02), indicating successful infection. Percentage of root length of hyphal colonization (hyphae, %), arbuscular colonization (arbuscules, %) and vesicle formation (vesicle, %) was quantified in 5 plants per combination, using the intersection method. Infection sites per cm per root were analysed after 5 weeks of cultivation at 24 °C. A t-test was performed to determine the statistical difference between overexpression of NIN and empty vector for the different structures.

To examine the percentage of root length colonisation by the fungus the intersect method was performed (McGonigle et al., 1990), where the abundance of certain fungal structures like hyphae, arbuscule and vesicles is taken into account. Gifu hairy roots overexpressing *NIN* showed successful infection and were fully colonized with hyphae, arbuscules and vesicles.

The quantification confirmed a comparable percentage of root length colonization in hairy roots overexpressing *NIN* and hairy roots transformed with the empty vector control for the amount of vesicles and hyphae formed (Figure 26). Interestingly, there was a slight reduction in the abundance of arbuscles in hairyroots overexpressing *NIN* compared to roots transformed with the empty vector control (Figure 26).

As expected, these results confirmed that the molecular mechanism induced by overexpression of *NIN* does not interfere with the AM signalling pathway, as all structures induced by AM fungi are formed in Gifu. Furthermore, these findings suggest a mechanism interfering with a factor required specifically for RNS, and strengthen the idea that *NIN* itself is a likely candidate as it is not required for AM symbiosis.

7.13 Overexpression of *NIN* triggers the process of cell division

NIN is a transcription factor that is nodulation specific and is crucial for the initiation of nodule formation (Schauser et al., 1999). NIN functions as transcriptional activator and one target is *LjNF-YA1* that is also required for root nodule organogenesis (Soyano et al., 2013). NF-YA is part of a heterodimer complex NF-Y, which is involved in cell cycle regulation and likely triggers cortical cell division in nodule formation (Laloum et al., 2014).

Interestingly, Soyano and collegues could show that overexpression of *NIN* induces nodule like structures in the absence of bacteria. Further the expression of the molecular nodule marker *Enod40* was detected in those structures (Soyano et al., 2013).

To investigate whether the published results could be reproduced, I performed hairy root experiments in *L. japonicus* Gifu plants overexpressing *NIN*, under the same conditions as described in Soyano et al. (2013) and as my previous experiments.

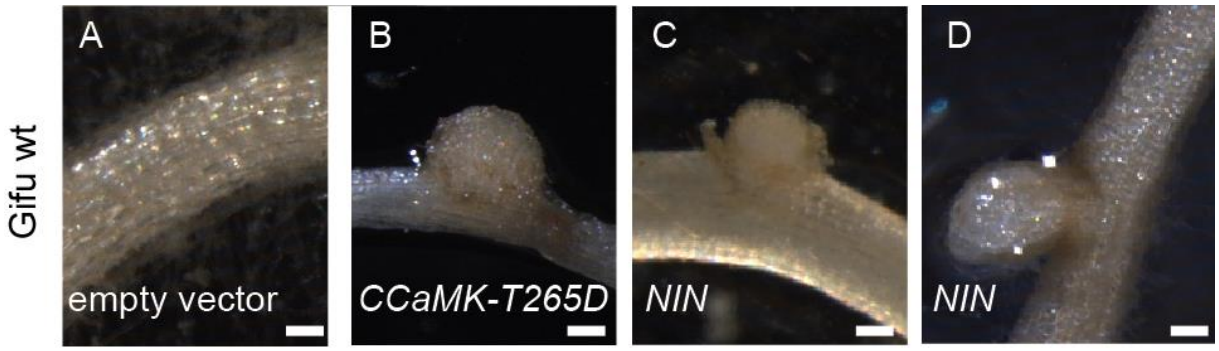

Figure 27: Spontaneous nodule formation and induction of nodule-like structures in Gifu hairy roots

Spontaneous nodules were not induced in the hairy roots transformed with the empty vector control (A), while hairy roots overexpressing *CCaMK-T265D* did form spontaneous nodules (B). Nodule-like structures were also formed on hairy roots overexpressing *NIN* (C and D). Spontaneous nodulation was examined 6 weeks past transplantation to pots, in the absence of rhizobia, using a stereomicroscope in bright field view. Scale bar: 0.1 mm

Interestingly, the formation of spontanteous structures like bumps and nodules were also observed in hairy roots overexpressing *NIN* (Figure 27C and D), indicating a potential of *NIN* to induce cell division. In hairy roots tansformed with the empty vector these spontaneous structures were absent (Figure 27A). Round shaped spontaneous nodules were developed on hairy roots overexpressing the gain-of-function CCaMK version carrying a replacement of threonin (T) at position 265 by aspartic acid (D) (Figure 27B) (Madsen et al., 2010).

Furthermore, longitudinal sections of these stuctures induced by NIN overexpression show a nodule-like character (Figure 28A). The frequency of such spontaneous structures induced by NIN overexpression was determined at 14 % (Figure 28B).

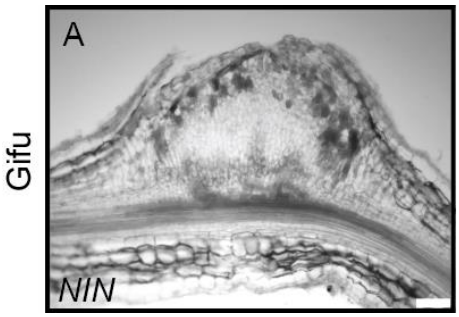

B

construct	Number of plants with nodule like structures	Number of total plants
empty vector	0	64
NIN	9	64

Figure 28: Overexpression of *NIN* induced the formation of nodule-like structures in the absence of rhizobia

(A) Microtome sectioned nodule-like structure were induced in Gifu hairy roots overexpressing *NIN* were analysed after 6 weeks of cultivation in the absence of *M. loti*. Longitudinal 50 µm section; Scale bar: 100 µm. (B) Quantification on the frequency of the development of spontaneous nodule-like structures in hairy roots experiments in the Gifu hairy roots counted 6 weeks past transplantion in pots in the absence of rhizobia.

Repetitive inspection of the root systems showed that hairy roots overexpressing *NIN* were thicker compared to roots transformed with the empty vector control. To confirm and quantify this observation, transversal sections of Gifu hairy roots overexpressing *NIN* and of roots transformed with the empty vector control were performed. Then the root diameter was measured, different cell types inspected and the cell layers in those roots counted.

In comparison to the control plants with a mean diameter of 308 mm, the diameter of hairy roots overexpressing *NIN* was significantly increased to 408 nm, showing bigger sized cortical cells and partly an additional cortical cell layer (Figure 29). Other cell types were represented equally the hairy roots transformed with the empty vector and in hairy roots overexpressing *NIN*.

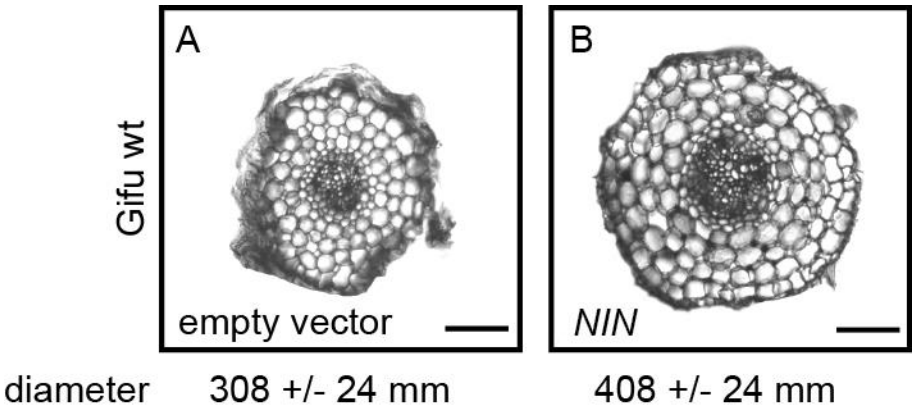

Figure 29: Root diameter was increased in Gifu hairy roots overexpressing *NIN*

(A) A diameter of 308 mm was measured in light micrographs of cross sections of Gifu hairyroots transformed with the empty vector (B) While hairy roots overexpressing *NIN* induced an increase in diameter of the root to 408 mm. Roots were sectioned 4 weeks past transformation. An average diameter was calculated from 6 independent root systems in 3 independent transformation events. Sections were sliced in the region of 1 cm distance to the root origin of the plant. Scale bars: 100 µm

Taken together these results underline the positive role of *NIN* in root nodule organogenesis, with its potential to trigger cortical cell division leading to nodule formation and thicker root diameters.

8 Discussion

8.1 NIN – CYCLOPS – CCaMK: two dimers or a trimer?

CYCLOPS and CCaMK form a complex in the nucleus (Yano et al., 2008), raising the question whether there are additional members in this complex that play an active role in the signalling pathway (Yano et al., 2008; Singh et al., 2014). The dimer formation of CCaMK with CYCLOPS was delimited to a functional kinase domain of CCaMK and the activation domain of CYCLOPS (Yano et al., 2008).

In the current work, NIN was found to interact with CYCLOPS *in planta* and in yeast (Figure 5, Figure 4), and that it has a possible function in the nucleus where all three players are localised (Figure 3) (Yano et al., 2008). The interaction of NIN with CYCLOPS was independent of the phosphorylation status of CYCLOPS, which is also the case for the CYCLOPS-CCaMK interaction (Singh et al., 2014). The interaction between NIN and CYCLOPS was further quantified by FLIM-FRET analysis (Figure 7). Identification and analysis of the specific interaction domains of the NIN and CYCLOPS proteins will be required to clarify a possible mode of action for the interplay.

NIN is a transcriptional target of the CCaMK/CYCLOPS complex that activates downstream genes in the root nodule signalling pathway (Singh et al., 2014). It becomes increasingly important to understand the molecular mechanism through which the complex acts and regulates. As overexpression of CCaMK-T265D induces spontaneous nodule formation in the *cyclops-3* mutant, it was believed that another transcription factor bypasses the action of CYCLOPS (Tirichine et al., 2006; Yano et al., 2008) and which may be NIN. However, no direct interaction was observed between CCaMK and NIN (Figure 5). Interestingly a gain-of-function version of CCaMK can stimulate the induction of NIN in the cortex but not in the epidermis tissue, suggesting that the action of NIN is localized to specific tissues of the root (Tirichine et al., 2006). Therefore, it would be interesting to further analyse the interaction of NIN with different variants of CCaMK, especially gain-of-function versions. As all interaction analyses were performed in leaf cells or in yeast, symbiosis specific factors might also be missing for a positive interaction between CCaMK and NIN.

A direct protein-protein interaction of NIN and CCaMK might require a gain-of-function CCaMK version or a third protein partner. The observed interaction between NIN and CCaMK in the presence of CYCLOPS could indicate that CYCLOPS functions as a scaffold protein in a trimeric complex (Figure 5). A similar interaction was reported about a protein harbouring the PB1 domain that interacts with a kinase in the presence of a scaffold protein (Lamark et al., 2003). NIN harbours this conserved PB1 domain at the very C-terminus, an evolutionary conserved domain that facilitates hetero-dimerization with other proteins (Ponting et al., 2002; Schauser et al., 2005; Sumimoto et al., 2007). The formation of a trimer could be easily verified in protein-protein interaction studies like multicolour BiFC or Co-immunoprecipitation from *Nicotiana* and with the use of the golden gate tool box in *Lotus* hairy root experiments, where co-expression of multiple proteins is feasible (Binder et al., 2014).

NIN has been shown to be a transcriptional target of the NSP1/NSP2 complex and of the NSP2 interacting protein IPN2 (Hirsch et al., 2009; Kang et al., 2011), therefore it would be important to test whether NIN can interact with members of transcriptional activating complexes other than CCaMK/CYCLOPS. The co-expression of different complexes could lead to a synergistic effect and further upregulate *NIN* expression or the different complexes could interfere with each other and thus downregulate *NIN* expression. For example, Laloum and co-workers showed a synergistic mode of action between the players NSP1 and NSP2 with NF-YA. The trimeric complex triggers a higher upregulation of *ERN1* than that achieved by the NSP1/NSP2 complex or NF-YA alone (Laloum et al., 2014).

CCaMK has already been reported to be part of a trimeric protein complex (Kang et al., 2015). In the yeast two-hybrid system the CCaMK interacting protein 73 (CIP73), a Scythe-N domain containing, ubiquitin like protein with unknown function was identified to interact with CCaMK (Kang et al., 2011). RNA interference (RNAi)-mediated knockdown of CIP73 expression impaired nodulation (Kang et al., 2011). Later, the same approach was applied to find interaction partners of CIP73, identifying a HSC/HSP70-interacting protein (Raymond et al.; Kang et al., 2015). CCaMK, CIP73 and HIP were shown to co-localise in the nucleus through the use of a multicolour BiFC system (Waadt et al., 2008; Kang et al., 2015).

Interestingly, *HIP* expression is downregulated during nodule development and nodule senescence (Kang et al., 2015). Using RNAi to lower *HIP* expression levels led to an increase in nodulation, suggesting a negative role of *HIP* in nodulation (Kang et al., 2015).

As CYCLOPS and CIP73 are both phosphorylation targets of CCaMK, NIN could also be a phosphorylation target of CCaMK. Previously it was shown that CCaMK can phosphorylate NIN in a calcium-dependent manner (Diploma thesis, 2010). The obtained results suggested that NIN is a phosphorylation target of CCaMK, as is CYCLOPS, strengthening the hypothesis that CCaMK, CYCLOPS and NIN form a trimeric complex.

This study presents the first evidence of NIN being part of a protein complex, as so far no protein interaction partners of NIN have been identified. To better understand the interplay of the regulatory networks will be a task for future research, especially to relate active networks to specific tissues and time points in symbiosis.

8.2 Dual Role of NIN in symbiosis: Activator and Repressor

When *NIN* was first identified in *L. japonicus*, the gene was described as transcriptional activator and essential for nodule inception (Schauser et al., 1999). Later, *NIN* was considered a repressor in symbiotic signalling, due to an extended expression pattern of *ENOD11* in the *nin* mutant (Marsh et al., 2007). *ENOD11* expression is restricted to a confined region in wild-type plants (Journet et al., 2001; Marsh et al., 2007), leading to the hypothesis that *NIN* plays an active negative regulatory role, restricting the expression of *ENOD11* in roots. Here, I demonstrated that the co-expression of *NIN* and *CYCLOPS-DD* lowered the transactivation potential of *NIN* in comparison to the sole activation by CYCLOPS-DD in transactivation assays performed both in leaf cells and in roots (Figure 8, Figure 9). These results further demonstrate that NIN functions as a repressor that can also block its own transcriptional activation. Which molecular mechanism could trigger this repression mode?

The expression of the transcriptional activator *ERN1* is sufficient for the induction of *ENOD11* in the epidermis, as observed in transactivation assays in *N. benthamiana* and *M. truncatula* (Andriankaja et al., 2007; Cerri et al., 2012), similar to CYCLOPS-DD activating the transcription of *NIN* (Figure 8, Figure 9) (Singh et al., 2014).

ERN transcription factors belong to the family of AP2/ERF proteins. AP2/ERF activators and repressors join in a coordinated interplay to regulate the fine-tuning of gene expression in antagonistic signalling pathways (McGrath et al., 2005; Nakano et al., 2006). ERN family members are involved in the regulation of gene expression of the pre-infection stage, enabling the association between the bacteria and the plant (Andriankaja et al., 2007). Interestingly, it was shown that another ERN transcription factor named ERN3 acts as a repressor of *ENOD11* expression, as the co-expression of ERN1 and ERN3 led to a reduced transactivation activity (Andriankaja et al., 2007). This is in line with the observation in our experiments where NIN acts as a repressor for the regulation of *NIN* transcription via CYCLOPS-DD (Figure 8), pointing towards a similar repression mechanism.

The DNA binding domain of ERN3 was not required to repress *ENOD11* expression, suggesting a mechanistic action independent of DNA binding (Andriankaja et al., 2007). Since NIN harbours a conserved RWP-RK domain that is involved in DNA binding (Schauser et al., 1999; Schauser et al., 2005; Schauser et al., 2005), it would be interesting to test if a NIN protein without the DNA binding domain would also show a comparable suppression potential to verify a similar mode of action. While there are several ERN proteins present in legume plants that function in different roles, NIN is the only known protein of its family that is involved in the process of nodulation (Schauser et al., 1999; Andriankaja et al., 2007). This strengthens the idea that NIN might fulfil functions to both negatively and positively regulate gene expression (Soyano et al., 2013; Soyano et al., 2014; Yoro et al., 2014).

As other transcription factors bind to the *NIN* promoter and upregulate its expression, the question arises if NIN could also prevent the activation by the NSP1/NSP2 complex, as it does with the CCaMK/CYCLOPS complex (Hirsch et al., 2009; Singh et al., 2014). No connection between NIN and the NSP complex has been described and it would be interesting to investigate and maybe find a missing link between different transcriptional activation protein complexes in the symbiosis pathway. Would the co-expression of NIN repress the transactivation activity of the NSP1/NSP2 complex on the *NIN* promoter, as it did in combination with CYCLOPS-DD?

These experiments would further clarify if the observed repression mode is specific for the CYCLOPS-DD mediated pathway or if it is a general mechanism that is triggered by any activating transcription factor for the induction of *NIN*.

In contrast to the negative regulatory function of NIN observed in this work, there are several publications showing that NIN functions as transcriptional activator (Soyano et al., 2014; Qiu et al., 2015; Vernie et al., 2015). For example, *SCARN* expression is induced by NIN, as was shown in transactivation assays performed in *N. benthamiana* leaf cells (Qiu et al., 2015). In addition NIN is able to upregulate both *CRE1* and *NF-YA1* promoter activity, where *CRE1* seems to be more strongly activated compared to *NF-YA* (Soyano et al., 2013; Vernie et al., 2015). *MtCRE1* gene encodes a cytokinin receptor (homolog to *LjHAR1*) required for nodulation (Gonzalez-Rizzo et al., 2006) (Plet et al., 2011); while NF-YA is involved in cell cycle activation (Soyano et al., 2013; Laloum et al., 2014). Thus, NIN acts as positive regulator of gene transcription in these cases.

Strikingly, NIN seems to unite both functions as activator and repressor in a bifunctional transcription factor (this work, (Soyano et al., 2014; Yoro et al., 2014; Qiu et al., 2015; Vernie et al., 2015). This is in contrast to ERN transcription factors, where each function is distributed to a separate ERN member, with ERN1 enabling activation of *ENOD11* induction, while ERN3 functions as a repressor in *Medicago* (Andriankaja et al., 2007).

Various NIN-like proteins exist in leguminous plants (4 NLPs in *L. japonicus*) (Schauser et al., 2005; Suzuki et al., 2013) and non-leguminous plants (9 NLPs in *Arabidopsis*) with probably redundant roles in nitrate signalling (Castaings et al., 2009; Chardin et al., 2014). NLPs have been shown to function as transcriptional activators with their N-terminal activation domain inducing nitrate signalling (Konishi and Yanagisawa, 2014). Although NLPs and NIN are homologous in their conserved C-terminal RWP-RK domain, NIN is unique to leguminous plants and in symbiosis, due to a deletion within its N-terminal region leading to a loss in nitrate responsiveness (Schauser et al., 2005; Suzuki et al., 2013). Hence NIN and NLPs function in different signalling pathways.

However, the transactivation activity of NLP1 on nitrate-response element was reduced in the presence of NIN, showing the same pattern as for the CYCLOPS DD mediated *NIN* activation in co-expression experiments with NIN (Figure 8, Figure 9)(Suzuki et al., 2013). One hypothesis is that NIN and NLPs function in antagonistic ways to regulate gene expression, repressing or activating the nodulation process (Suzuki et al., 2013; Soyano et al., 2014; Soyano et al., 2015).

8.3 The *NIN* promoter - a target for different transcription factors

Transcription factors bind to specific DNA elements to enhance or repress transcription at a defined locus (Carrera and Treisman, 2008). NIN has been characterised as a transcription factor due to its conserved RWP-RK domain, which functions in DNA binding (Schauser et al., 1999; Schauser et al., 2005; Soyano et al., 2015). The RWP-RK domain consists of an unusual DNA binding domain with a basic region followed by a heptad leucine or isoleucine repeat (Schauser et al., 1999). Interestingly, this domain also features structures of bZIP transcriptions factors with an amphipathic leucine-zipper structure but with an unusual longer stretch between the zipper and the basic sequence (Schauser et al., 1999; Sornaraj et al., 2016).

Here, we could show that NIN is able to bind to *NIN-RE*, an element that is in close proximity to *CYC-RE* on the *NIN* promoter (Figure 11, Figure 14). The identified *NIN-RE* consists of a bipartite sequence TTTGxxxxxxxAGG, which is similar to the previous published conserved NIN binding site (NBS) that was found via random binding site analysis (Soyano et al., 2013). In comparison to this NBS, our identified NBS consists also of a sequence rich in T (TTT, left part) and of an adenine followed by two guanines (AGG, right part) (Figure 11) (Soyano et al., 2013; Soyano et al., 2015). In addition, Soyano and colleagues predicted two NIN binding sites within the *NIN* promoter (-1849 bp and -338 bp) in ChIP experiments (Soyano et al., 2014), supporting the findings in our EMSAs (Figure 11, Figure 12).

Similar binding sequences for NIN were also identified in the *CRE1* promoter. NIN binding to the *CRE1* promoter activates *CRE1* expression in cortex cells (Vernie et al., 2015). Although NIN can bind to its promoter in EMSA, it does not activate its own transcription (Figure 8, Figure 9, Figure 11), which is supported by the work of Qui and colleagues (Qiu et al., 2015).

Furthermore, in competition assays we could verify that NIN binds via its DNA binding domain in a sequence specific manner to the identified *NIN-RE* binding sequence, as the unlabelled *NIN-RE* fully competed with labelled *NIN-RE* in EMSAs, while a *PAL* element and the mutated *NIN-RE* did not interfere with the binding to *NIN-RE* (Figure 13). *NIN-RE* was mutated in the T rich region to an A (left part) and in the AGG region to TCC (right part), similar to the nucleotide sequence mutated in (Soyano et al., 2013).

NIN-RE	ATATAAGTTTGCATTTTTAGGTACACAAATTT	this work
mNIN-RE	ATATAAGATTGCATTTTTTCCTACACAAATTT	this work
yB1a	TGTATCTTTAGAGCTTTCCAAGGGATATTT	Soyano et al., 2013
myB1	TGTATCAAAAGAGCTTTCGTTGGGATATTT	Soyano et al., 2013

Figure 30: alignment of NBS for NIN in this work and Soyano

NIN binding to the *NIN-RE* resulted in two shifted bands in EMSAs (Figure 11, Figure 12, Figure 13, Figure 14). The higher band showed a specific binding affinity compared to the lower band, as the upper band was outcompeted with unlabelled *NIN-RE* and the lower band was not. Thus, the lower band could be *NIN-RE* bound in a different stoichiometric complex or it could be an unspecific DNA-protein association. In other reports NIN binding properties were also demonstrated in EMSAs, however, only the higher shifted band was bound specifically by NIN (Soyano et al., 2013; Soyano et al., 2014, 2015). Moreover, in a recent publication one can clearly see two bands but only the upper specific band was discussed as bound by NIN (Qiu et al., 2015). To further determine the specificity in EMSA it would be required to measure relative binding activity and stoichiometry of NIN to the *cis* responsive element (Flores et al., 2015).

Due to a deletion in the N-terminal part of *NIN, NIN* has lost its sensitivity towards nitrate, in contrast to NLPs (Schauser et al., 2005). Nevertheless NIN is still able to bind to nitrate responsive elements (NRE), although with a weaker affinity compared to *LjNLP1* and *AtNIR1* (Suzuki et al., 2013). Interestingly, the same binding pattern with two shifted bands was shown for these NIN-like proteins, with the upper band presenting a specific binding and the lower band a non-specific binding *in vitro* (Suzuki et al., 2013). There has been no functional explanation for the requirement of this binding to *NRE*, as NIN is unable to activate nitrate responsive genes (Suzuki et al., 2013). Maybe NIN binds to *NRE* to prevent NLP binding and therefore blocks nitrate signalling, as NIN is highly upregulated in symbiosis in a N-deficient environment.

Several plant genes have been described to act in cooperation at neighbouring binding sites, making gene regulation more specific (Buttner and Singh, 1997; Riechmann and Meyerowitz, 1998; Diaz et al., 2002; Brown et al., 2003). The *NIN* promoter binding site for CYCLOPS-DD was identified to be a palindromic sequence of TGCCA, named "CYC-box", in the region between –717 bp and – 683 bp upstream of the transcriptional start site (Singh et al., 2014). Both NIN_C and $CYCLOPS_{BD}$ were incubated together with the *CYC-RE* resulting in a super shift in EMSA, indicating that both proteins can be simultaneously bound, next to each other (Figure 14).

It seems to be a common feature for transcription factors that the NBSs of two different DNA binding proteins are located in close proximity to each other or even partially overlap. Examples for that include CAAT binding TF, DOF TF, HD-ZIP protein and W-box binding sites for WRKY transcriptions factors (Kusnetsov et al., 1999; Yanagisawa and Schmidt, 1999; Andriankaja et al., 2007). Accordingly, *NIN* is also a transcriptional target of many known players involved in the symbiosis signalling pathway, with different identified binding elements (Hirsch and Oldroyd, 2009; Singh et al., 2014).

The *NIN* promoter is also a target for NSP1, which has the preferred binding site AATTT, and direct binding was verified to the *NIN* promoter region between -892 bp and -13 bp (Hirsch et al., 2009). Interestingly, our newly identified *NIN-RE* harbours an AATTT sequence for a putative NSP1 binding site only 6 bp downstream from the AGG recognition site for NIN binding.

NIN-RE ATATAAGTTTGCATTTTTAGGTACACAAATTT

Figure 31: Putative NSP1 binding site present on *NIN-RE*

The identified cis-binding element *"NIN-RE"* of NIN is shown, with the consensus NBS of NIN highlighted in green and a putative NSP1 binding site depicted in blue.

Therefore, it would be interesting to test if NSP1 and NIN could simultaneously bind to the *NIN-RE* cis-element, which should result in a supershift in EMSA, similar to the combined binding of NIN and CYCLOPS to the *CYC* responsive cis-element (Figure 14). In summary, *NIN* expression appears to be tightly controlled by the interplay of a massive regulatory network of different TFs.

8.4 Inhibition of nodulation: local or systemic repression caused by *NIN* overexpression

The *nin* mutant phenotype is non-nodulating, indicating that NIN is required for nodulation (Schauser et al., 1999). Still, so far no published data could successfully demonstrate complementation of *nin* mutants (Figure 18) (Yokota et al., 2010; Yoro et al., 2014; Clavijo et al., 2015). One reason might be that most *nin* mutants still produce a transcriptional product of *NIN* which might negatively regulate normal nodule development. While overexpression of a gene under a strong constitutive promoter can often complement a mutant phenotype (e.g. *NSP2*), in some cases mutants require expression of the gene under the native promotor for successful complementation, e.g. in case of the *ern1* mutant (Middleton et al., 2007; Cerri et al., 2012). Partial complementation of a *nin* mutant (*nin-2*) was shown for the infection process, by transforming a 5 kb (4877 bp) *NIN* promoter fragment into *L. japonicus* (Yokota et al., 2010), suggesting that the expression of *NIN* has to be tightly regulated to respond in certain tissues with an adequate expression level. Nodule formation was also partially complemented in *Lotus* and *Medicago* with the native promoter of *NIN* or the constitutive *poly-ubiqiutin* promoter driving *NIN* expression (Soyano et al., 2014; Yoro et al., 2014; Clavijo et al., 2015; Vernie et al., 2015).

It seems clear that the spatio-temporal expression of *NIN* has to be tightly regulated to induce the right signals for a functional mutant complementation of root nodule symbiosis. Regulatory elements upstream of the utilized 5 kb promoter sequence may be required for successful complementation, but they have not been identified so far (this work) (Yoro et al., 2014; Clavijo et al., 2015). The fact that NLPs failed to cross-complement *nin* mutants (Yokota et al., 2010), highlights the unique role NIN has acquired during evolution with a function in symbiosis (Soyano et al., 2014).

NIN overexpression driven by the *poly-ubiquitin* promoter led to inhibition of nodulation with arrested infection at the stage of micro-colony formation (Figure 15, Figure 16) (Maekawa et al., 2009). We therefore concluded that the observed inhibition in transactivation of the *NIN* promoter caused by NIN overexpression has a negative regulatory effect on infection thread formation and nodule number. Interestingly, the arrested infection phenotype at the micro colony stage observed upon overexpression of *NIN* resembles the *cyclops* mutant phenotype (Figure 16) (Yano et al., 2008). In contrast, the *nin* mutant phenotype shows excessive curling of responsive root hairs but no entrapped microcolony (Schauser et al., 1999). Overexpression of *CYCLOPS* or *NSP2*, both required for RNS, did not trigger the same negative effect on nodulation (Figure 15, Figure 21, Figure 23) (Kaló et al., 2005; Yano et al., 2008; Yokota et al., 2010), supporting the hypothesis that the negative regulation observed is a unique feature of *NIN* overexpression.

An inhibition of nodulation was only observed in transformed hairy roots (Figure 15), suggesting a local response due to the overexpression of *NIN*. In agreement with this is the observation that overexpression of *NIN* triggers an inhibition of nodulation in a mutant background involved in systemic inhibition of nodulation (Figure 19). In the original paper that identified *NIN* as an essential player in symbiosis, it was also hypothesized that NIN might act locally (Schauser et al., 1999). This was due to the observation of *nin* revertants showing densely packed nodules in a defined area of the root (Schauser et al., 1999). Moreover, a local repression effect on rhizobia infection was detected when *NIN* was expressed under a cortex specific promoter (Yoro et al., 2014). *NIN* has been shown to have a bifunctional role, in both the infection and the nodulation

process (Figure 15; Figure 16; Figure 27) (Schauser et al., 1999; Soyano et al., 2014; Yoro et al., 2014).

Soyano and collegues showed that overexpression of *NIN* under the *35S* promoter induced the formation of two distinct morphologies in the root architecture, with both malformed structures and also normal root structures (Soyano et al., 2014). This is in contrast to my work, as only normal root architecture was observed in all tested mutants upon overexpression of *NIN* (Figure 15, Figure 19). The difference in observed root architecture might be due to the usage of a different promoter (Soyano: *35S* promoter; this work: *poly-ubiqutin* promoter) and the addition of a glucocorticoid receptor (GR) to induce the 35S promoter activity (Soyano et al., 2014). In hairy roots showing normal architecture during overexpression of *NIN*, both Soyano and I report a reduction of nodulation only in GFP-positive, *NIN* overexpressing hairy roots, while the GFP-negative roots showed normal nodulation, in line with the empty vector control (this work) (Soyano et al., 2014). However, reports on roots forming malformed structures due to *NIN* overexpression demonstrate a systemic repression of nodulation, with no nodule development on either GFP-positive or GFP-negative roots (Soyano et al., 2014). They argue for a mechanism whereby *NIN* overexpression promotes CLE-RS peptide upregulation, which in turn blocks nodulation in a systemic response (Soyano et al., 2014). Hence there might be different modes of action regulated by *NIN* for local and systemic regulation of nodule development in plants.

Furthermore the domain of NIN that is responsible for the local inhibition of nodulation still needs to be identified. For example, inhibition of nodule formation was also observed for another transcriptional target of *NIN*, *SCARN,* that is required for root hair infection (Qiu et al., 2015). The negative regulatory domain of SCARN was pinpointed to the N-terminal part (Qiu et al., 2015). Interestingly, the C-terminal part of SCARN harbouring a WA domain with a function in G-acting binding led to an increased number of nodules on transformed roots in Gifu plants (Qiu et al., 2015). By analysing N- or C-terminal truncated versions of NIN, the domains of NIN involved in the negative regulation could be dissected and thus the molecular mechanism underlying the regulation could be clarified.

8.5 Involvement of *NIN* in nodule development by inducing cell division

The formation of spontaneous nodules (*snf*) was first observed with gain-of-function mutations in CCaMK (T265I, *snf1*) and LHK1 (L266F*, snf2*), which are both dependent on *NIN* expression (Tirichine et al., 2006; Tirichine et al., 2007; Hayashi et al., 2010). For the *snf2* mutant it was reported that cytokinin signalling is constantly active and triggers auxin accumulation in nodule primordia (Tirichine et al., 2007). The same effect of local auxin accumulation was detected by overexpression of *NIN,* which induced cortical cell division (Suzuki et al., 2013).

The induction of nodule-like structures was observed upon overexpression of *NIN* in 14% of transformed Gifu wild-type plants (Figure 27), similary to other works (Suzaki et al., 2012; Soyano et al., 2013; Soyano et al., 2014). This was observed in less frequent numbers compared to what was examined with overexpression of gof-CCaMK (67%) or gof-LHK1 (47%) (Madsen et al., 2010). For example, *NF-YA* was shown to be a transcriptional target of NIN and overexpression of *NF-YA* also induced swelling of root tips resembling malformed structures (Soyano et al., 2013). The paper lacked, however, convincing evidence that NIN can transactivate *NF-YA in planta* (Soyano et al., 2013). In *Medicago*, *NIN* overexpression was confirmed to induce spontaneous nodule-like structures with a high occurrence rate of 75% on transformed roots (Vernie et al., 2015). Furthermore Vernie and colleagues demonstrated that *NIN* expression driven by an epidermis (*pEXPA*) and by a cortex (*pNRT1.3*.) specific promoter still induced cortical cell division (Vernie et al., 2015). The role of *NIN* is well characterised in the cortex of legumes, where it functions as a positive factor for cortical cell division mediated by cytokinin, which in turn also leads to nodule primordia development (Heckmann et al., 2011; Soyano et al., 2013).

Transversal sections of Gifu hairy roots overexpressing *NIN* showed a larger diameter in comparison to hairy roots transformed with the empty vector control (Figure 29). The cells in the outer cortex appeared lager and an additional cell layer was visible (Figure 29). This observation is in line with work, which demonstrated that the outermost cortical cells contained larger nuclei due to a higher DNA amount, indicating endoreduplication (Bourdon et al., 2011). In addition, Soyano reported increased cell divisions caused by

NIN overexpression in pericycle cells, from which root primordia originate (Soyano et al., 2013). Based on the role of *Arabidopsis* RKD proteins in the induction of cell division, the RWP-RK domain of NIN was proposed to have a similar function (Koszegi et al., 2011; Waki et al., 2011).

I observed that *NIN* overexpression also inhibited spontaneous nodulation in both *snf1* and *snf2* mutants, suggesting that NIN might interfere with cytokinin signalling (Figure 21, Figure 23). Others demonstrated a relationship of *NIN* with the novel gene *tricot* (*Tco). Tco,* which encodes an AMP1-related carboxypeptidase, might be involved in the induction of *NIN* (Suzaki et al., 2013). Furthermore, when *Tco* was mutated an inhibition of nodulation in *snf2* was observed, supporting the hypothesis that NIN could interfere with cytokinin signalling (Suzaki et al., 2013).

8.6 A model for the negative feedback loop caused by NIN

When bacteria and plants engage in symbiosis, many plant cells actively respond to NF perception (Ehrhardt et al., 1996; Journet et al., 2001). However, only a few cells actually develop into a nodule. This process is independent from AON, as nodules are still formed in the *har1* mutant (Oldroyd and Downie, 2008; Okamoto et al., 2009; Reid et al., 2011). How this process is regulated and controlled remains unresolved. In the following model I will present a process that may answer this open question.

Based on the results obtained in this thesis, I propose here the following mechanistic model. Symbiosis signalling is activated, leading to calcium spiking in the plant (Ehrhardt et al., 1996). CCaMK, the postulated decoder of calcium spiking, phosphorylates its target CYCLOPS, forming a complex in the nucleus (Yano et al., 2008). Through the site-specific phosphorylation of CYCLOPS at serine 50 and 154, CYCLOPS gains DNA binding properties and is able to transactivate *NIN* (Singh et al., 2014). For the transcriptional activation of *NIN* the active CCaMK/CYCLOPS complex probably interacts with the basal transcription machinery (Singh et al., 2014) (Figure 32). The transcription of *NIN* is then upregulated, leading to an abundance of *NIN* expression in the cell. Consequently, NIN accumulates in the nucleus and engages in a trimeric complex with CCaMK and CYCLOPS.

A novel finding of my work is that NIN can bind to its own promoter in close vicinity to the *CYC-box* element of CYCLOPS-DD and thereby suppresses further activation of *NIN* expression in the CYCLOPS-DD mediated signaling pathway (Figure 11). In addition, co-binding of NIN and CYCLOPS to the *CYC-RE* is further stabilized through protein-protein interaction (Figure 7, Figure 14).

Hence, NIN creates a negative feedback loop on its transcriptional activation mediated by autoactive CYCLOPS-DD and prevents further *pNIN* activation, which would otherwise lead to an inhibition of nodulation (Figure 32).

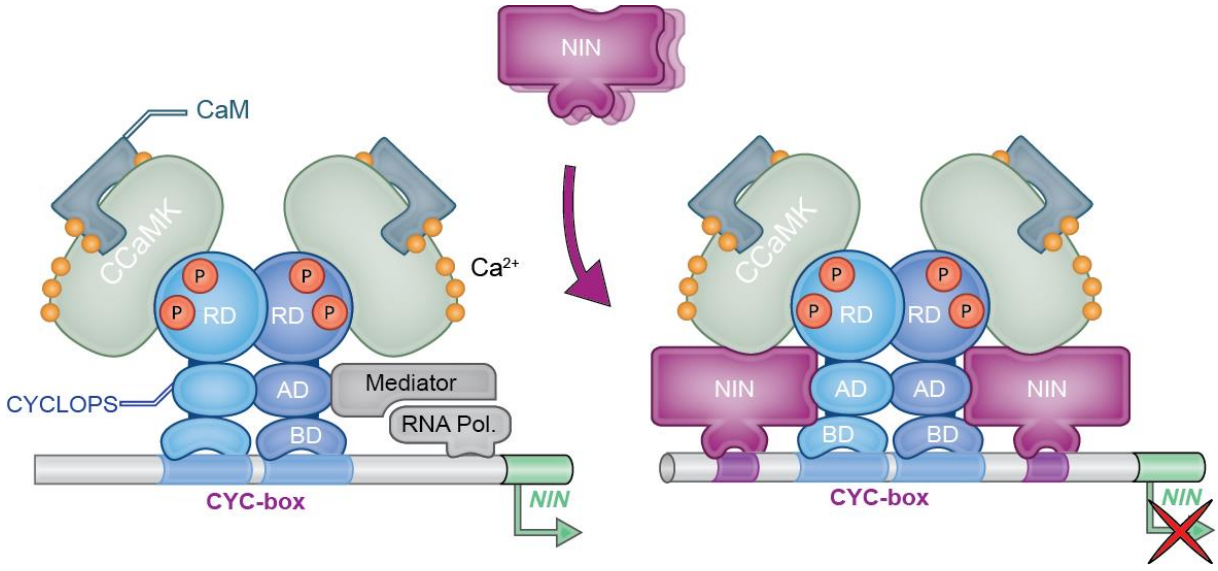

Figure 32: Model of mechanistic action of NIN creating a negative feedback loop on the activation of *NIN* expression mediated by the CCaMK/CYCLOPS complex.

Upon Calcium spiking, CCaMK gets activated and forms a complex with CYCLOPS in the nucleus. Phosphorylation of CYCLOPS by CCaMK induces a conformational change in CYCLOPS protein that turns CYCLOPS into a transcriptional activator. Then CYCLOPS is able to bind to DNA and activates the transcriptional target *NIN*. Consequently, the transcription of *NIN* is upregulated and leads to an increase in NIN protein level, which also accumulates in the nucleus. Hence, NIN engages in the complex formation with CCaMK/CYCLOPS. In addition, NIN can bind to its own promoter at cis binding elemts, which are located upstream and downstream of the cis binding element "CYC-box" bound by CYCLOPS. In turn, this prevents further activation of *NIN* expression in the CYCLOPS-DD mediated pathway, by blocking the transactivation property of CYCLOPS. This meachnism might explain the block of the formation of nodules in *Lotus japonicus* roots upon overexpression of *NIN*.

In the early phase of infection, *NIN* expression is highly upregulated, likely through the identified CYCLOPS-DD mediated pathway (Schauser et al., 1999; Yano et al., 2008; Madsen et al., 2010; Xie et al., 2012; Singh et al., 2014; Fournier et al., 2015). The expression pattern of *NIN* is associated with infected cells in the epidermis following the process of cortical cell division where nodule primordia are formed (Marsh et al., 2007; Soyano et al., 2013). Furthermore *NIN* expression in roots is activated in two stages in the early infection process (Schauser et al., 1999; Yano et al., 2008).

The observation that the co-expression of NIN and ERN1 leads to a reduction in the transactivation ability of ERN1 on the NF-responsive element of the *ENOD11* promoter (Vernie et al., 2015) is in line with my data presented in this work concerning CYCLOPS-DD and NIN (Figure 8). Both experiments observe the suppresion of gene expression caused by NIN co-expression on the binding cis elements of either ERN1 or CYCLOPS-DD (Figure 8) (Vernie et al., 2015), suggesting that NIN in combination with either protein might compete for binding to the *cis* element, or that co-binding prevents transactivation capability. However, an interaction between ERN1 and NIN similar to what was demonstrated for NIN and CYCLOPS in this work (Figure 5; Figure 7; Figure 4), has not yet been tested.

Strikingly, the binding of NIN to the *NIN* promoter can be outcompeted by addition of CYCLOPS protein in the EMSA reaction, suggesting that binding of activated CYCLOPS is more specific or has a higher affinity to the *NIN* promoter. So given equal protein amounts of NIN and CYCLOPS, activation of *NIN* expression is dominant (Figure 13). Thus NIN would need to be at an excessive amount to compete for binding to the *NIN* promoter, which is the case during the second phase of *NIN* activation in the symbiosis process (Yano et al., 2008).

In my model I speculate that *NIN* is upregulated in one cell, leading to an increase of protein in that cell. Then, NIN is able to move to neighboring cells and there prevents *NIN* activation, ensuring that limited specific infection sites are activated and discrete nodules are formed. This might involve short-distance cell-to-cell communication mediated by plasmodesmata, which are channels that traverse cell walls enabling transport through the connected cytoplasm of neighboring cells (Complainville et al., 2003).

The ability to move from the cytoplasm to the nucleus has already been demonstrated for NLPs in *Arabidopsis* (Konishi and Yanagisawa, 2013; Marchive et al., 2013). Others also hypothesized about a mobile signal that traffics between epidermis and cortex to ensure a controlled infection process and nodule development (Hayashi and Parniske, 2014; Held et al., 2014; van Zeijl et al., 2015).

The negative regulation caused by *NIN* is likely occuring within the first 24 hours of the infection process (Marsh et al., 2007; Yoro et al., 2014). A negative regulatory role of *NIN* was previously reported for the infection process, as infection was inhibited in the *daphne* mutant, harboring a mutation in the *NIN* promoter (Yoro et al., 2014). Moreover, *NIN* cannot activate its own transcription (Figure 8) (Vernie et al., 2015). I believe that the repressor function of *NIN* is directed at controlling the number of formed nodules by creating a negative feedback loop on its own expression at certain stages in symbiosis.

Further evidence to support my model is given by studies of ERN3, which might represses the association of the ERN1 activator to the DNA binding site on the *ENOD11* promoter by protein-protein interaction (Andriankaja et al., 2007). A negative feedback-loop triggered by protein-protein interaction is a common way to regulate gene expression during signaling cascades in plants. This type of regulation has also been reported for other ERF transcription factors (Fujimoto et al., 2000; Ohta et al., 2001). Recently, this mechanism has been described in *Arabidopsis* where two bHLH heterodimers (LHW and TSL1) form a complex to induce the transcription of a repressor gene (*SACL3*). In turn SACL3 prevents DNA binding of the LHW-TSL1 complex to the *SACL3* promoter, via protein-protein interaction with LHW, thus maintaining the root apical meristem (RAM) size (Katayama et al., 2015).

More and more evidence has been presented that stresses the role of *NIN* as a transcription factor with a dual role in gene regulation in the process of RNS, depending on the stage of symbiosis. Based on the obtained results, I propose that a tight regulation of *NIN* expression is required to direct its function in RNS to either exert a positive or a negative role within the signalling pathway regulating nodule organogenesis.

9 Materials and Methods

9.1 Materials

Device	**Manufacturer**
Confocal microscope, Leica TCS SP5	Leica Mikrosystems, Wetzlar
French Pressure cell press	SIM-Aminco Spectronic Instruments, Rochester
Incubators	Binder, Tuttlingen
Inverted Microscope Leica DMI6000B	Leica Mikrosystems, Wetzlar
LaminAir HB 2448	Heraeus Sepatech GmbH, Osterode
Microtiter plate reader	Tecan, Thermo Fisher Scientific
NanoDrop ND-Spectrophotometer	Kisker, Steinfurt
Sanyo ultra low (-80 °C freezer)	Heraeus Sepatech GmbH, Osterode
Stereomicroscope (Leica MZ16A)	Leica Microsystems, Wetzlar

9.2 Solutions

Name	**Components**
Bradford solution (1x)	dilution in ddH2O, stored at 4 °C
Blocking solution	TBS-T + 5 % Skimmed milk
Coomassie staining solution	10% acidic acid, 10% ethanol, 0,1% Coomassie brilliant blue
$CaCl_2$ solution	75 mM $CaCl_2$, 15 % Glycerol, 10 mM PIPES, pH 7
Extraction buffer (fluorometric Gus assay)	50 mM $NaPO_4$ pH 7; 10 mM EDTA pH 7; 0.1% Laurylsarcosine; 0.1% Triton-X100; 14,7 mM beta-Mercaptoethanol; protease inhibitor (1:1000)

GUS assay buffer	50 mM $NaPO_4$ pH 7; 10 mM EDTA pH 7; 0.1% Laurylsarcosine; 0.1% Triton-X100; 14,7 mM β-Mercaptoethanol; 1 mM 4-MUG
GUS staining solution	0.1 M $NaPO_4$, pH 7; 5 mM EDTA, pH 7; 1 mM K_3 $(Fe(CN)_6)$; 1 mM K4 $(Fe(CN)_6)$; 0.1% Trition-X100; 1 mM X-Gluc
Infiltration buffer	10 mM $MgCl_2$, 10 mM MES/KOH pH5.6, 150 μM acetosyringone
Lysis buffer (protein extraction from *N. benthamiana* leaves)	62.6 mM Tris, 2 % SDS, 10 % Gly-cerol, 5 % b-Mercaptoethanol, Protease inhibitor (1:1000)
6x SDS sample buffer	300 mM Tris/HCl (pH 6.6), 12 % SDS, 60 % Glycerol, 6 mM DTT, little bit Bromphenol blue
10 % SDS separating gel (per gel)	2 ml millipore water, 1.3 ml 1.5 M Tris, pH 8.8, 0.05 ml 10 % SDS, 1.7 ml 30 % Acrylamid, 0.05 ml 10 % APS, 0.002 ml TEMED
4 % SDS stacking gel (per gel)	0.68 ml millipore water, 0.13 ml 1M Tris pH 6.8, 0.01 ml 10 % SDS, 0.17 ml 30 % Acrylamid, 0.17 ml 10 % APS, 0.001 ml TEMED
SDS PAGE running buffer	25 mM Tris/HCl, 200 mM Glycine, 0.1 % SDS
Western Blot Transfer buffer, pH 8.3	25 mM Tris base, 192 mM Glycine, 10% Methanol
10x TBS, pH 7.6	24.2 g/l Tris base, 80 g/l NaCl
TAE-buffer	40 mM Tris-acetate, pH 8.6, 1 mM EDTA
Z-buffer (500 ml)	4.27 g NaH2PO4, 2.75 g NaH2PO4H2O, 0.375 g KCl, 0.125g MgSO4 7 H2O, pH 7, store at 4 °C (do not autoclave)

9.3 Media

B5 Medium	1.65 g Gamborg B5 salt; 10 g sucrose; 5 g Bactoagar; in 500 ml dd H_2O

Bactoagar	0.8% Bactoagar in 500 ml dd H_2O
Hoagland Solution	0,6 ml Hoagland Trace Elements; 1 ml KNO_3 (495 mM); 1 ml $Ca(NO_3)_2$ $4H_2O$ (43 mM); 2 mL $MgSO_4$ 7 H_2O (200 mM); 2 ml Fe-Citrat (22 mM)
LB Medium 1 % (w/v) Tryptone, 0.5 % (w/v)	LB Medium 1 % (w/v) Tryptone, 0.5 % (w/v) Yeast extract, 1 % (w/v) NaCl, pH 7.0(NaOH)
SD-Medium	SD-Medium 0.7 % Yeast nitrogen base without amino acids, 0.1 % Dropout mix, 2 % Glucosemonohydrate, pH 5.8
TY-Medium	TY-Medium 0.3 % (w/v) Yeast extract, 0.5 % (w/v) Tryptone, pH 7.0
YPAD Medium (liquid)	YPAD Medium (liquid) 1 % Bacto yeast extract, 2 % Bacto peptone, 2 % Glucose monohydrate, 0.004 % Adenine sulfate, pH 6.5

9.4 Chemicals

Chemicals	**Manufacturer**
Acetosyringone	Fluka, Buchs, CH
3-AT	Sigma-Aldrich, Taufkirchen
Bacterial Protease Inhibitor	Sigma-Aldrich, Taufkirchen
Biorad Protein Assay	Biorad, München
Carrier DNA (Hering Sperm, 10 mg/ml)	Promega, Mannheim
Dropout Supplement	Clontech, Mountain View, USA
Gamborg B5 salt	Sigma-Aldrich, Taufkirchen
Gelrite	Roth, Karlsruhe
LR Clonase II Enzyme Mix	Invitrogen Karlsruhe
Luminogen. TMA-6	GE Healthcare UK, Little Chalfont Buckinghamshire
4-MU	Sigma-Aldrich Taufkirchen
MUG	Sigma-Aldrich Taufkirchen
Plant Protease Inhibitor	Sigma-Aldrich Taufkirchen

Polyethylenglycol (MW 3350)	GE Healthcare Freiburg

9.5 Antibodies

Antibody	**Description**	**Dilution**	**Source**
Anti-HA-HRP	primary antibody conjugated with HRP, IgG, monoclonal, rat.	1:2000	Roche, Penzberg
Anti-GFPpoly	a-GFP primary antibody, IgG, polyclonal, mouse	1:3000	Rockland
Anti-myc	primary antibody	1:1000	Roche, Penzberg
Anti-dsRed	primary antibody	1: 5000	Clonetech
Anti-mouse IRdye800	secondary antibody conjugated with HRP, IgG, monoclonal, goat	1:10000	Biomol, Hamburg
Anti-rabbit HRP	secondary antibody	1:20000	Amersham

9.6 Plant Material

Plant species	**ecotype**	**genotype**	**reference**
Lotus japonicus	Gifu B-129	wild-type	Larsen, 1995
Lotus japonicus	MG-20	wild-type	
Lotus japonicus	Gifu	*snf1-1*	Tirichine et al., 2006
Lotus japonicus	Gifu	*snf2-2*	Tirichine et al., 2007
Lotus japonicus	Gifu	*har1-3*	(Barbulova et al., 2007)

Lotus japonicus	Gifu	*nin-2*, *nin-8*	(Schauser et al., 1999) (Perry et al., 2009)

Lotus japonicus Gifu (accession number B-129) and ecotype Miyakojima MG-20 were used as the wild-type along with five symbiotic mutants, *nin-2*, *har1-3*, *cyclops-3*, *snf1-1* and *snf2-2* in hairy root experiments.

9.7 Bacterial Strains

strain	**description**	**resistance**
Agrobacterium AR1193	MATa trp1-901 leu23,112 ura3-52 his3-200 gal4 gal80 LYS2::GAL1UASGAL1TATA-HIS3 MEL1 GAL2UAS-GAL2TATAADE2, URA3::MEL1UASMEL1TATA-lacZ, Stougaard *et al.*, 1987	rifampicin (100μg/ml), carbenicillin (50 μg/ml)
Agrobacterium agl1	Lazo *et al.*; 1991 Oct; 963-7	rifampicin (100μg/ml), carbenicillin (50 μg/ml)
Agrobacterium GV3101	Koncz & Schell, 1986	rifampicin (100 mg/ml), gentamycin (50 mg/ml)
E. coli, Top10	F-, mcrA, Δ (mrr-hsdRMS-mcrBC), φ 80lacZ ΔM15, Δ lacX74,recA1, araD139,Δ (araleu) 7697, galU, galKrpsL (StrR), endA1, nupG, λ-	
Mesorhizobium loti MAFF 303099	wild-type with RFP transgene (DsRed)	

Root transformation was performed with *A. rhizogenes* (AR1193) and nodulation experiments were done with *M. loti* MAFF303099 expressing *Ds*RED constitutively (Maekawa et al., 2009). *E.coli* strains DH5alpha, DB3.1 and TOP10 were used for plasmid transformation and propagation of the plasmid. *E.coli* Rosetta strain was used for protein expression of NIN and CYCLOPS. *A. tumefaciencs* strains agl1 and GV3101 were used for transient expression in *Nicotiana* leaf cells. Yeast strain AH109 was used for yeast transformation and in the yeast-two hybrid analysis.

9.8 Oligonucleotides

Oligonucleotides were designed in CLC Main Workbench and the web-based program primer3plus (Untergasser et al., 2012). They were ordered from Sigma-Aldrich (Germany).

Primer (5´-3´)

Contruct	Primer Sequence forward and reverse
NIN-546-878 coding sequence = NIN_C	ATGGTCTCTCACCATGTCTTCTTATA CCTTTGGAAGCCG_f ATGGTCTCACCTTTTAAGATGGGCT GCTATTGCG_r
NIN-546-643 coding sequence = RW	ATGGTCTCTCACCATGTCTTCTTATA CCTTTGGAAGCCG_f *Bsa*I ATGGTCTCACCTTTTACTGTATGGC ACCCTCAGCA_r *Bsa*I

EMSA probes and competitors (5´-3´)

CYC-RE *NIN-RE* wild-type	(Singh et al., 2014) ATATAAGTTTGCATTTTTAGGTACACAAATTT_f AAATTTGTGTACCTAAAAATGCAAACTTATAT_r
NIN-RE mutated	ATATAAGATTGCATTTTTTCCTACACAAATTT_f AAATTTGTGTAGGAAAAAATGCAATCTTATAT_r
NC-RE	TAAGTTTGCATTTTTAGGTACACAAATTTTGTACGATT GCCATGTGGCACGCA_f GCGTGCCACATGGCAATCGTACAAAATTTGTGTACCTA AAAATGCAAACTTAT_r
Pal	TACGATTGCCATGTGGCACGC_f TGCGTGCCACATGGCAATCGT_r

9.9 Plasmid construction

pENTR_*Bsa*I:cNIN-546-878 = (NIN_C)	Phusion PCR product of cNIN-546-878 nucleotide sequence amplified from pENTR:cNIN with *NIN-546-878*_fwd/rev cloned into *Bsa*I sites of pENTR_*Bsa*I-GW-*Bsa*I
pENTR_*Bsa*I:cNIN-546-643 = (RW)	Phusion PCR product of cNIN-546-643 nucleotide sequence amplified from pENTR:cNIN with *NIN-546-643*_fwd/rev cloned into *Bsa*I sites of pENTR_*Bsa*I-GW-*Bsa*I
pDEST17:cNIN-546-878 = (NIN_C) and pDEST17:cNIN-546-643 = (RW) (N-terminal 6xHis-tag)	LR reaction (Invitrogen) of pDEST17 (Invitrogen) and pENTR_BsaI:cNIN-546-878 or pENTR_BsaI:cNIN-546-643
pDEST15:CYCLOPS, phosphosite and truncated versions(N-terminal GST-tag)	Singh et al., 2014
pENTR:cNIN	Phusion PCR amplified cDNA NIN was cloned into pENTR/D TOPO via TOPO reaction (Invitrogen)
pENTR:cNSP2	Phusion PCR amplified cDNA NSP2 was cloned into pENTR/D TOPO via TOPO reaction (Invitrogen)
p35S:TSapphire-GW	Singh et al., 2014
p35S:Tsapphire-CYCLOPS and 99hosphor-site mutants	Singh et al., 2014

p35S:mOrange	Singh et al., 2014
Tsapphire-mOrange chimeric fusion	Bayle et al., 2008
p35S:mOrange-GW	Singh et al., 2014
p35S:CCaMK-mOrange	Singh et al., 2014
p35S:NIN-mOrange	LR reaction (Invitrogen) pENTR:cNINΔstop and p35S:GW-mOrange (Bayle et al., 2008)
pSPYNE35S:CYCLOPS and phosphosite mutants	Singh et al., 2014
pSPYNE35S:NIN	LR reaction (Invitrogen) of pENTR:cNIN with pSPYNE35S:GW
pSPYCE35S:CCaMK	Yano et al., 2008
pGWB735 CYCLOPS and phosphosite mutants	Singh et al., 2014
pUb:3xHAgCYCLOPS	Singh et al., 2014
pUb:cNIN	LR reaction (Invitrogen) of pENTR:cNIN and pUB:GWGFP (Maekawa et al., 2008)
pUb:cNSP2	LR reaction (Invitrogen) of pENTR:cNSP2 and pUB:GWGFP (Maekawa et al., 2008)
pUb:gNIN:myc-pUb:gCYCLOPSDD:HA-35S:GFP	LIII GG cut-ligation of LII promUb:gNIN:myc, LII promUb:gCYCLOPSDD:HA and LII 35S:GFP and insulators

Plasmids for the golden gate tool box	Binder et al., 2014
p35S:cNIN-YFP	LR reaction (Invitrogen) of pENTR:cNIN and M1((p35S:GW:YFP)
p35S:cNIN-C-YFP	LR reaction (Invitrogen) of pENTR:cNIN-C and M18 (p35S:GW:YFP)
pNIN:GUS	Singh et al., 2014
2xCYC-RE:GUS	Singh et al., 2014
BD-NIN	LR reaction (Invitrogen) of pENTR:cNIN and pBD-GAL4 Cam (Stratagene)
AD-NIN	LR reaction (Invitrogen) of pENTR:cNIN and pGAD424 (Clontech)
AD-CYCLOPS	Yano et al., 2008
BD-CYCLOPS (1-159 aa)	Yano et al., 2008
BD-CCaMK	Yano et al., 2008

10 Methods

10.1 Molecular biology methods

10.1.1 Polymerase-chain reaction

For cloning experiments the amplification of DNA fragments was performed using Phusion high fidelity polymerase (NEB) in either HF or GC buffer. Colony PCR was performed with Taq polymerase in standard buffer (NEB).

These components were mixed as follows:

Phusion PCR

component	volume
template (200 ng/µl)	1 µl
5x HF buffer	10 µl
dNTPs (5 mM)	1 µl
primer forward (2 µM)	5 µl
primer reverse (2 µM)	5 µl
Phusion(NEB con.)	1 µl
sterile ddH_2O	27 µl
total	50 µl

Standard PCR-program for Phusion polymerase:
98 °C:30 sec; (98 °C:10 sec, X °Ca 30 sec,72 °C:15-30s/1 kb) x 35; 72 °C 10 min; 4 °C

10.1.2 Electrophoresis of DNA

1 % Agarose solution was prepared with TAE buffer and boiled. Then, ethidium bromide was added to the mixture. Gel was left at RT to polymerize. Samples and DNA ladder were loaded into the sample wells. The gel was run with 120 Volts for 30 minutes. The separated fragments were visualized by a gel documentation system.

10.1.3 Extraction of PCR products from agarose gels/PCR clean-up

The gel containing DNA sample was placed on a UV table and exposed very shortly to UV. A scalpel was used to cut out the DNA fragment and transfer it to a 1.5 ml reaction tube. The extraction procedure of DNA from agarose gels was performed with the Gel Extraction kit from Fermentas according to the manufacturer´s instructions.
Alternatively, the PCR product was directly cleaned up with the PCR clean-up kit from Fermentas according to the manufacturer's instructions. The cleaned PCR product was further used in cloning reactions.

10.1.4 Plasmid isolation and estimation of DNA concentration

Plasmid DNA was isolated from 2 ml of overnight cultures of *E.coli* grown at 37°C using the GeneJET Plasmid Miniprep Kit (Thermo Scientific) according to the manufacturer's instructions. The concentration of the isolated DNA was measured with a Nanodrop spectrophotometer according to the manufacturer´s instructions.

10.1.5 Restriction endonuclease digestion of DNA

The restriction enzyme digest-mix was prepared on ice with the following components (one reaction):

Component	**Volume**
10x NEB buffer	1 µl
BSA (10mg/ml)	1 µl
Enzyme (3 units)	0.3 µl
DNA (250ng/µl)	1 µl
sterile ddH_2O	6.7 µl
total volume	10 µl

The reaction was incubated at the recommended temperature for 2 hours. The reaction was stopped with 10x DNA-loading buffer and run on a 1 % agarose gel to separate the cut fragments according to its size.

10.2 Cloning and Vector construction of *NIN*

The coding region of *NIN* was amplified using cDNA from Gifu wt roots and genomic *NIN* was amplified using genomic DNA from Gifu wt roots. The genomic sequence of *NIN* was cloned with the Golden Gate strategy (Binder et al.; details see golden gate cloning). *NIN-C* (aa) cDNA was cloned from the vector template of *NIN-FL*. For the construction of genomic *NIN* three type IIS sites had to be removed, therefore the gene was divided into 3 fragments and rejoined in a LI vector. The LII construct for *NIN* was combined as *pUb:gNIN:myc*. For the co-expression of *CYCLOPS-DD* and *NIN* together with a GFP transformation marker, a LIII vector was assembled (pUb:gNIN:myc-pUb:CYCLOPS-DD:HA-*35S:GFP)* with insulators separating the genes.

10.2.1 Golden gate cloning (cut-ligation reaction)

BsaI, BpiI and Esp3I cut-ligation:

For convenience all plasmids were diluted to a final concentration of 100 ng/µl.

The cut-ligation for Golden Gate cloning was set up as follows:

Compound	**volume**
Destination vector	1 µl
Enzyme (BsaI/BpiI/Esp3I) (5-10 units)	0,5 µl
T4 ligase buffer (10x)	1,5 µl
T4 ligase	0,75 µl
different insert vectors	1 µl
dd H_2O	ad 15 µl

For BsaI cut-ligations 0.15 µl of bovine serum albumin (10mg/ml) were added. Reactions were incubated in a thermocycler for 20-40 cycles, cycling between 37°C for 2 min and 16°C for 5 min, followed by 37°C for 5 min, 50°C for 5 minutes and 80°C for 5 minutes. 3-5 µl of the reaction were transformed into *E. coli* TOP10 or DB3.1 (for insertion of *ccdB* cassettes).

Blunt-end cut-ligation (subcloning):

For blunt-end cloning of PCR fragments into pUC57 vector an optimized cut-ligation protocol was used.

Compound	**volume**
StuI/NruI (5-10 units)	0,5 µl
T4 Ligase	1 µl

T4 ligase buffer	2 µl
100 mM ATP	0,2 µl
pUC57	25-50 ng
Insert	6:1 (6x)
H_2O	up to 20

Standard cut-ligation program: (37 °C:5 min; 20°C:5 min)x 20-40; 80 °C:10 min

0.4 µl of fresh enzyme (StuI/NruI) was added together with 0.4 µl of antarctic phosphatase (NEB) and 2 µl of phosphatase reaction buffer. Samples were incubated for another 30 min at 37°C, then heat inactivated at 80°C for 20 min.

5 µl of the reaction was transformed into *E. coli* Top10 by heat shock and plated on LB plates containing the appropriate antibiotic supplemented with 40 µg/ml X-Gal (5-Brom-4-chlor-3-indoxyl-β-D-galactopyranosid) and 100 µM IPTG (Isopropyl β-D-thiogalactopyranoside). Plasmids were isolated from white colonies and validated by sequencing.

10.2.2 Cloning: LR-reaction

LR reactions were set up like stated in the table below. The reaction mix was incubated at 25 °C for 1,5 hours.

Component	**Volume**
entry-vector (100 ng)	0.75 µl
destination-vector (300 ng)	0.75 µl
LR clonase Mix	1 µl

The whole reaction mix was transformed into E. coli by heat shock transformation.

10.2.3 TOPO Cloning

The TOPO cloning reaction was set up like listed in the table below, then the reaction was incubated for 1 hour at 21 °C.

Component	volume
pENTR-D-TOPO vector (50 ng)	0.5 µl
Salt	0.5 µl
Insert (50 ng)	1 µl
Aqua	1 µl

The whole volume of the TOPO-reaction was transformed into *E. coli* Top10 by heat shock.

10.2.4 Transformation of *E. coli* cells (heat shock method)

Chemically competent *E. coli* TOP10 or DB3.1 cells were used for transformation. Cells were thawed on ice for 2 minutes and 50 µl of the suspension was added to a 1.5 ml microliter tube. 1-5 µl of plasmid DNA or ligation reaction were added and mixed by gentle pipetting. The reaction was incubated on ice for 2 minutes, and then a heat shock of 42°C was applied for 30 seconds. The tubes were immediately returned to ice and 500 µl of LB medium was added. After incubation at 37°C on a shaker (200 rpm) for 30 min to 1 h, 50-200 µl of the suspension was plated on LB plates containing the appropriate antibiotics and incubated overnight at 37°C. Successful transformations were screened by colony PCR and/or following plasmid extraction by restriction digestions and sequencing.

10.2.5 Transformation of *Agrobacterium* cells (Electroporation method)

Electrocompetent *A. rhizogenes* AR1193 or *A. tumefaciens* AGL1 cells were used for transformation. The cells were thawed on ice for 2 minutes and mixed together in chilled 1.5 ml microliter tubes with 1-2 µl of plasmid DNA (10-50 ng) by gentle pipetting. The mixed suspension was pipetted into chilled electroporation cuvettes. For electroporation the following settings were used: Voltage 1.2 kV, conductance = 25/25/125 Fd; resistance = 400 Ω. After the pulse, the cells were immediately mixed with 500 µl of LB medium and transferred to 1.5 ml microliter tubes. Cells were incubated at 28°C for 1 hour and 20-100 µl were plated on LB plates containing the appropriate antibiotics. Successful transformations were screened by colony PCR.

10.2.6 Sequencing

DNA sequence analysis was performed by the "Sequencing Service of the Faculty of Biology" with an ABI3730 48 capillary sequencer (Applied Biosystems) using Big Dye Terminator 3.1. Sequencing runs were set up according to the "cycle, clean & run" protocol with 100 – 500 ng of plasmid DNA and 3.2 pmol of sequencing primer in a total volume of 7 µl.

10.3 Cultivation methods

10.3.1 Bacterial growth conditions

E. coli was grown at 37 °C in LB medium overnight. *Agrobacterium* strains were grown at 28 °C for 1-2 days in LB medium, *M. loti* strains were grown at 28 °C for 2 to 4 days in TY medium. Liquid cultures were shaken at 200 rpm.

10.4 Plant cultivation

10.4.1 *N. benthamiana* transformation

BiFC and localisation stduies were performed in 5 weeks old *Nicotiana benthamiana* plants following *A. tumefaciens* GV3101 pM90RK (Koncz and Schell, 1986) and Agl1 strain mediated transient transformation, respectively (Lazo et al., 1999; Walter et al., 2004).

Bacteria cultures of 2 ml LB-medium with selective antibiotics were inoculated with 1 Agrobacteria colony carrying the constructs of interest. The cultures were incubated 1-2 days at 28°C shaking at 170-220 rpm, and then the OD600 of the cultures was measured. Cultures were centrifuged at 4000 rpm for 5 min at RT, the pellet was resuspended in freshly prepared infiltration buffer and adjusted to a final OD600 of 0.5. Then, the resuspended cultures were incubated in the dark for 2 hours at RT. Agrobacterium cultures carrying constructs for testing a putative interaction/localisation were mixed with an Agrobacterium strain carrying the P19 silencing suppressor (Voinnet et al., 2003; Lakatos et al., 2004) in equal ratios. Bacterial mixtures were infiltrated into the lower side of the leaf of *N. benthamiana* plants via a small wound. After infiltration the plants were kept in a Binder growth chamber at 22°C for 16 hours day and 8 hours night cycle for 72 hours, which was determined to be the best time point for the expression of NIN. Leaf

samples were cut out, and the expression of fluorescent proteins was detected with an inverted epifluorescence or a confocal laser-scanning microscope, respectively. After microscopy, 3 leaf discs per sample were harvested and frozen in liquid nitrogen for protein extraction and western blot analysis.

10.4.2 Plant germination and growth

L. japonicus seeds were scarified with sandpaper, sterilized with 2% NaOCl containing 0.1% sodium dodecylsulfate with an incubation time of 5 minutes, then washed 5 times with 1 ml sterile ddH_2O and incubated for at least 6 hours or overnight in sterile water rotating on a wheel. Swollen seeds were transferred to 0.8% bactoagar plates and germinated in the dark (wrapped in aluminium foil) for 3 days (in vertical position). The plants were unwrapped from the foil and grown at 24°C in a 16 h light / 8 h dark cycle. Hairy root transformation was performed with 6-7 days old seedlings.

10.4.3 Lotus hairy root Transformation

Following germination *L. japonicus* seedlings were grown on 0.8% bacto agar plates for 3 days in the dark and 4 days in the light at 24 °C prior to transformation. *A. rhizogenes* AR1193 (Stougaard et al., 1987a) carrying the desired plasmids were precultivated on agar plates containing the appropriate antibiotics for 2-3 days. Bacteria from a single colony were taken and dissolved in 200 µl dd H_2O and grown for 1 day.

For hairy root transformation the bacteria were scraped off the LB plates onto a Petri dish and diluted in 1 ml of sterile water. The roots were cut at the hypocotyls with a scalpel that was covered with bacterial suspension. The wound was dipped into the bacteria and the plants were placed on agar plates containing B5 medium. The plates were covered with aluminum foil and co-cultivated in the dark at approximately 24 °C in a growth chamber. After 2 days the aluminum foil was partly removed (two thirds of the bottom of the plates was still covered to limit light exposure of the roots) and the plants were incubated for 3 days in 16 h light/8 h dark condition at 24°C in a growth chamber. The plants were transferred to B5 plates containing Cefotaxime (333 µg/ml) in order to halt the growth of the *Agrobacteria*. The plants were then cultivated at 24 °C in 16 h light/8 h dark conditions until emergence of hairy roots (2 to 3 weeks).

10.4.4 Nodulation assay

L. japonicus plants were inoculated with *Mesorhizobium loti* MAFF303099 expressing dsRed ((Maekawa, 2009 #295)). The bacteria were inoculated from a preculture plate and grown in 20 ml liquid TY medium containing 10 μg/ml gentamycin for 4 days. Cultures were centrifuged for 10 minutes at 3000 g, then suspended in 1 ml sterile water. OD_{600} was measured and the suspension was diluted in Hoagland medium to an OD_{600} of 0.05.

For nodulation of transformed *L. japonicus* hairy roots, plants were transferred from the B5 agar plates into open pots containing 300 g of sand/vermiculite (1:1) supplemented with 50 ml Hoagland medium. The plants were grown for one week at 24°C, and then inoculated evenly with 10 ml of *M. loti* MAFF303099 dsRED (OD_{600} of 0.05). Nodulation was assayed four weeks later.

In sterile assays the plants were cultivated in open pots containing 300 g of sand/vermiculite (1:1) supplemented with 50 ml Hoagland medium (10-15 plants per pot). The plants were watered with sterile water twice a week and supplemented with 50 ml Hoagland once a week. Spontanous nodulation was scored 5 weeks after transplantation.

10.4.5 AM Assay

Seeds of *L. japonicus* ecotype Gifu B-129 wild-type were scarified and surface sterilized with 1 % NaClO. Imbibed seeds were germinated on 1 % Bacto Agar (Difco) at 18 °C or 24 °C for 5-6 days. Seedlings were cultivated in chive (*Allium schoenoprasum*) nurse pots containing '*G. intraradices*-like' BEG195 (Stockinger et al., 2009) as described (Kistner et al., 2005) except that sand/vermiculite (1/1 vol.) was used as substrate. After 5 weeks of growth in open pots at 24 °C, 16 h light/ 8 h dark cycles, roots were harvested and cleared with 10 % KOH at 90 °C for 15 min. AM fungal structures were stained with ink and quantified under the inverted-fluorescence microscope using the intersections method (McGonigle et al., 1990).

10.4.6 Nodule sectioning

Mature nodules were embedded in 6% low melting agarose and sections (50 μm) were cut using the vibratome VT100S (Leica). Sections were stained with toluidine blue (0.05%)

and pictures were taken with a Leica DM16000 inverted light microscope using brightfield illumination.

10.5 Biochemical methods

10.5.1 Histochemical GUS Staining

GUS staining was performed with 3 week old transformed *L. japonicus* roots or with *N. benthamiana* leaves that carried a *pNIN*:GUS reporter 60 hours after transformation. Samples were infiltrated with a GUS staining solution (1 mM X-Gluc (5-bromo-4-chloro-3-indolyl-b-glucuronic acid), 0.1 M NaPO4 pH7, 5 mM EDTA, 0,1% Triton X-100, 1mM $K_3(Fe(CN)_6)$, 1 mM $K_4(Fe(CN)_6)$, enzymatic reaction was incubated for 3 hours at 37 °C and subsequently washed with 100 % Ethanol.

10.5.2 Fluorimetric GUS assay

Leaf samples from infiltrated *N. benthamia* plants were harvested 72 hours after infiltration and frozen in liquid nitrogen. Frozen samples were homogenized with beads in a retch mill (2x40 sec, 30/sec). Then, 200 µl extraction buffer was added to the samples and vortexed for 1 minute. Samples were rotated for 10 minutes at 4 °C and then centrifuged at 14000 rpm at 4 °C for 15 minutes. The supernatant was transferred to a new tube and used for the fluorimetric GUS assay. 10 µl of cell extract was added to GUS buffer and the reaction was incubated at 37°C for certain time points (3 min, 6 min, 9 min). The reaction was stopped by addition of 100 µl $NaCO_3$ (0,2 M). The reaction mix was measured with a tecan reader for fluorescence (4-MU) at an excitation wavelength of 360 nm and a detection wavelength of 465 nm. Protein concentration was estimated with the Bradford test. 1 µl of cell extract was mixed with 100 µl Bradford reagent and measured at the absorption of 595 nm.

10.5.1 Protein extraction from *N. benthamina* leaves

Frozen samples of 3 leaf discs per tested combination was ground with a tissue lyser with a frequency of 30/sec for 1.5 minutes. Per sample tube 300 µl of lysis buffer were added and then vortexed for 1 minute. All samples were kept on ice for a few minutes and then rotated on a wheel for 5 minutes at 4 °C. Then, the protein samples were heated at 95 °C for 5 minutes and then centrifuged at 16000 rpm for 20 minutes. The protein extracts

were separated on an SDS-PAGE and expressed proteins were detected via western blot analysis.

10.5.2 SDS PAGE

Each protein sample was mixed with 5x SDS sample buffer and incubated at 95 °C for 3 minutes. Then, all samples were shortly centrifuged prior to loading on a gel. A pre-stained protein ladder was loaded to correlate separated protein sizes from the samples. Samples were loaded on the gel and run at 150 V for 1 hour. The SDS-gel was then either stained with Coomassie staining solution or subjected in a western blot with protein transfer on a membrane.

10.5.3 Western blot

The PVDF-membrane was activated by incubation in 100 % ethanol for 15 seconds and then transferred to transfer buffer for 5 minutes. A sandwich for the transfer of proteins from an SDS-gel to the membrane was put together with 4 Whatman filter papers and 2 western sponges. The blot was run at 130V for 90 minutes. After transfer of the proteins from the gel to the membrane, the PVDF-membrane was washed with TBS once and then washed with TBS-T twice (each time for 10 minutes). For blocking the membrane was incubated in TBS-T with 5 % milk for 1 hour at RT on a shaker or overnight at 4 °C. The membrane was washed 3 times with TBS-T for 10 minutes on a shaker. Antibodies were diluted in TBS-T with 5 % milk and added to the membrane for 2 hours at RT or overnight at 4°C. The membrane was washed again 3 times with TBS-T for 10 minutes. A secondary antibody conjugated with HRP was added to the membrane for the duration of 1 hour. Additional washing was performed 3 times with TBS-T for 10 minutes. Horseradish peroxidase (HRP) activity was detected using chemiluminescence.

10.5.4 Protein expression and purification

Expression of NIN deletion constructs was induced in *E. coli* Rosetta pLaqI (Novagen) for 12 hr at 18 °C by addition of 0.5 mM IPTG. His-tagged proteins were purified by metal affinity chromatography using TALON resin (Clontech) as described by the protocol of the manufacturer. Buffer conditions were modified accordingly (binding and wash buffer: 20 mM PIPES, 500 mM KCl, 2 mM β-mercapto-ethanol, 10 mM imidazole, pH 7.0; elution buffer: 20 mM PIPES, 200 mM KCl, 2 mM β-mercapto-ethanol, 250 mM

imidazole, pH 7.0). Expression and purification of GST-CYCLOPS phosphosite and truncated versions was performed as described (Sing et al., 2014). Protein concentration was determined by the Bradford Method (Bio-Rad), using BSA (Sigma) as a standard. Protein purity was analyzed by SDS-PAGE and Coomassie staining of the gel.

10.5.5 Electrophoretic mobility shift assay

Binding reaction composition and practical application was as described in Sing et al.. 2014. 100 fmol 5' CY5 labeled DNA and 15 pmol NIN_C and RW, 25 pmol NIN_N, 20 pmol CYC_{BD}, 35 pmol CYC_{Min} and 75 pmol CYC_{DD} were used (competitor DNA and variant molar amounts of protein are indicated within the figure). Reactions were solved on 4 % native polyacrylamide gels. CY5 labeled DNA was visualized with the Typhoon TriO phosphoimager (Amersham Biosciences). Complementary pairs of labeled and unlabeled oligonucleotide probes are listed in 9.8.

10.5.6 Bradford assay for protein standard curve and protein concentration measurement

Bradford reagent was diluted with ddH_2O in a ratio of 1:5 and filter sterilized. A dilution series of 1000 µg, 500 µg, 250 µg and 125 µg BSA was prepared, by diluting a 100mg/l BSA stock solution. The reaction mixes were incubated for a maximum of 10 minutes at RT and the OD of each sample was measured at 595 nm. For the determination of protein concentrations, 20 µl of protein sample were mixed with 980 µl Bradford solution. Then the concentration of proteins was calculated from the BSA standard curve using MS Excel.

10.5.7 Yeast two-hybrid

Yeast two-hybrid interaction assay was performed in the the yeast AH109 according to the user manual (Yeast Protocols Handbook, Clonetech). AH109 yeast strain were transformed with the lithium acetate method (Woods and Gietz, 2001). Transformants were screened on SD medium containg 0,67 % yeast nitrogen base, 2% glucose, but lacking appropriate nutrients.

A single colony of AH109 was inoculated into 20 ml YPAD-medium and grown in a shaker at 30 °C overnight. The OD of the yeast culture was measured at 546 nm. The Culture was adjusted to an OD of 0.2 and then grown until an OD of 0.6-0.8. Culture was

pelleted for 5 minutes at 700 g and resuspended in 1 ml sterile H2O (an amount sufficient for 10 single- or co-transformations).
A master mix was prepared with the following components (one transformation) and vortexed briefly:

component	volume
50 % PEG	240 µl
1 M LiAc	36 µl
ssDNAa	30 µl
total	306 µl

Per transformation 300 µl of master mix were used and mixed with 7. 5 µl of plasmid-DNA (200 ng/µl) and 100 µl yeast cells. The mix was vortexed for 1 minute. The mixtures were incubated in a water bath at 42 °C for 45 minutes. Then a centrifugation step was performed at 700 g for 5 minutes. The Pellet was resuspended in 100 µl sterile 0.9 % NaCl and plated onto selective SD(-)LW plates. The plates were incubated at 30 °C for 2-3 days and grown yeast colonies were subjected to a yeast two hybrid test.
10 independent clones of each combination were picked and inoculated into 500 µl sterile water in a 12 well plate. Then the cultures were incubated at 30°C shaking at 170-220 rpm overnight. The next day, all cultures were adjusted to an OD546 of 1.0. For each construct dilutions of 10^1, 10^2 and 10^3 were prepared in sterile ddH_2O. A metallic stamp was used to transfer 10 µl of each diluted sample to the selective SD plates. All plates were and incubated at 30 °C for 2-3 days and yeast growth was analysed.

10.6 Microscopy

Confocal laser scanning microcopy (CLSM) was performed with a Leica SP5 microscope. *N. benthamiana* leaves were vacuum infiltrated prior to imaging and imaged with a HCX PL Fluotar 63x objective. For image acquisition the resolution was set to 512 x 512 pixels and the frame average to 2. Using the argon laser at 20% power, GFP was excited with the 488 nm laser line and detected at 500-530 nm, YFP with the 514 nm spectral line and detected at 530-550 nm, mOrange was excited with the 514 nm laser line and detected at 545 nm to 600 nm. TSapphire was excited with a 405 diode laser and detected at 485 nm

to 535 nm. Images of *L. japonicus* root systems were taken using a Leica M165 FC epifluorescence stereomicroscope equipped with a GFP and RFP filter.

10.6.1 FLIM-FRET

Nicotiana benthamiana leaves were co-infiltrated with *Agrobacterium tumefaciens* bacteria carrying the respective plasmid constructs. 60 hpi leave discs were harvested and used for the interaction study. For CLSM T-Sapphire was excited with a 405 diode laser, whereas mOrange was excited with a 514 nm argon laser line (Bayle et. al., 2008). The emission of TSapphire was detected with a 485 nm to 535 nm band pass emission filter, while mOrange was detected with a 545 nm to 600 nm band-pass emission filter. A Ti-Sapphire Mai Tai multiphoton (MP) laser from Spectra Physics was tuned at 800 nm for the excitation of TSapphire fluorescence, which runs at 80 mHz with a 100 fs pulse length. For a single FLIM measurement a number of 20 scanning cycles (5s/cycle) were applied to get a suitable photon count rate at a spatial resolution of 256x256 pixels. As the FLIM setup a Leica SP5 microscope with an implemented FLIM PMT detector from Becker and Hickl were used. Hence the Becker and Hickl photon count software TCSPC2.80 was used for recording the light signals. For lifetime calculations a region of interest was set around the nucleus and the double exponential model was applied for all interaction pairs in the Becker and Hickl SPCImage software. Both scatter and shift were fixed to zero. The FRET efficiency was calculated as described in Bayle et al., 2008.

10.6.2 Statistics

All statistical analyses and data plots have been performed and generated with R version 3.0.2. For statistical analysis of the numbers of nodules, AM structures and FLIM-FRET a t-test and ANOVA was applied.

11 List of Figures

12 List of Tables

13 List of Abbreviations

° C	degree(s) Celsius
µ	micro
A / ala	alanine
aa	amino acid
AD	activation domain
AM	arbuscular mycorrhiza
Amp	Ampicilin
ANOVA	analysis of variance
AON	autoregulation of nodulation
BD	binding domain
BiFC	bimolecular fluorescence complementation
BF	bright field
bp	base pair
CaM	Calmodulin
CaMBD	Calmodulin binding domain
CCaMK	Calcium Calmodulin dependent Kinase
CIP	CCaMK interacting protein
cDNA	complementary DNA
CLE	CLAVATA3/ENDOSPERM SURROUNDING REGION
CLE-RS	CLE root signal
CLSM	confocal laser microscopy
CNCG	cyclic nucleotide-gated channel
D / asp	aspartic acid
Da	Dalton
dd H_2O	double distilled water / Millipore filtered water
dpi	days post infection/inoculation

dpt	days post transformation
EMSA	Electrophoretic mobility shift assay
ENOD11	Early Nodulin11
ERF	Ethylene Response Factor
ERN	ERF required for nodulation
FLIM	Fluorescence Lifetime Imaging Microscopy
FRET	Förster Resonance Energy Transfer
g	gravitational acceleration / gram(s)
Gent	gentamycin
GFP	Green Fluorescent Protein
GG	golden gate
GOI	gene of interest
GUS	β-glucuronidase
h	hour(s)
HAR1	Hypernodulation aberrant root formation
HRP	horse radish peroxidase
IPTG	isopropyl β-D-thiogalactopyranoside
IT	infection thread
Kan	kanamycin
k	kilo
LB	lysogeny broth / Luria-Bertani broth
L	litre(s)
LHK	Lotus histidine kinase
Lj	*Lotus japonicus*
LysM	lysin motif
M	molar
m	meter(s) / mili
min	minute(s)

mO	mOrange
n	nano
NBS	NIN binding site
NF	nodulation factor
NFR1	Nod Factor Receptor 1
NF-Y	Nuclear Factor-Y subunit
NIN	nodule inception
NLS	nuclear localization signal
NLP	NIN like protein
NPL	pectate lyase
NRE	Nitrate responsive element
NUP	nucleoporin
NSP	nodulation signalling pathway
OD	optical density
p	p-value
p35S	cauliflower mosaic virus 35S promoter
PCR	polymerase chain reaction
RAM	root apical meristem
RFP	Red Fluorescent Protein
RLK	receptro like kinase
RNS	root nodule symbiosis
ROI	region of interest
rpm	rounds per minute
RT	room temperature
s	second(s)
S / ser	serine
snf	spontaneous nodule formation
SYMREM1	Symbiotic Remorin 1
SYMRK	Symbiosis Receptor-like Kinase

T / thr	threonine
TALEs	transciption activator-like effectors
TF	transcription factor
TM	transmembrane domain
TS	TSapphier
Tukey's HSD	Tukey's Honestly Significant Difference
UAS	upstream activated sequence
promUb	poly Ubiquitin promoter
VLD	Visin like domain
wt	wild-type
X-Gal	5-Brom-4-chlor-3-indoxyl-β-D-galactopyranosid
X-Gluc	5-bromo-4-chloro-3-indolyl glucuronide
Y2H	yeast two-hybrid
YFP	Yellow Fluorescent Protein

14 Declaration of contribution of other researches

Jayne Lambert, the author of this thesis contributed to the experiments displayed in figure 1-32 as follows:

Figure 1: designed by Andreas Binder and modified by Jayne Lambert

Figure 2-6, 10, 15-32: Experiments were designed, performed and analysed by Jayne Lambert, statistical analysis was done by Jayne Lambert, who also prepared the corresponding figures

Figure 7-9: Experiments were designed by Jayne Lambert, performed and analysed by Jayne Lambert and Isabel Seidler, pictures were taken by Jayne Lambert, and figures were prepared by Jayne Lambert

Figure 11-14: Experiments were designed by Jayne Lambert and Katja Katzer, EMSAs were performed by Katja Katzer, and figures were prepared by Jayne Lambert and Katja Katzer

15 References

Andriankaja A, Boisson-Dernier A, Frances L, Sauviac L, Jauneau A, Barker DG, de Carvalho-Niebel F (2007) AP2-ERF transcription factors mediate Nod factor dependent *MtENOD11* activation in root hairs via a novel cis-regulatory motif. Plant Cell **19:** 2866-2885

Ané J, Kiss G, Riely B, Penmetsa R, Oldroyd G, Ayax C, Lévy J, Debellé F, Baek J, Kalo P, Rosenberg C, Roe B, Long S, Dénarié J, Cook D (2004) *Medicago truncatula* DMI1 required for bacterial and fungal symbioses in legumes. Science **303:** 1364-1367

Antolin-Llovera M, Ried MK, Parniske M (2014) Cleavage of the SYMBIOSIS RECEPTOR-LIKE KINASE Ectodomain Promotes Complex Formation with Nod Factor Receptor 5. Current Biology **24:** 422-427

Barbulova A, Rogato A, D'Apuzzo E, Omrane S, Chiurazzi M (2007) Differential effects of combined N sources on early steps of the Nod factor-dependent transduction pathway in *Lotus japonicus*. Mol Plant Microbe Interact **20:** 994-1003

Bateman A, Bycroft M (2000) The structure of a LysM domain from E. coli membrane-bound lytic murein transglycosylase D (MltD). J Mol Biol **299:** 1113-1119

Bayle V, Nussaume L, Bhat R (2008) Combination of novel green fluorescent protein mutant TSapphire and DsRed variant mOrange to set up a versatile in planta FRET-FLIM assay. Plant Physiol **148:** 51-60

Binder A, Lambert J, Morbitzer R, Popp C, Ott T, Lahaye T, Parniske M (2014) A Modular Plasmid Assembly Kit for Multigene Expression, Gene Silencing and Silencing Rescue in Plants. Plos One **9**

Bolanos L, Redondo-Nieto M, Rivilla R, Brewin NJ, Bonilla I (2004) Cell surface interactions of Rhizobium bacteroids and other bacterial strains with symbiosomal and peribacteroid membrane components from pea nodules. Mol Plant Microbe Interact **17:** 216-223

Bolle C (2004) The role of GRAS proteins in plant signal transduction and development. Planta **218:** 683-692

Bonfante P, Genre A, Faccio A, Martini I, Schauser L, Stougaard J, Webb J, Parniske M (2000) The *Lotus japonicus LjSym4* gene is required for the successful symbiotic infection of root epidermal cells. Mol Plant Microbe Interact **13:** 1109-1120

Borisov A, Madsen L, Tsyganov V, Umehara Y, Voroshilova V, Batagov A, Sandal N, Mortensen A, Schauser L, Ellis N, Tikhonovich I, Stougaard J (2003) The *Sym35* gene required for root nodule development in pea is an ortholog of *Nin* from *Lotus japonicus*. Plant Physiol **131:** 1009-1017

Bourdon M, Coriton O, Pirrello J, Cheniclet C, Brown SC, Poujol C, Chevalier C, Renaudin JP, Frangne N (2011) In planta quantification of endoreduplication using fluorescent in situ hybridization (FISH). Plant J **66:** 1089-1099

Breakspear A, Liu C, Roy S, Stacey N, Rogers C, Trick M, Morieri G, Mysore KS, Wen J, Oldroyd GE (2014) The Root Hair "Infectome" of *Medicago truncatula* Uncovers changes in cell cycle genes and reveals a requirement for auxin signaling in rhizobial infection. The Plant Cell Online**:** tpc. 114.133496

Brewin B, Woodley P, Drummond M (1999) The basis of ammonium release in nifL mutants of Azotobacter vinelandii. J Bacteriol **181:** 7356-7362

Broghammer A, Krusell L, Blaise M, Sauer J, Sullivan JT, Maolanon N, Vinther M, Lorentzen A, Madsen EB, Jensen KJ, Roepstorff P, Thirup S, Ronson CW, Thygesen MB, Stougaard J (2012) Legume receptors perceive the rhizobial lipochitin oligosaccharide signal molecules by direct binding. Proc Natl Acad Sci U S A **109:** 13859-13864

Brown RL, Kazan K, McGrath KC, Maclean DJ, Manners JM (2003) A role for the GCC-box in jasmonate-mediated activation of the *PDF1.2* gene of *Arabidopsis*. Plant Physiol **132:** 1020-1032

Buttner M, Singh KB (1997) *Arabidopsis thaliana* ethylene-responsive element binding protein (AtEBP), an ethylene-inducible, GCC box DNA-binding protein interacts with an ocs element binding protein. Proc Natl Acad Sci U S A **94:** 5961-5966

Buzas DM, Gresshoff PM (2007) Short- and long-distance control of root development by *LjHAR1* during the juvenile stage of *Lotus japonicus*. J Plant Physiol **164:** 452-459

Carrera I, Treisman JE (2008) Message in a nucleus: signaling to the transcriptional machinery. Curr Opin Genet Dev **18:** 397-403

Castaings L, Camargo A, Pocholle D, Gaudon V, Texier Y, Boutet-Mercey S, Taconnat L, Renou J, Daniel-Vedele F, Fernandez E, Meyer C, Krapp A (2009) The nodule inception-like protein 7 modulates nitrate sensing and metabolism in *Arabidopsis*. Plant J **57:** 426-435

Cermak T, Doyle EL, Christian M, Wang L, Zhang Y, Schmidt C, Baller JA, Somia NV, Bogdanove AJ, Voytas DF (2011) Efficient design and assembly of custom TALEN and other TAL effector-based constructs for DNA targeting. Nucleic Acids Research **39:** e82

Cerri MR, Frances L, Kelner A, Fournier J, Middleton PH, Auriac MC, Mysore KS, Wen J, Erard M, Barker DG, Oldroyd GE, de Carvalho-Niebel F (2016) The symbiosis-related ERN transcription factors act in concert to coordinate rhizobial host root infection. Plant Physiol **171:** 1037-1054

Cerri MR, Frances L, Laloum T, Auriac MC, Niebel A, Oldroyd GE, Barker DG, Fournier J, de Carvalho-Niebel F (2012) *Medicago truncatula* ERN transcription factors: regulatory interplay with NSP1/NSP2 GRAS factors and expression dynamics throughout rhizobial infection. Plant Physiol **160:** 2155-2172

Chabaud M, Genre A, Sieberer BJ, Faccio A, Fournier J, Novero M, Barker DG, Bonfante P (2011) Arbuscular mycorrhizal hyphopodia and germinated spore exudates trigger Ca2+ spiking in the legume and nonlegume root epidermis. New Phytologist **189:** 347-355

Chardin C, Girin T, Roudier F, Meyer C, Krapp A (2014) The plant RWP-RK transcription factors: key regulators of nitrogen responses and of gametophyte development. J Exp Bot **65:** 5577-5587

Charpentier M, Bredemeier R, Wanner G, Takeda N, Schleiff E, Parniske M (2008) *Lotus japonicus* CASTOR and POLLUX are ion channels essential for perinuclear calcium spiking in legume root endosymbiosis. Plant Cell **20:** 3467-3479

Charpentier M, Sun J, Vaz Martins T, Radhakrishnan GV, Findlay K, Soumpourou E, Thouin J, Very AA, Sanders D, Morris RJ, Oldroyd GE (2016) Nuclear-localized cyclic nucleotide-gated channels mediate symbiotic calcium oscillations. Science **352:** 1102-1105

Charron D, Pingret JL, Chabaud M, Journet EP, Barker DG (2004) Pharmacological evidence that multiple phospholipid signaling pathways link Rhizobium nodulation factor perception in Medicago truncatula root hairs to intracellular responses, including Ca2+ spiking and specific ENOD gene expression. Plant Physiol **136:** 3582-3593

Clavijo F, Diedhiou I, Vaissayre V, Brottier L, Acolatse J, Moukouanga D, Crabos A, Auguy F, Franche C, Gherbi H, Champion A, Hocher V, Barker D, Bogusz D, Tisa LS, Svistoonoff S (2015) The *Casuarina NIN* gene is transcriptionally activated throughout Frankia root infection as well as in response to bacterial diffusible signals. New Phytol

Complainville A, Brocard L, Roberts I, Dax E, Sever N, Sauer N, Kondorosi A, Wolf S, Oparka K, Crespi M (2003) Nodule initiation involves the creation of a new symplasmic field in specific root cells of medicago species. Plant Cell **15:** 2778-2791

Delaux PM, Radhakrishnan GV, Jayaraman D, Cheema J, Malbreil M, Volkening JD, Sekimoto H, Nishiyama T, Melkonian M, Pokorny L, Rothfels CJ, Sederoff HW, Stevenson DW, Surek B, Zhang Y, Sussman MR, Dunand C, Morris RJ, Roux C, Wong GK, Oldroyd GE, Ane JM (2015) Algal ancestor of land plants was preadapted for symbiosis. Proc Natl Acad Sci U S A **112:** 13390-13395

Delaux PM, Sejalon-Delmas N, Becard G, Ane JM (2013) Evolution of the plant-microbe symbiotic 'toolkit'. Trends Plant Sci **18:** 298-304

Den Herder G, Parniske M (2009) The unbearable naivety of legumes in symbiosis. Curr Opin Plant Biol **12:** 491-499

Denarie J, Debelle F, Prome JC (1996) Rhizobium lipo-chitooligosaccharide nodulation factors: signaling molecules mediating recognition and morphogenesis. Annu Rev Biochem **65:** 503-535

Diaz I, Vicente-Carbajosa J, Abraham Z, Martinez M, Isabel-La Moneda I, Carbonero P (2002) The GAMYB protein from barley interacts with the DOF transcription factor BPBF and activates endosperm-specific genes during seed development. Plant J **29:** 453-464

Ehrhardt D, Wais R, Long S (1996) Calcium spiking in plant root hairs responding to Rhizobium nodulation signals. Cell **85:** 673-681

Endre G, Kereszt A, Kevei Z, Mihacea S, Kaló P, Kiss G (2002) A receptor kinase gene regulating symbiotic nodule development. Nature **417:** 962-966

Engler C, Gruetzner R, Kandzia R, Marillonnet S (2009) Golden gate shuffling: A one-pot DNA shuffling method based on type IIs restriction enzymes. PLoS ONE **4:** e5553

Engler C, Kandzia R, Marillonnet S (2008) A one pot, one step, precision cloning method with high throughput capability. PLoS ONE **3:** e3647

Engler C, Marillonnet S (2011) Generation of Families of Construct Variants Using Golden Gate Shuffling. *In* C Lu, J Browse, JG Wallis, eds, cDNA Libraries, Vol 729. Humana Press, pp 167-181

Esseling JJ, Lhuissier FG, Emons AM (2003) Nod factor-induced root hair curling: continuous polar growth towards the point of nod factor application. Plant Physiol **132:** 1982-1988

Fisher RF, Long SR (1992) *Rhizobium*--plant signal exchange. Nature **357:** 655-660

Flores JK, Kariawasam R, Gimenez AX, Helder S, Cubeddu L, Gamsjaeger R, Ataide SF (2015) Biophysical Characterisation and Quantification of Nucleic Acid-Protein Interactions: EMSA, MST and SPR. Curr Protein Pept Sci **16:** 727-734

Fournier J, Teillet A, Chabaud M, Ivanov S, Genre A, Limpens E, de Carvalho-Niebel F, Barker DG (2015) Remodeling of the infection chamber before infection thread formation reveals a two-step mechanism for rhizobial entry into the host legume root hair. Plant Physiol **167:** 1233-1242

Fournier J, Timmers AC, Sieberer BJ, Jauneau A, Chabaud M, Barker DG (2008) Mechanism of infection thread elongation in root hairs of *Medicago truncatula* and dynamic interplay with associated rhizobial colonization. Plant Physiol **148:** 1985-1995

Fried MG (1989) Measurement of protein-DNA interaction parameters by electrophoresis mobility shift assay. Electrophoresis **10:** 366-376

Fujimoto SY, Ohta M, Usui A, Shinshi H, Ohme-Takagi M (2000) Arabidopsis ethylene-responsive element binding factors act as transcriptional activators or repressors of GCC box-mediated gene expression. Plant Cell **12:** 393-404

Gage D (2004) Infection and invasion of roots by symbiotic, nitrogen-fixing rhizobia during nodulation of temperate legumes. Microbiol Mol Biol Rev **68:** 280-300

Geurts R, Fedorova E, Bisseling T (2005) Nod factor signaling genes and their function in the early stages of Rhizobium infection. Curr Opin Plant Biol **8:** 346-352

Gleason C, Chaudhuri S, Yang T, Muñoz A, Poovaiah B, Oldroyd G (2006) Nodulation independent of rhizobia induced by a calcium-activated kinase lacking autoinhibition. Nature **441:** 1149-1152

Gonzalez-Rizzo S, Crespi M, Frugier F (2006) The *Medicago truncatula* CRE1 cytokinin receptor regulates lateral root development a nd early symbiotic interaction with *Sinorhizobium meliloti*. Plant Cell **18:** 2680-2693

Groth M, Takeda N, Perry J, Uchida H, Draxl S, Brachmann A, Sato S, Tabata S, Kawaguchi M, Wang TL, Parniske M (2010) NENA, a *Lotus japonicus* homolog of Sec13, is required for rhizodermal infection by arbuscular mycorrhiza fungi and rhizobia but dispensable for cortical endosymbiotic development. Plant Cell **22:** 2509-2526

Gutjahr C, Parniske M (2013) Cell and developmental biology of arbuscular mycorrhiza symbiosis. Annual Review of Cell and Developmental Biology, Vol 29 **29:** 593-617

Harrison MJ (1999) Molecular and cellular aspects of the arbuscular mycorrhizal symbiosis. Annu Rev Plant Physiol Plant Mol Biol **50:** 361-389

Hayashi M, Parniske M (2014) Symbiosis and pathogenesis: What determines the difference? Current Opinion in Plant Biology **20:** V-VI

Hayashi T, Banba M, Shimoda Y, Kouchi H, Hayashi M, Imaizumi-Anraku H (2010) A dominant function of CCaMK in intracellular accommodation of bacterial and fungal endosymbionts. Plant J **63:** 141-154

Heckmann A, Lombardo F, Miwa H, Perry J, Bunnewell S, Parniske M, Wang T, Downie J (2006) *Lotus japonicus* nodulation requires two GRAS domain regulators, one of which is functionally conserved in a non-legume. Plant Physiol **142:** 1739-1750

Heckmann AB, Sandal N, Bek AS, Madsen LH, Jurkiewicz A, Nielsen MW, Tirichine L, Stougaard J (2011) Cytokinin induction of root nodule primordia in

Lotus japonicus is regulated by a mechanism operating in the root cortex. Mol Plant Microbe Interact **24:** 1385-1395

Held M, Hou H, Miri M, Huynh C, Ross L, Hossain MS, Sato S, Tabata S, Perry J, Wang TL, Szczyglowski K (2014) *Lotus japonicus* cytokinin receptors work partially redundantly to mediate nodule formation. Plant Cell **26:** 678-694

Hirsch S, Kim J, Munoz A, Heckmann AB, Downie JA, Oldroyd GE (2009) GRAS proteins form a DNA binding complex to induce gene expression during nodulation signaling in Medicago truncatula. Plant Cell **21:** 545-557

Hirsch S, Oldroyd GE (2009) GRAS-domain transcription factors that regulate plant development. Plant Signal Behav **4:** 698-700

Horvath B, Yeun LH, Domonkos A, Halasz G, Gobbato E, Ayaydin F, Miro K, Hirsch S, Sun J, Tadege M, Ratet P, Mysore KS, Ane JM, Oldroyd GE, Kalo P (2011) *Medicago truncatula IPD3* is a member of the common symbiotic signaling pathway required for rhizobial and mycorrhizal symbioses. Mol Plant Microbe Interact **24:** 1345-1358

Hrabak EM, Chan CW, Gribskov M, Harper JF, Choi JH, Halford N, Kudla J, Luan S, Nimmo HG, Sussman MR, Thomas M, Walker-Simmons K, Zhu JK, Harmon AC (2003) The *Arabidopsis* CDPK-SnRK superfamily of protein kinases. Plant Physiol **132:** 666-680

Imaizumi-Anraku H, Takeda N, Charpentier M, Perry J, Miwa H, Umehara Y, Kouchi H, Murakami Y, Mulder L, Vickers K, Pike J, Downie JA, Wang T, Sato S, Asamizu E, Tabata S, Yoshikawa M, Murooka Y, Wu GJ, Kawaguchi M, Kawasaki S, Parniske M, Hayashi M (2005) Plastid proteins crucial for symbiotic fungal and bacterial entry into plant roots. Nature **433:** 527-531

Jarsch IK, Ott T (2011) Perspectives on remorin proteins, membrane rafts, and their role during plant-microbe interactions. Mol Plant Microbe Interact **24:** 7-12

Jones K, Kobayashi H, Davies B, Taga M, Walker G (2007) How rhizobial symbionts invade plants: the Sinorhizobium-Medicago model. Nat Rev Microbiol **5:** 619-633

Journet EP, El-Gachtouli N, Vernoud V, de Billy F, Pichon M, Dedieu A, Arnould C, Morandi D, Barker DG, Gianinazzi-Pearson V (2001) *Medicago truncatula ENOD11*: a novel RPRP-encoding early nodulin gene expressed during mycorrhization in arbuscule-containing cells. Mol Plant Microbe Interact **14:** 737-748

Kaló P, Gleason C, Edwards A, Marsh J, Mitra R, Hirsch S, Jakab J, Sims S, Long S, Rogers J, Kiss G, Downie J, Oldroyd G (2005) Nodulation signaling in legumes requires NSP2, a member of the GRAS family of transcriptional regulators. Science **308:** 1786-1789

Kanamori N, Madsen L, Radutoiu S, Frantescu M, Quistgaard E, Miwa H, Downie J, James E, Felle H, Haaning L, Jensen T, Sato S, Nakamura Y, Tabata S, Sandal N, Stougaard J (2006) A nucleoporin is required for induction of Ca2+ spiking in legume nodule development and essential for rhizobial and fungal symbiosis. Proc Natl Acad Sci U S A **103:** 359-364

Kang H, Xiao A, Huang X, Gao X, Yu H, He X, Zhu H, Hong Z, Zhang Z (2015) A *Lotus japonicus* cochaperone protein interacts with the ubiquitin-like domain protein CIP73 and plays a negative regulatory role in nodulation. Mol Plant Microbe Interact **28:** 534-545

Kang H, Zhu H, Chu X, Yang Z, Yuan S, Yu D, Wang C, Hong Z, Zhang Z (2011) A novel interaction between CCaMK and a protein containing the Scythe_N ubiquitin-like domain in *Lotus japonicus*. Plant Physiol **155:** 1312-1324

Katayama H, Iwamoto K, Kariya Y, Asakawa T, Kan T, Fukuda H, Ohashi-Ito K (2015) A negative feedback loop controlling bHLH complexes is involved in vascular cell division and differentiation in the root apical meristem. Curr Biol **25:** 3144-3150

Kerppola TK (2008) Bimolecular fluorescence complementation (BiFC) analysis as a probe of protein interactions in living cells. Annu Rev Biophys **37:** 465-487

Kistner C, Parniske M (2002) Evolution of signal transduction in intracellular symbiosis. Trends Plant Sci **7:** 511-518

Kistner C, Winzer T, Pitzschke A, Mulder L, Sato S, Kaneko T, Tabata S, Sandal N, Stougaard J, Webb K, Szczyglowski K, Parniske M (2005) Seven *Lotus japonicus* genes required for transcriptional reprogramming of the root during fungal and bacterial symbiosis. Plant Cell **17:** 2217-2229

Konishi M, Yanagisawa S (2013) Arabidopsis NIN-like transcription factors have a central role in nitrate signalling. Nature Communications **4:** 1617

Konishi M, Yanagisawa S (2014) Emergence of a new step towards understanding the molecular mechanisms underlying nitrate-regulated gene expression. Journal of experimental botany **65:** 5589-5600

Kosuta S, Hazledine S, Sun J, Miwa H, Morris RJ, Downie JA, Oldroyd GE (2008) Differential and chaotic calcium signatures in the symbiosis signaling pathway of legumes. Proceedings of the National Academy of Sciences **105:** 9823-9828

Kosuta S, Held M, Hossain MS, Morieri G, Macgillivary A, Johansen C, Antolin-Llovera M, Parniske M, Oldroyd GE, Downie AJ, Karas B, Szczyglowski K (2011) *Lotus japonicus symRK-14* uncouples the cortical and epidermal symbiotic program. Plant J **67:** 929-940

Koszegi D, Johnston AJ, Rutten T, Czihal A, Altschmied L, Kumlehn J, Wust SE, Kirioukhova O, Gheyselinck J, Grossniklaus U, Baumlein H (2011) Members of the RKD transcription factor family induce an egg cell-like gene expression program. Plant J **67:** 280-291

Krusell L, Madsen LH, Sato S, Aubert G, Genua A, Szczyglowski K, Duc G, Kaneko T, Tabata S, de Bruijn F, Pajuelo E, Sandal N, Stougaard J (2002) Shoot control of root development and nodulation is mediated by a receptor-like kinase. Nature **420:** 422-426

Kucukoglu M, Nilsson O (2015) *CLE* peptide signaling in plants - the power of moving around. Physiol Plant **155:** 74-87

Kusnetsov V, Landsberger M, Meurer J, Oelmuller R (1999) The assembly of the CAAT-box binding complex at a photosynthesis gene promoter is regulated by light, cytokinin, and the stage of the plastids. J Biol Chem **274:** 36009-36014

Lakatos L, Szittya G, Silhavy D, Burgyan J (2004) Molecular mechanism of RNA silencing suppression mediated by p19 protein of tombusviruses. Embo j **23:** 876-884

Laloum T, Baudin M, Frances L, Lepage A, Billault-Penneteau B, Cerri MR, Ariel F, Jardinaud MF, Gamas P, de Carvalho-Niebel F, Niebel A (2014) Two CCAAT-box-binding transcription factors redundantly regulate early steps of the legume-rhizobia endosymbiosis. Plant J **79:** 757-768

Laloum T, De Mita S, Gamas P, Baudin M, Niebel A (2013) CCAAT-box binding transcription factors in plants: Y so many? Trends Plant Sci **18:** 157-166

Lamark T, Perander M, Outzen H, Kristiansen K, Overvatn A, Michaelsen E, Bjorkoy G, Johansen T (2003) Interaction codes within the family of mammalian Phox and Bem1p domain-containing proteins. J Biol Chem **278:** 34568-34581

Lefebvre B, Klaus-Heisen D, Pietraszewska-Bogiel A, Herve C, Camut S, Auriac MC, Gasciolli V, Nurisso A, Gadella TW, Cullimore J (2012) Role of N-glycosylation sites and CXC motifs in trafficking of medicago truncatula Nod factor perception protein to plasma membrane. J Biol Chem **287:** 10812-10823

Lefebvre B, Timmers T, Mbengue M, Moreau S, Hervé C, Tóth K, Bittencourt-Silvestre J, Klaus D, Deslandes L, Godiard L, Murray JD, Udvardi MK, Raffaele S, Mongrand S, Cullimore J, Gamas P, Niebel A, Ott T (2010) A remorin protein interacts with symbiotic receptors and regulates bacterial infection. Proc Natl Acad Sci U S A **107:** 2343-2348

Levy J, Bres C, Geurts R, Chalhoub B, Kulikova O, Duc G, Journet EP, Ane JM, Lauber E, Bisseling T, Denarie J, Rosenberg C, Debelle F (2004) A putative Ca2+ and calmodulin-dependent protein kinase required for bacterial and fungal symbioses. Science **303:** 1361-1364

Li HL, Wang W, Mortimer PE, Li RQ, Li DZ, Hyde KD, Xu JC, Soltis DE, Chen ZD (2015) Large-scale phylogenetic analyses reveal multiple gains of actinorhizal nitrogen-fixing symbioses in angiosperms associated with climate change. Sci Rep **5:** 14023

Liu W, Kohlen W, Lillo A, Op den Camp R, Ivanov S, Hartog M, Limpens E, Jamil M, Smaczniak C, Kaufmann K, Yang WC, Hooiveld GJ, Charnikhova T, Bouwmeester HJ, Bisseling T, Geurts R (2011) Strigolactone biosynthesis in *Medicago truncatula* and rice requires the symbiotic GRAS-type transcription factors NSP1 and NSP2. Plant Cell **23:** 3853-3865

Madsen E, Madsen L, Radutoiu S, Olbryt M, Rakwalska M, Szczyglowski K, Sato S, Kaneko T, Tabata S, Sandal N, Stougaard J (2003) A receptor kinase gene of the LysM type is involved in legume perception of rhizobial signals. Nature **425:** 637-640

Madsen EB, Antolin-Llovera M, Grossmann C, Ye J, Vieweg S, Broghammer A, Krusell L, Radutoiu S, Jensen ON, Stougaard J, Parniske M (2011) Autophosphorylation is essential for the in vivo function of the Lotus japonicus Nod factor receptor 1 and receptor-mediated signalling in cooperation with Nod factor receptor 5. Plant J **65:** 404-417

Madsen LH, Tirichine L, Jurkiewicz A, Sullivan JT, Heckmann AB, Bek AS, Ronson CW, James EK, Stougaard J (2010) The molecular network governing nodule organogenesis and infection in the model legume *Lotus japonicus*. Nat Commun **1:** 10

Maekawa T, Maekawa-Yoshikawa M, Takeda N, Imaizumi-Anraku H, Murooka Y, Hayashi M (2009) Gibberellin controls the nodulation signaling pathway in *Lotus japonicus*. Plant J **58:** 183-194

Magori S, Kawaguchi M (2009) Long-distance control of nodulation: molecules and models. Mol Cells **27:** 129-134

Marchive C, Roudier F, Castaings L, Bréhaut V, Blondet E, Colot V, Meyer C, Krapp A (2013) Nuclear retention of the transcription factor *NLP7* orchestrates the early response to nitrate in plants. Nature Communications **4:** 1713

Markmann K, Giczey G, Parniske M (2008) Functional adaptation of a plant receptor-kinase paved the way for the evolution of intracellular root symbioses with bacteria. PLoS Biol **6:** e68

Marsh J, Rakocevic A, Mitra R, Brocard L, Sun J, Eschstruth A, Long S, Schultze M, Ratet P, Oldroyd G (2007) *Medicago truncatula NIN* is essential for rhizobial-independent nodule organogenesis induced by autoactive calcium/calmodulin-dependent protein kinase. Plant Physiol **144:** 324-335

McGrath KC, Dombrecht B, Manners JM, Schenk PM, Edgar CI, Maclean DJ, Scheible WR, Udvardi MK, Kazan K (2005) Repressor- and activator-type ethylene response factors functioning in jasmonate signaling and disease resistance identified via a genome-wide screen of *Arabidopsis* transcription factor gene expression. Plant Physiol **139:** 949-959

Messinese E, Mun JH, Yeun LH, Jayaraman D, Rouge P, Barre A, Lougnon G, Schornack S, Bono JJ, Cook DR, Ane JM (2007) A novel nuclear protein interacts with the symbiotic DMI3 calcium- and calmodulin-dependent protein kinase of *Medicago truncatula*. Mol Plant Microbe Interact **20:** 912-921

Middleton P, Jakab J, Penmetsa R, Starker C, Doll J, Kaló P, Prabhu R, Marsh J, Mitra R, Kereszt A, Dudas B, VandenBosch K, Long S, Cook D, Kiss G, Oldroyd G (2007) An *ERF* transcription factor in *Medicago truncatula* that is essential for Nod factor signal transduction. Plant Cell **19:** 1221-1234

Mitra R, Gleason C, Edwards A, Hadfield J, Downie J, Oldroyd G, Long S (2004) A Ca2+/calmodulin-dependent protein kinase required for symbiotic nodule development: Gene identification by transcript-based cloning. Proc Natl Acad Sci U S A **101:** 4701-4705

Miwa H, Sun J, Oldroyd G, Downie J (2006) Analysis of calcium spiking using a cameleon calcium sensor reveals that nodulation gene expression is regulated by calcium spike number and the developmental status of the cell. Plant J **48:** 883-894

Morbitzer R, Elsaesser J, Hausner J, Lahaye T (2011) Assembly of custom TALE-type DNA binding domains by modular cloning. Nucleic Acids Res **39:** 5790-5799

Mortier V, Holsters M, Goormachtig S (2012) Never too many? How legumes control nodule numbers. Plant Cell Environ **35:** 245-258

Murakami Y, Miwa H, Imaizumi-Anraku H, Kouchi H, Downie J, Kawaguchi M, Kawasaki S (2006) Positional cloning identifies *Lotus japonicus NSP2*, a putative transcription factor of the GRAS family, required for *NIN* and *ENOD40* gene expression in nodule initiation. DNA Res **13:** 255-265

Murray J, Karas B, Sato S, Tabata S, Amyot L, Szczyglowski K (2007) A cytokinin perception mutant colonized by *Rhizobium* in the absence of nodule organogenesis. Science **315:** 101-104

Murray JD (2011) Invasion by invitation: rhizobial infection in legumes. Mol Plant Microbe Interact **24:** 631-639

Nakano T, Suzuki K, Ohtsuki N, Tsujimoto Y, Fujimura T, Shinshi H (2006) Identification of genes of the plant-specific transcription-factor families cooperatively regulated by ethylene and jasmonate in Arabidopsis thaliana. J Plant Res **119:** 407-413

Nishida H, Handa Y, Tanaka S, Suzaki T, Kawaguchi M (2016) Expression of the *CLE-RS3* gene suppresses root nodulation in *Lotus japonicus*. J Plant Res **129:** 909-919

Nishimura R, Hayashi M, Wu G, Kouchi H, Imaizumi-Anraku H, Murakami Y, Kawasaki S, Akao S, Ohmori M, Nagasawa M, Harada K, Kawaguchi M (2002) *HAR1* mediates systemic regulation of symbiotic organ development. Nature **420:** 426-429

Ohta M, Matsui K, Hiratsu K, Shinshi H, Ohme-Takagi M (2001) Repression domains of class II *ERF* transcriptional repressors share an essential motif for active repression. Plant Cell **13:** 1959-1968

Okamoto S, Ohnishi E, Sato S, Takahashi H, Nakazono M, Tabata S, Kawaguchi M (2009) Nod Factor/Nitrate-Induced *CLE* Genes that Drive *HAR1*-Mediated Systemic Regulation of Nodulation. Plant and Cell Physiology **50:** 67-77

Oldroyd GE, Downie JA (2008) Coordinating nodule morphogenesis with rhizobial infection in legumes. Annu Rev Plant Biol **59:** 519-546

Oldroyd GE (2013) Speak, friend, and enter: signalling systems that promote beneficial symbiotic associations in plants. Nature Reviews Microbiology **11:** 252-263

Oldroyd GE, Murray JD, Poole PS, Downie JA (2011) The rules of engagement in the legume-rhizobial symbiosis. Annual review of genetics **45:** 119-144

Op den Camp RH, Polone E, Fedorova E, Roelofsen W, Squartini A, Op den Camp HJ, Bisseling T, Geurts R (2012) Nonlegume *Parasponia andersonii* deploys a broad rhizobium host range strategy resulting in largely variable symbiotic effectiveness. Mol Plant Microbe Interact **25:** 954-963

Ovchinnikova E, Journet EP, Chabaud M, Cosson V, Ratet P, Duc G, Fedorova E, Liu W, den Camp RO, Zhukov V, Tikhonovich I, Borisov A, Bisseling T, Limpens E (2011) *IPD3* controls the formation of nitrogen-fixing symbiosomes in *pea* and *Medicago* Spp. Mol Plant Microbe Interact **24:** 1333-1344

Pawlowski, K., and Sprent, J.I. (2008). Comparison between actinorhizal and legume symbiosis, in *Nitrogen-fixing Actinorhizal Symbioses,* eds. K. Pawlowski & W. Newton. Springer Netherlands), 261-288.

Parniske M (2008) Arbuscular mycorrhiza: the mother of plant root endosymbioses. Nat Rev Microbiol **6:** 763-775

Perry J, Brachmann A, Welham T, Binder A, Charpentier M, Groth M, Haage K, Markmann K, Wang TL, Parniske M (2009) TILLING in *Lotus japonicus* identified large allelic series for symbiosis genes and revealed a bias in functionally defective ethyl methanesulfonate alleles toward glycine replacements. Plant Physiol **151:** 1281-1291

Peters NK, Frost JW, Long SR (1986) A plant flavone, luteolin, induces expression of *Rhizobium meliloti* nodulation genes. Science **233:** 977-980

Pietraszewska-Bogiel A, Lefebvre B, Koini MA, Klaus-Heisen D, Takken FL, Geurts R, Cullimore JV, Gadella TW (2013) Interaction of Medicago truncatula lysin motif receptor-like kinases, NFP and LYK3, produced in *Nicotiana benthamiana* induces defence-like responses. PLoS One **8:** e65055

Plet J, Wasson A, Ariel F, Le Signor C, Baker D, Mathesius U, Crespi M, Frugier F (2011) *MtCRE1*-dependent cytokinin signaling integrates bacterial and plant cues to coordinate symbiotic nodule organogenesis in Medicago truncatula. Plant J **65:** 622-633

Ponting C, Ito T, Moscat J, Diaz-Meco M, Inagaki F, Sumimoto H (2002) OPR, PC and AID: all in the PB1 family. Trends Biochem Sci **27:** 10

Qiu L, Lin JS, Xu J, Sato S, Parniske M, Wang TL, Downie JA, Xie F (2015) SCARN a novel class of SCAR protein that is required for root-hair infection during legume nodulation. PLoS Genet **11:** e1005623

Radutoiu S, Madsen L, Madsen E, Felle H, Umehara Y, Grønlund M, Sato S, Nakamura Y, Tabata S, Sandal N, Stougaard J (2003) Plant recognition of symbiotic bacteria requires two LysM receptor-like kinases. Nature **425:** 585-592

Raymond J, Siefert J, Staples C, Blankenship R (2004) The natural history of nitrogen fixation. Mol Biol Evol **21:** 541-554

Reid DE, Ferguson BJ, Hayashi S, Lin YH, Gresshoff PM (2011) Molecular mechanisms controlling legume autoregulation of nodulation. Ann Bot **108:** 789-795

Remigi P, Zhu J, Young JP, Masson-Boivin C (2016) Symbiosis within symbiosis: evolving nitrogen-fixing legume symbionts. Trends Microbiol **24:** 63-75

Riechmann JL, Meyerowitz EM (1998) The AP2/EREBP family of plant transcription factors. Biol Chem **379:** 633-646

Ried MK, Antolin-Llovera M, Parniske M (2014) Spontaneous symbiotic reprogramming of plant roots triggered by receptor-like kinases. Elife **3**

Roche P, Lerouge P, Ponthus C, Prome JC (1991) Structural determination of bacterial nodulation factors involved in the *Rhizobium meliloti*-alfalfa symbiosis. J Biol Chem **266:** 10933-10940

Rodríguez-Llorente I, Pérez-Hormaeche J, El Mounadi K, Dary M, Caviedes M, Cosson V, Kondorosi A, Ratet P, Palomares A (2004) From pollen tubes to infection threads: recruitment of Medicago floral pectic genes for symbiosis. Plant J **39:** 587-598

Ryder SP, Recht MI, Williamson JR (2008) Quantitative analysis of protein-RNA interactions by gel mobility shift. Methods Mol Biol **488:** 99-115

Saito K, Yoshikawa M, Yano K, Miwa H, Uchida H, Asamizu E, Sato S, Tabata S, Imaizumi-Anraku H, Umehara Y, Kouchi H, Murooka Y, Szczyglowski K, Downie J, Parniske M, Hayashi M, Kawaguchi M (2007) *NUCLEOPORIN85* is required for calcium spiking, fungal and bacterial symbioses, and seed production in *Lotus japonicus*. Plant Cell **19:** 610-624

Sakuma T, Ochiai H, Kaneko T, Mashimo T, Tokumasu D, Sakane Y, Suzuki K, Miyamoto T, Sakamoto N, Matsuura S, Yamamoto T (2013) Repeating pattern of non-RVD variations in DNA-binding modules enhances TALEN activity. Sci Rep **3:** 3379

Schauser L, Roussis A, Stiller J, Stougaard J (1999) A plant regulator controlling development of symbiotic root nodules. Nature **402:** 191-195

Schauser L, Wieloch W, Stougaard J (2005) Evolution of NIN-like proteins in *Arabidopsis*, rice, and *Lotus japonicus*. J Mol Evol **60:** 229-237

Schüβler A, Schwarzott D, Walker C (2001) A new fungal phylum, the Glomeromycota: phylogeny and evolution *Dedicated to Manfred Kluge (Technische Universität Darmstadt) on the occasion of his retirement. Mycological Research **105:** 1413-1421

Shimoda Y, Han L, Yamazaki T, Suzuki R, Hayashi M, Imaizumi-Anraku H (2012) Rhizobial and fungal symbioses show different requirements for calmodulin binding to calcium calmodulin-dependent protein kinase in *Lotus japonicus*. Plant Cell **24:** 304-321

Sieberer BJ, Chabaud M, Fournier J, Timmers AC, Barker DG (2012) A switch in Ca2+ spiking signature is concomitant with endosymbiotic microbe entry into cortical root cells of *Medicago truncatula*. The Plant Journal **69:** 822-830

Singh S, Katzer K, Lambert J, Cerri M, Parniske M (2014) CYCLOPS, a DNA-binding transcriptional activator, orchestrates symbiotic root nodule development. Cell Host Microbe **15:** 139-152

Singh S, Parniske M (2012) Activation of calcium- and calmodulin-dependent protein kinase (CCaMK), the central regulator of plant root endosymbiosis. Curr Opin Plant Biol **15:** 444-453

Smit P, Raedts J, Portyanko V, Debelle F, Gough C, Bisseling T, Geurts R (2005) NSP1 of the GRAS protein family is essential for rhizobial Nod factor-induced transcription. Science **308:** 1789-1791

Sornaraj P, Luang S, Lopato S, Hrmova M (2016) Basic leucine zipper (bZIP) transcription factors involved in abiotic stresses: A molecular model of a wheat bZIP factor and implications of its structure in function. Biochim Biophys Acta **1860:** 46-56

Soyano T, Hirakawa H, Sato S, Hayashi M, Kawaguchi M (2014) *Nodule Inception* creates a long-distance negative feedback loop involved in homeostatic regulation of nodule organ production. Proceedings of the National Academy of Sciences **111:** 14607-14612

Soyano T, Kouchi H, Hirota A, Hayashi M (2013) *Nodule inception* directly targets NF-Y subunit genes to regulate essential processes of root nodule development in Lotus japonicus. PLoS Genet **9:** e1003352

Soyano T, Shimoda Y, Hayashi M (2015) *Nodule Inception* antagonistically regulates gene expression with nitrate in Lotus japonicus. Plant Cell Physiol **56:** 368-376

Stockinger H, Walker C, Schussler A (2009) '*Glomus intraradices* DAOM197198', a model fungus in arbuscular mycorrhiza research, is not *Glomus intraradices*. New Phytol **183:** 1176-1187

Stracke S, Kistner C, Yoshida S, Mulder L, Sato S, Kaneko T, Tabata S, Sandal N, Stougaard J, Szczyglowski K, Parniske M (2002) A plant receptor-like kinase required for both bacterial and fungal symbiosis. Nature **417:** 959-962

Streeter J, Wong PP (1988) Inhibition of legume nodule formation and N2 fixation by nitrate. Critical Reviews in Plant Sciences **7:** 1-23

Sumimoto H, Kamakura S, Ito T (2007) Structure and function of the PB1 domain, a protein interaction module conserved in animals, fungi, amoebas, and plants. Sci STKE **2007:** re6

Suzaki T, Kim CS, Takeda N, Szczyglowski K, Kawaguchi M (2013) *TRICOT* encodes an AMP1-related carboxypeptidase that regulates root nodule development and shoot apical meristem maintenance in *Lotus japonicus*. Development **140:** 353-361

Suzaki T, Yano K, Ito M, Umehara Y, Suganuma N, Kawaguchi M (2012) Positive and negative regulation of cortical cell division during root nodule development in *Lotus japonicus* is accompanied by auxin response. Development **139:** 3997-4006

Suzuki W, Konishi M, Yanagisawa S (2013) The evolutionary events necessary for the emergence of symbiotic nitrogen fixation in legumes may involve a loss of nitrate responsiveness of the NIN transcription factor. Plant Signal Behav **8**

Swainsbury DJ, Zhou L, Oldroyd GE, Bornemann S (2012) Calcium ion binding properties of *Medicago truncatula* calcium/calmodulin-dependent protein kinase. Biochemistry **51:** 6895-6907

Takeda N, Maekawa T, Hayashi M (2012) Nuclear-localized and deregulated calcium- and calmodulin-dependent protein kinase activates rhizobial and mycorrhizal responses in *Lotus japonicus*. Plant Cell **24:** 810-822

Timmers A, Auriac M, Truchet G (1999) Refined analysis of early symbiotic steps of the *Rhizobium-Medicago* interaction in relationship with microtubular cytoskeleton rearrangements. Development **126:** 3617-3628

Tirichine L, Imaizumi-Anraku H, Yoshida S, Murakami Y, Madsen L, Miwa H, Nakagawa T, Sandal N, Albrektsen A, Kawaguchi M, Downie A, Sato S, Tabata S, Kouchi H, Parniske M, Kawasaki S, Stougaard J (2006) Deregulation of a Ca2+/calmodulin-dependent kinase leads to spontaneous nodule development. Nature **441:** 1153-1156

Tirichine L, Sandal N, Madsen L, Radutoiu S, Albrektsen A, Sato S, Asamizu E, Tabata S, Stougaard J (2007) A gain-of-function mutation in a cytokinin receptor triggers spontaneous root nodule organogenesis. Science **315:** 104-107

Toth K, Stratil TF, Madsen EB, Ye J, Popp C, Antolin-Llovera M, Grossmann C, Jensen ON, Schussler A, Parniske M, Ott T (2012) Functional domain analysis of the Remorin protein LjSYMREM1 in *Lotus japonicus*. PLoS One **7:** e30817

Untergasser A, Cutcutache I, Koressaar T, Ye J, Faircloth BC, Remm M, Rozen SG (2012) Primer3--new capabilities and interfaces. Nucleic Acids Res **40:** e115

van Zeijl A, Op den Camp RH, Deinum EE, Charnikhova T, Franssen H, Op den Camp HJ, Bouwmeester H, Kohlen W, Bisseling T, Geurts R (2015) *Rhizobium* Lipo-chitooligosaccharide signaling triggers accumulation of cytokinins in *Medicago truncatula* roots. Mol Plant **8:** 1213-1226

Vernie T, Kim J, Frances L, Ding Y, Sun J, Guan D, Niebel A, Gifford ML, de Carvalho-Niebel F, Oldroyd GE (2015) The NIN transcription factor coordinates diverse nodulation programs in different tissues of the *Medicago truncatula* root. Plant Cell **27:** 3410-3424

Voinnet O, Rivas S, Mestre P, Baulcombe D (2003) An enhanced transient expression system in plants based on suppression of gene silencing by the p19 protein of *tomato* bushy stunt virus. Plant J **33:** 949-956

Waadt R, Schmidt LK, Lohse M, Hashimoto K, Bock R, Kudla J (2008) Multicolor bimolecular fluorescence complementation reveals simultaneous formation of alternative CBL/CIPK complexes in planta. Plant J **56:** 505-516

Waki T, Hiki T, Watanabe R, Hashimoto T, Nakajima K (2011) The *Arabidopsis* RWP-RK protein RKD4 triggers gene expression and pattern formation in early embryogenesis. Curr Biol **21:** 1277-1281

Weber E, Gruetzner R, Werner S, Engler C, Marillonnet S (2011) Assembly of designer TAL effectors by golden gate cloning. PLoS One **6:** e19722

Weerasinghe RR, Bird DM, Allen NS (2005) Root-knot nematodes and bacterial nod factors elicit common signal transduction events in *Lotus japonicus*. Proc Natl Acad Sci U S A **102:** 3147-3152

Woods RA, Gietz RD (2001) High-efficiency transformation of plasmid DNA into *yeast*. Methods Mol Biol **177:** 85-97

Wopereis J, Pajuelo E, Dazzo FB, Jiang Q, Gresshoff PM, De Bruijn FJ, Stougaard J, Szczyglowski K (2000) Short root mutant of *Lotus japonicus* with a dramatically altered symbiotic phenotype. Plant J **23:** 97-114

Xie F, Murray JD, Kim J, Heckmann AB, Edwards A, Oldroyd GE, Downie JA (2012) Legume pectate lyase required for root infection by *rhizobia*. Proceedings of the National Academy of Sciences **109:** 633-638

Yanagisawa S, Schmidt RJ (1999) Diversity and similarity among recognition sequences of Dof transcription factors. Plant J **17:** 209-214

Yang W, de Blank C, Meskiene I, Hirt H, Bakker J, van Kammen A, Franssen H, Bisseling T (1994) *Rhizobium* nod factors reactivate the cell cycle during infection and nodule primordium formation, but the cycle is only completed in primordium formation. Plant Cell **6:** 1415-1426

Yano K, Yoshida S, Müller J, Singh S, Banba M, Vickers K, Markmann K, White C, Schuller B, Sato S (2008) CYCLOPS, a mediator of symbiotic intracellular accommodation. Proceedings of the National Academy of Sciences **105:** 20540-20545

Yokota K, Soyano T, Kouchi H, Hayashi M (2010) Function of GRAS proteins in root nodule symbiosis is retained in homologs of a non-legume, rice. Plant Cell Physiol **51:** 1436-1442

Yoro E, Suzaki T, Toyokura K, Miyazawa H, Fukaki H, Kawaguchi M (2014) A positive regulator of nodule organogenesis, Nodule inception, acts as a negative regulator of rhizobial infection in *Lotus japonicus*. Plant physiology **165:** 747-758

Yoshida S, Parniske M (2005) Regulation of plant symbiosis receptor kinase through serine and threonine phosphorylation. J Biol Chem **280:** 9203-9209

Zhang XC, Wu X, Findley S, Wan J, Liba ult M, Nguyen HT, Cannon SB, Stacey G (2007) Molecular evolution of lysin motif-type receptor-like kinases in plants. Plant Physiol **144:** 623-636

16 Acknowledgement

17 Curriculum Vitae

18 Eidesstattliche Versicherung

Ich versichere hiermit an Eides statt, dass die vorliegende Dissertation von mir selbstständig und ohne unerlaubte Hilfe angefertigt ist.

München, den 27. Oktober 2016

Jayne Carol Lambert

19 Erklärung

Hiermit erkläre ich, dass die Dissertation nicht ganz oder in wesentlichen Teilen einer anderen Prüfungskommission vorgelegt worden ist. Ich habe nicht versucht, anderweitig eine Dissertation einzureichen oder mich einer Doktorprüfung zu unterziehen.

München, den 27. Oktober 2016

Jayne Carol Lambert